

Lappeenrannan teknillinen yliopisto  
*Lappeenranta University of Technology*

*Hanne Jussila*

**CONCENTRATED WINDING MULTIPHASE PERMANENT  
MAGNET MACHINE DESIGN AND ELECTROMAGNETIC  
PROPERTIES – CASE AXIAL FLUX MACHINE**

*Thesis for the degree of Doctor of Science  
(Technology) to be presented with due  
permission for public examination and  
criticism in the Auditorium 1382 at  
Lappeenranta University of Technology,  
Lappeenranta, Finland on the 21st of  
December, 2009, at noon.*

Acta Universitatis  
Lappeenrantaensis  
**374**

Supervisor Professor Juha Pyrhönen  
Lappeenranta University of Technology  
Finland

Reviewers Professor Emeritus Tapani Jokinen  
Helsinki University of Technology  
Finland

D.Sc. Jussi Huppunen  
KONE Oyj  
Finland

Opponent Professor Pavol Rafajdus  
University of Žilina  
Slovak Republic

ISBN 978-952-214-882-7  
ISBN 978-952-214-883-4 (PDF)  
ISSN 1456-4491

Lappeenrannan teknillinen yliopisto  
Digipaino 2009

## ABSTRACT

Hanne Jussila

### **Concentrated Winding Multiphase Permanent Magnet Machine Design and Electromagnetic Properties – Case Axial Flux Machine**

Lappeenranta 2009

119 p.

Acta Universitatis Lappeenrantaensis 374

Diss. Lappeenranta University of Technology

ISBN 978-952-214-882-7, ISBN 978-952-214-883-4 (PDF), ISSN 1456-4491

Concentrated winding permanent magnet machines and their electromagnetic properties are studied in this doctoral thesis. The thesis includes a number of main tasks related to the application of permanent magnets in concentrated winding open slot machines. Suitable analytical methods are required for the first design calculations of a new machine. Concentrated winding machines differ from conventional integral slot winding machines in such a way that adapted analytical calculation methods are needed.

A simple analytical model for calculating the concentrated winding axial flux machines is provided. The next three main design tasks are discussed in more detail in the thesis. The magnetic length of the rotor surface magnet machines is studied, and it is shown that the traditional methods have to be modified also in this respect. An important topic in this study has been to evaluate and minimize the rotor permanent magnet Joule losses by using segmented magnets in the calculations and experiments. Determination of the magnetizing and leakage inductances for a concentrated winding machine and the torque production capability of concentrated winding machines with different pole pair numbers are studied, and the results are compared with the corresponding properties of integral slot winding machines.

The thesis introduces a new practical permanent magnet motor type for industrial use. The special features of the machine are based on the option of using concentrated winding open slot constructions of permanent magnet synchronous machines in the normal speed ranges of industrial motors, for instance up to  $3000 \text{ min}^{-1}$ , without excessive rotor losses.

By applying the analytical equations and methods introduced in the thesis, a 37 kW  $2400 \text{ min}^{-1}$  12-slot 10-pole axial flux machine with rotor-surface-mounted magnets is designed. The performance of the designed motor is determined by experimental measurements and finite element calculations.

Keywords: axial flux machine, concentrated winding, Joule loss, inductance, magnetic length, segmented magnet, open slot

UDC 621.313.82 : 621.3.013.1 -026.32

## ACKNOWLEDGEMENTS

This research work for this thesis has been carried out during the years 2006–2009 at Lappeenranta University of Technology. The research was partly funded by AXCO-motors Oy.

I would like to thank all the people involved in the preparation of this thesis. Especially I express my gratitude to Professor Juha Pyrhönen, the supervisor of this thesis, for his valuable guidance and encouragement. I would like to thank Dr. Asko Parviainen and Dr. Mikko Valtonen from AXCO-motors Oy, for their guidance during this thesis. I wish also thank Dr. Pia Lindh, Dr. Janne Nerg and Dr. Markku Niemelä for the collaboration and encouragement during the years.

Special thanks are reserved for Dr. Hanna Niemelä for her professional help to review and improve the language of this work. I also thank the laboratory personnel for the assistance during the construction of the prototype machines as well as practical arrangements in the laboratory.

I am grateful to the preliminary examiners of the thesis, Professor Emeritus Tapani Jokinen and Dr. Jussi Huppunen for their valuable comments and improvements to the manuscript.

The financial support by the Lappeenranta University of Technology Foundation, Lahja and Lauri Hotinen Fund, the Finnish Foundation for Technology Promotion, Walter Ahlström Foundation, Ulla Tuominen Foundation and the Finnish Cultural Foundation (South Karelia Regional Fund) is gratefully appreciated.

I also express my gratitude to my colleagues, friends and especially my family for their help and support during this process.

Lappeenranta, December, 2009

Hanne Jussila



## CONTENTS

ABSTRACT .....	3
ACKNOWLEDGEMENTS .....	5
CONTENTS .....	7
ABBREVIATIONS AND SYMBOLS.....	9
1 INTRODUCTION .....	15
1.1 Harmonics of concentrated windings .....	22
1.2 Scope of the work and outline of the thesis .....	26
1.3 Scientific contributions of the work .....	29
1.4 Most relevant scientific publications.....	29
2 ANALYTICAL METHODS FOR CALCULATION OF AXIAL FLUX CONCENTRATED WINDING PM MACHINES.....	33
2.1 Modelling of concentrated winding axial flux machines .....	34
2.2 Analytical calculation of the magnetic flux density in the air gap.....	45
2.2.1 Slotting effect.....	48
2.3 Torque and inductances .....	52
2.4 Joule losses of permanent magnets.....	61
2.4.1 Joule losses caused by winding harmonics .....	62
2.4.2 Joule losses caused by permeance harmonics .....	69
2.5 Other losses .....	73
2.6 Summary .....	76
3 TORQUE CAPBILITIES OF DIFFERENT WINDING CONSTRUCTIONS .....	77
3.1 Machine parameters.....	78
3.2 Inductances and torques of concentrated winding machines and integral slot winding machines in the case of semi-closed slot openings .....	79
3.3 Inductances and torques of concentrated winding machines in the cases of a semi-closed slot opening and a totally open slot.....	87
3.4 Summary .....	88
4 PROTOTYPE MACHINE AND TEST RESULTS .....	90
4.1 Stator resistance.....	96
4.2 Load measurements .....	100
4.3 Maximum pull-out torques .....	105
4.4 Cogging torque with the 2D and 3D FEA .....	106
4.5 Summary .....	107

5 CONCLUSION.....108  
    5.1 Future Work .....109  
REFERENCES.....111

## ABBREVIATIONS AND SYMBOLS

### Roman letters

$A$ ,	linear current density [A/m]
$A_{wh}$ ,	linear current density of the working harmonic [A/m]
$B$ ,	magnetic flux density [Vs/m <sup>2</sup> ], [T]
$B_n$ ,	normal component of magnetic flux density [T]
$B_{n,wh}$ ,	normal component of magnetic flux density of the working harmonic [T]
$B_{PM}$ ,	magnetic flux density [T]
$B_r$ ,	remanent flux density [T]
$b$ ,	width [m]
$b_4$ ,	stator slot width [m]
$b_1$ ,	slot opening width [m]
$b_{PM}$ ,	permanent magnet width [m]
$b_{PM,segment}$ ,	permanent magnet segment width [m]
$D$ ,	diameter [m]
$D_r$ ,	outer diameter of the rotor [m]
$D_i$ ,	inner diameter of the stator [m]
$D_{i,axial}$ ,	inner diameter of the axial flux machine [m]
$D_o$ ,	outer diameter of the stator [m]
$D_{o,axial}$ ,	outer diameter of the axial flux machine [m]
$D_\delta$ ,	air gap diameter [m]
$d$ ,	thickness [m]
$E_{PM}$ ,	electromotive force (emf) [V], RMS
$e$ ,	electromotive force (emf) [V]
$F$ ,	force [N]
$F_{tan}$ ,	tangential force [N]
$f$ ,	frequency [Hz]
$g$ ,	coefficient, constant
$H$ ,	magnetic field strength [A/m]
$h$ ,	height [m]
$h_{PM}$ ,	height of magnet [m]
$h_{ys}$ ,	height of stator yoke [m]
$I_s$ ,	current [A], RMS
$i_s$ ,	current [A], instantaneous value $i(t)$
$i_u$ ,	slot current [A], instantaneous value $i(t)$
$J$ ,	current density [A/m <sup>2</sup> ], magnetic polarization
$J_{PM}$ ,	current density in permanent magnet [A/m <sup>2</sup> ]
$K_n$ ,	coefficient
$k$ ,	constant

$k_{ad}$ ,	additional loss coefficient
$k_C$ ,	Carter factor
$k_d$ ,	distribution factor
$k_e, k_{eh}, k_{exe}, k_h$ ,	constant
$k_{Feys}, k_{Fets}$ ,	constant
$k_p$ ,	pitch factor
$k_{sq}$ ,	skewing factor
$k_w$ ,	winding factor
$k_{w1}$ ,	winding factor for the fundamental wave
$k_{w,wh}$ ,	winding factor for the working harmonic
$k_p$ ,	coefficient
$L_d$ ,	direct-axis inductance [H]
$L_{md}$ ,	magnetizing inductance of an $m$ -phase synchronous machine, in d-axis [H]
$L_{mq}$ ,	magnetizing inductance of an $m$ -phase synchronous machine, in q-axis [H]
$L_q$ ,	quadrature-axis inductance [H]
$L_{s\sigma}$ ,	stator leakage inductance [H]
$L_u$ ,	slot leakage inductance [H]
$L_w$ ,	end winding leakage inductance [H]
$L_z$ ,	tooth tip leakage inductance [H]
$L_\delta$ ,	air gap leakage inductance [H]
$l$ ,	length [m]
$l'$ ,	effective core length [m]
$l_{ew}$ ,	average conductor length of winding overhang [m]
$l_{Fe}$ ,	stator stack core length [m]
$l_{mf}$ ,	main flux path length [m]
$l_r$ ,	rotor core length [m]
$l_w$ ,	length of coil ends [m]
$m$ ,	number of phases, mass [kg]
$N_{PM}$ ,	number of permanent magnet segments
$N_s$ ,	number of turns in series per stator winding
$n$ ,	exponent
$n_s$ ,	rotation speed (rotation frequency) [1/s]
$P$ ,	power, losses [W]
$P_{Cu}$ ,	copper losses [W]
$P_{Fe,ec}$ ,	iron Joule losses [W]
$P_{hy}$ ,	hysteresis loss [W]
$P_{in}$ ,	input power [W]
$P_{out}$ ,	output power [W]
$P_{ad}$ ,	additional loss [W]
$P_{PM, ec}$ ,	permanent magnet Joule loss [W]
$P_\rho$ ,	mechanical loss [W]

$p$ ,	number of pole pairs, ordinal
$Q$ ,	number of slots
$q$ ,	number of slots per pole and phase,
$R_s$ ,	resistance [ $\Omega$ ]
$r$ ,	radius [m]
$r_{PM}$ ,	radius of permanent magnet [m]
$r_r$ ,	outer radius of the rotor [m]
$r_i$ ,	inner radius of the stator [m]
$r_{i, axial}$ ,	inner radius of the axial flux machine [m]
$r_o$ ,	outer radius of the stator [m]
$r_{o, axial}$ ,	outer radius of the axial flux machine [m]
$r_\delta$ ,	air gap radius [m]
$S$ ,	cross-sectional area [ $m^2$ ]
$s_{sq}$ ,	skewing pitch
$T$ ,	torque [Nm], period
$T_N$ ,	rated torque [Nm]
$T_{max}$ ,	maximum pull-out torque, peak torque [Nm]
$t$ ,	time [s]
$U$ ,	voltage [V], RMS
$U_s$ ,	voltage [V], RMS
$V$ ,	volume [ $m^3$ ]
$V_{PM}$ ,	volume of permanent magnet [ $m^3$ ]
$v$ ,	speed, velocity [m/s]
$v_r$ ,	rotor speed, velocity [m/s]
$W$ ,	coil span (width), [m]
$w$ ,	width [m]
$x$ ,	coordinate, length
$y$ ,	coordinate, length, winding step
$y_Q$ ,	full step

### Greek letters

$\alpha$ ,	angle [rad], [ $^\circ$ ], coefficient, temperature coefficient
$\alpha_{PM}$ ,	relative permanent magnet width
$\beta$ ,	angle [rad], [ $^\circ$ ]
$\gamma_n$ ,	angle [rad], [ $^\circ$ ]
$\delta$ ,	air gap (length) [m], skin depth [m], load angle [rad], [ $^\circ$ ]
$\delta_{PM}$ ,	magnetic air gap (influence of physical air gap and permanent magnet taken into account) [m]
$\delta'_{PM}$ ,	equivalent air gap (influence of physical air gap and permanent magnet and Carter factor taken into account) [m]

$\delta_{ef}$ ,	effective air gap (in addition to previous, influence of iron taken into account) [m]
$\eta$ ,	efficiency, constant
$\theta$ ,	angle [rad], [°]
$\kappa$ ,	factor for reduction of slot opening
$\lambda$ ,	permeance factor, inductance factor, relative permeance factor
$\lambda_{ew}, \lambda_w, \lambda_w$ ,	end winding leakage factor
$\lambda_u$ ,	slot leakage factor
$\lambda_z$ ,	tooth tip leakage factor
$\mu$ ,	permeability [Vs/Am, H/m]
$\mu_r$ ,	relative permeability
$\mu_{r, PM}$ ,	relative permeability of PM
$\mu_0$ ,	permeability of vacuum, $4 \cdot \pi \cdot 10^{-7}$ [Vs/Am, H/m]
$\nu$ ,	ordinal of harmonic
$\rho$ ,	resistivity [ $\Omega\text{m}$ ], density [ $\text{kg}/\text{m}^3$ ]
$\rho_{Fe}$ ,	iron resistivity [ $\Omega\text{m}$ ]
$\rho_{PM}$ ,	permanent magnet resistivity [ $\Omega\text{m}$ ]
$\sigma$ ,	specific conductivity [S/m], leakage factor
$\sigma_{PM}$ ,	permanent magnet conductivity
$\sigma_{tan}$ ,	tangential stress [Pa]
$\sigma_{Fe}$ ,	iron conductivity [S/m]
$\sigma_\delta$ ,	air gap leakage factor
$\tau_p$ ,	pole pitch [m]
$\tau_u$ ,	slot pitch [m]
$\Phi$ ,	magnetic flux [Vs, Wb]
$\varphi$ ,	phase shift angle [rad], [°]
$\Psi$ ,	magnetic flux linkage [Vs]
$\Omega$ ,	mechanical angular speed [rad/s]
$\omega$ ,	electric angular velocity [rad/s], angular frequency [rad/s]
$\omega_s$ ,	stator electric angular velocity [rad/s], stator angular frequency [rad/s]

## Subscripts

ar, mean,	arithmetic mean
axial,	parameter of the axial flux machine
Cu,	copper
Fe,	iron
geom, mean,	geometric mean
i,	inner
o,	outer

PM,	permanent magnet
r,	rotor
s,	stator
t,	tooth
u,	slot
y,	yoke
wh,	working harmonic

### Superscripts

$\wedge$ ,	peak/maximum value, amplitude
'	imaginary, apparent, referred, virtual
$\bar{\sigma}$ ,	bar above the symbol denotes average value

### Acronyms

AC,	alternating current
AFPM,	axial flux permanent magnet
$BH$ ,	energy product
$BH_{\max}$ ,	maximum energy product
DC,	direct current
DTC,	direct torque control
EC,	eddy current
emf,	electromagnetic force
FEA,	Finite Element Analysis
NdFeB,	neodymium-iron-boron
PM,	permanent magnet
PMSM,	permanent magnet synchronous motor (or machine)
p.u.,	per unit
RMS,	root mean square



## 1 INTRODUCTION

The progress in the field of permanent magnet material technology has resulted in very powerful permanent magnet materials at a relatively competitive price, and as a result of that, the era of large industrial permanent magnet machines has started. For example, with neodymium-iron-boron (NdFeB) magnets, which have been commercially available since the mid 1980s, a maximum energy product ( $BH_{\max}$ ) of 400 kJ/m<sup>3</sup> and a remanent flux density  $B_r$  of 1.4 T can be achieved with a proper manufacturing process (Neorem 2009, International Magnetics Association 2000). Nowadays, NdFeB magnets are available with shapes, sizes and grades of great variety.

Permanent magnet synchronous machines (PMSM) provide significant advantages in terms of electrical efficiency compared with the traditional electrically excited synchronous machines. This is because the Joule losses of the field winding are eliminated by applying permanent magnets (PM) instead of rotor windings. Because permanent magnets are part of the magnetic circuit of the machine, they significantly affect the total reluctance of the machine. The relative permeability  $\mu_r$  of modern PM materials such as NdFeB is about equal to 1.05, leading to the fact that the equivalent air gap length in rotor surface magnet PMSMs in the direct-axis direction is considerable, thus resulting in small magnetizing inductance values, which is beneficial from the viewpoint of high pull-out torque production. The main drawback of the application of permanent magnets is that the rotor magnetization cannot be controlled. For example, in order to gain field weakening, demagnetizing stator current is required, which is not very efficient. However, the progress in the PM machine design, power electronics and particularly in different motor control schemes such as direct torque control (DTC) and sensorless vector control have resulted in a wide variety of industrial applications of electric drive systems where PMSMs are applied.

PM motor technology is also penetrating into the field of network-driven machines (Polinder et al. 2006, El-Rafaie and Jahns 2007, Kinnunen 2007), in which a mechanical gearbox is eliminated and thus the efficiency, performance and reliability of the drive system are enhanced. Of course, the same benefits hold true also for frequency-converter-driven speed-controlled applications. A specially designed direct drive PMSM may, in some applications, efficiently compete with a traditional induction motor drive with a gear both with respect to the space needed and the overall efficiency of the drive.

Compared with induction motors, clear benefits in terms of energy efficiency, power factor and speed control accuracy without speed encoders can be obtained by utilizing permanent magnet motor technology. Efficiency and

power factor benefits are, however, achieved best in drives applying multiple pole motors. For example, the designer of PMSMs has more freedom in selecting machine layout features and parameters such as the number of pole pairs, which in turn provides benefits in integrated machine systems. Furthermore, the power factor of an induction machine decreases rapidly as the number of poles is increased, which can be indirectly seen in the following equation describing the direct axis magnetizing inductance of an integral slot winding machine (Pyrhönen, Jokinen, Hrabovcová 2008)

$$L_{\text{md}} = \frac{2m\mu_0}{\pi} \frac{\tau_p}{p\pi\delta_{\text{ef}}} l' (k_{\text{w1}} N_s)^2, \quad (1.1)$$

where  $m$  is the number of the phase,  $\mu_0$  is the permeability of air,  $\tau_p$  is the pole pitch,  $l'$  is the effective length of the stator core,  $p$  the number of pole pairs,  $\delta_{\text{ef}}$  the effective air gap length taking also the effect of iron into account,  $k_{\text{w1}}$  the winding factor for the fundamental wave and  $N_s$  number of turns in series per stator winding. Distributed fractional slot windings are outside the scope of this work, and hence, the discussion and references on distributed windings concern integral slot windings only.

The magnetizing current of an induction motor is about inversely proportional to the magnetizing inductance. As the pole pitch  $\tau_p$  is inversely proportional to the number of pole pairs  $p$ , the magnetizing inductance is thereby inversely proportional to the square of the number of pole pairs  $L_{\text{md}} \cong 1/p^2$ , and hence, the induction machine power factor rapidly decreases as the number of poles increases.

An interesting field where PMSMs are applied is axial flux machines, which are often called disc-type machines because of their pancake shape. Axial flux permanent magnet (AFPM) machines are, because of their short axial length, an attractive alternative to traditional radial flux PMSMs in electric vehicles, pumps, fans, valve control, centrifuges, machine tools, robots, industrial equipment and in small- to medium-scale power generators (Gieras et al. 2008).

Integrating an electric motor with a pump, a fan or a compressor or using an electric motor integrated into the propulsion of an electric vehicle, a windmill, a lift or the like seem to be future trends in the applications of electrical machines to different drives (Reichert 2004). Axial flux machines are, in principle, easily integrated into the above-mentioned applications. Also the high efficiency of permanent magnet machines in different applications makes the application attractive.

In pump and fan applications, an axial flux permanent magnet machine is a very interesting machine type because of its high power factor and high efficiency compared with the axial flux induction motor introduced by Valtonen (2007). In some cases it seems to be easier to integrate such a motor type into a working machine construction. Valtonen used an induction rotor where a mechanically strong aluminium winding also acts as the rotor mechanical core. The magnetic flux carriers inserted in the strong winding are made of solid steel that fast deteriorates the power factor of the machine despite its high efficiency. The power factor in axial flux induction machines having solid steel active parts varies usually between 0.6 and 0.8 while permanent magnet machines provide power factors in the range of 0.90–0.95. A high power factor is beneficial as it results in a lowest possible stator current. Consequently, a low current capability frequency converter may be selected. The highest power factors close to unity, however, consume extra permanent magnet material, and often the best power factor is in the range of 0.9–0.95 in PMSM drives.

The manufacturing process of AFPM machines can be simplified considerably compared with traditional radial flux machines: The stator may be manufactured from narrow electrical steel bands, and hence, the waste of the lamination material is kept to minimum. Only the punching waste from the stator slots is recycled. However, the manufacturing process of an axial flux stator core is technically demanding and calls for high accuracy; nevertheless, the process can be automated. In radial flux machines with both the stator and the rotor made of laminations, the amount of wasted lamination material is relatively small but substantially larger than in an axial flux machine, as between the stator roundels there always remains some unused material. The best benefit, however, may be the easiness of the winding manufacturing process, which can be performed in a plane compared with working inside a cylinder, which is the case in inner rotor radial flux machines. With the two-stator-single-rotor construction, where the magnetic flux travels through the permanent magnets from one stator to another the rotor of the machine can be kept totally ironless. This makes the manufacturing of the permanent magnet rotor very simple and inexpensive. The adverse effect is, of course, that two stators are needed.

Concentrated windings together with the axial flux technology provide a further manufacturing benefit. When open stator slots and concentrated windings are used, prefabricated coils can just be inserted around the stator teeth, and the winding process becomes very low-cost compared for example with double-layer short-pitched normal integral slot windings. Furthermore, the space needed by the end-windings is minimized. Hence, concentrated winding axial flux permanent magnet motors are very cost effective from the manufacturing point of view. The shortening of the end windings and a high power factor

make it possible to minimize the stator Joule losses. The end-windings of an axial flux concentrated winding machine and a traditional integral slot winding machine are presented as an example in Fig. 1.1. In this work, concentrated winding refers to a fractional slot winding with concentrated coils, e.g. the number of slots per pole and phase  $q \leq 0.5$ . Even when using open slots, the concentrated winding machine may provide very low cogging torque values, and hence, the torque quality of the motor can be good. Cogging torque is the torque resulting from the interaction between the permanent magnets of the rotor and the stator slots. Cogging occurs even when there is no current in the stator (Baracat et al. 2001, Hanselmann 2003, Gieras et al. 2006).



Fig. 1.1. a) End winding of a concentrated winding machine and b) an integral slot winding machine

The cogging of the motor as a function of the relative magnet width, that is, the magnet width divided by the pole pitch, was analyzed in (Salminen 2004, 2006). We may conclude that for a certain number of slots per pole and phase  $q$ , the amount of cogging torque decreases as the number of slots increases. The minimum cogging values seem to be found when  $q$  is close to 0.33. On the contrary, the largest cogging torque may be expected when  $q$  equals to 0.25 or 0.5 (Salminen 2004, Salminen et al. 2006).

When the motor is running, there occur also additional oscillatory torque components because of the interaction of the magnets with the stator space harmonics and with the magnetic flux waves created by the current harmonics. These oscillatory components are generally referred to as torque ripple (Cros and Viarouge 2002, Magnussen and Sadarangani 2003, Ishak et al. 2004,

Salminen et al. 2005, Gieras 2006). The lowest peak-to-peak torque ripple values were obtained for machines with  $q$  close to 0.33. The torque ripple tends to have more than one local minima. For example, local minima can be found for two or three different permanent magnet widths, depending on the number of slots per pole and phase. Thereby it may be concluded that the minimum cogging torque and the minimum torque ripple are found when  $q$  is close to the value of 0.33 (Salminen 2004, Salminen et al. 2006).

Many examples of PMSMs with concentrated windings can be found in the literature, most of these being radial flux machines: a 20 kW 2000 min<sup>-1</sup> for a hybrid electric propulsion system (Magnussen and Sadarangani 2003, Magnussen et al. 2003, Magnussen et al. 2004), a 5 kW 50 min<sup>-1</sup> machine for an industrial application (Libert and Soulard 2004), a 45 kW 1000 min<sup>-1</sup> machine (Deak et al. 2006, 2008) and a 18.5 kW 1700 min<sup>-1</sup> machine for automotive applications (Wang et al. 2005). Salminen (2004) focused on 45 kW 400 min<sup>-1</sup> concentrated winding machines, for example paper mill applications.

The latest development and applications are found in 0.26 kW–10 kW radial flux permanent magnet machines with concentrated windings: a 6 kW 600 min<sup>-1</sup> machine for traction purpose (El-Refaie et al. 2006, El-Refaie and Jahns 2006), a 10 kW 370–440 min<sup>-1</sup> machine for an in-wheel drive application (Rix et al. 2007), a 5–10 kW 200–240 min<sup>-1</sup> machine for wind turbines (Cistelean et al. 2007) and a 0.26 kW 250 min<sup>-1</sup> for a bicycle application (Wrobel and Mellor 2005).

Some examples of concentrated winding axial flux machines can also be found in the literature: a 1.6 kW 250 min<sup>-1</sup> axial flux permanent magnet machine, designed to operate as a generator in a small-scale wind power application (Parviainen et al. 2005), 1 kW and 200 min<sup>-1</sup> laboratory prototype concentrated winding AFPM machines with air-cored stators (Kamper et al. 2007, 2008) and a nine-phase axial flux PM generator with concentrated windings for a direct drive turbine (Vizireanu et al. 2006).

In the above-mentioned work, a comparison of the PMSMs equipped with open stator slots and semi-closed stator slots with different pole pair – slot combinations was carried out in terms of pull-out torque production capability and electrical efficiency. Using semi-closed slots, the stator winding losses and the eddy-current losses in the permanent magnets were lower than with similar motors having open slots (Parviainen 2005, Salminen 2004, Lindh et al. “Concentrated Wound PM Motors with Semiclosed Slots and with Open Slots” *IEEE Energy Conversion* (forthcoming)). The flux travelling from the permanent magnet rotor to the stator is higher with semi-closed slots, and thus in open slot structures with the same main dimensions, a higher number of

winding turns are needed to induce an appropriate voltage. The semi-closed slot structures had slightly higher stator iron losses than the corresponding open slot structures because of the higher amount of flux in the stator teeth and yoke. The permanent magnet flux density pulsation is, of course, larger in open slot constructions than in semi-closed slot structures. The open slot structures gave slightly higher pull-out torques (because of low inductances), but the efficiencies of open slot structures remained somewhat lower than those of corresponding semi-closed structures, mainly because of high stator winding losses. Figure 1.2 clearly indicates the effect of wide teeth tips on the flux of the machine.

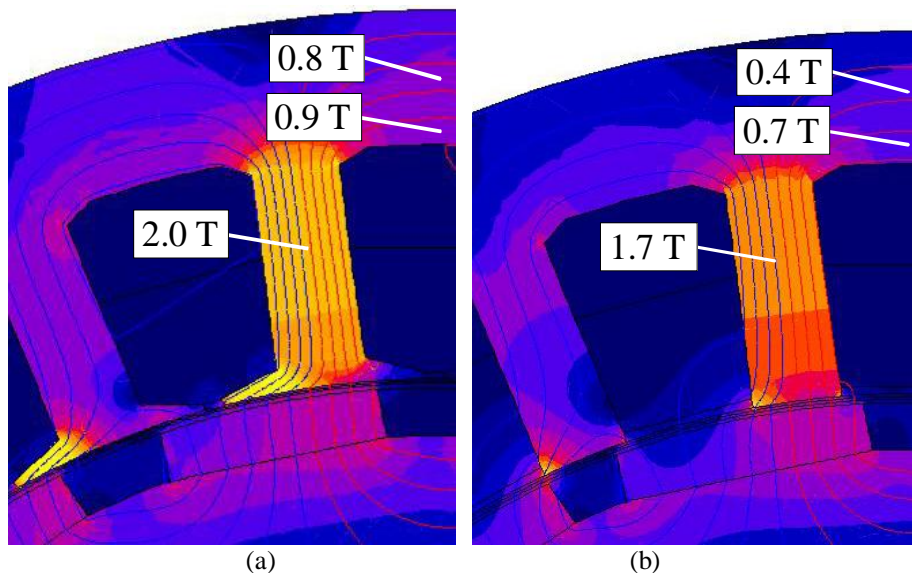


Fig. 1.2. Effect of wide and narrow tooth tips on the flux of otherwise similar machines. The flux paths and flux densities of a 24-slot 16-pole machine a) with semi-closed slots and b) with open slots are shown (Lindh et al. "Concentrated Wound PM Motors with Semiclosed Slots and with Open Slots." *IEEE Energy Conversion* (forthcoming)).

The only significant problem related to the design of open slot concentrated winding machines is that there can be large eddy current losses produced by the flux variations in the permanent magnets (Polinder and Hoeijmakers 1999, Toda et al. 2004). This is a problem especially when using sintered magnets. If, however, sintered NdFeB magnets are divided into several insulated sections (Polinder and Hoeijmakers 1999, Toda et al. 2004, Zhu et al. 2004, Deak et al. 2006, Ede et al. 2007, Deak et al. 2008), acceptable loss levels may be found, but the magnet configuration must be carefully analyzed to attain an acceptable eddy current loss level in the magnets. Plastic-bonded magnets, with a

maximum energy product of  $100 \text{ kJ/m}^3$  and a remanent flux density  $B_r$  of  $0.78 \text{ T}$  (Neorem Magnets, 2009), typically have very low eddy current losses (Kume et al. 2005, El-Rafaie and Jahns 2007, El-Rafaie and Jahns 2008), but other magnetic properties of such magnet materials available on the market are not satisfactory at the moment.

If eddy current losses in permanent magnets can be minimized thereby keeping the magnets at as low temperature as possible during machine operation, the open slot concentrated winding design can be very competitive and provide a new energy saving choice for industrial and many other purposes. The effect of temperature on the demagnetization characteristics of a typical NdFeB magnet made by NEOREM 495a / NEOREM 595a is shown in Fig. 1.3. When the operating temperature of the magnet is increased above a critical temperature and the demagnetizing field strength is large enough, it will result in irreversible demagnetization of the magnet. Such a situation may take place for instance during a sudden short circuit of the machine stator terminal. As industrial machines must tolerate such a situation, selection of the magnet material and motor design have to be carried out carefully taking this issue into account. NEOREM 495a tolerates a negative flux density at 100 degrees Celsius and about zero flux density at 150 degrees Celsius. Axial flux single stator designs have a large rotor yoke surface against cooling air, which usually results in a considerably cooler rotor than in a corresponding radial flux machine with an inner rotor. This makes the selection of the magnet material in a single-sided axial flux machine somewhat easier.

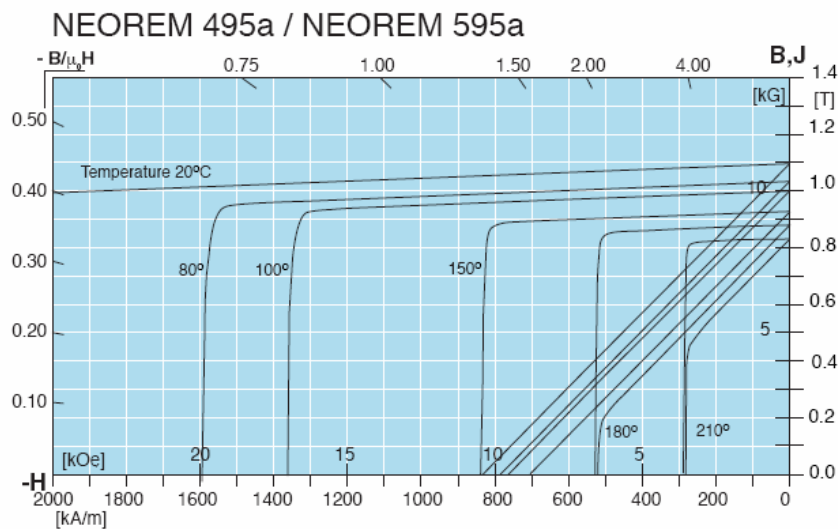


Fig. 1.3. Demagnetization characteristics of NEOREM 495a/NEOREM 595a NdFeB permanent magnet material at different temperatures (Neorem Magnets, 2009).

### 1.1 Harmonics of concentrated windings

In integral slot winding machines, the energy conversion process is related to the fundamental component of the flux density, which is produced by the interaction of the stator and rotor fundamental current linkages (Pyrhönen, Jokinen, Hrabovcová 2008). The concentrated winding machines, however, operate at some of the stator current linkage harmonics (Jokinen 1973, Atallah 2000). For instance in this case, we study the behaviour of a 12-slot 10-pole three-phase machine with the number of slots per pole and phase  $q = 0.4$ . Such a machine operates at the fifth harmonic, not the fundamental component of the flux density. The fundamental has a low winding factor and the flux related to the fundamental is, hence, low. In the theory of concentrated machines there seem to be two alternative approaches: Either the machine is really considered to operate at the fifth harmonic when all the harmonics of the machine are 1,  $-5$ ,  $+7$ ,  $-11$ ,  $+13$  and so on, or the fifth harmonic of the machine is denominated the fundamental when the real first harmonic is regarded as a sub-harmonic of the order  $-1/5$  (Zhu et al. 1991, Atallah et al. 2000, Ede et al. 2007). All the other harmonics of the machine are then treated accordingly.

As the 12-10-machine happens to produce harmonics of the same order as integral slot winding machines, it is easy to apply the traditional way of treating the harmonics similarly as in an integral slot winding machine. The 12-10 machine is regarded as a base machine having a base winding embedded in 12 stator slots and a rotor consisting of 10 permanent magnet poles with  $p = 5$ . When in a 12-stator slot concentrated winding three-phase machine  $p$  of the base winding is odd (in practice  $p = 5$  or  $p = 7$ ), the harmonics  $\nu$  of a three-phase machine ( $m = 3$ ) are according to the equation

$$\nu = 1 \pm 2km, \quad (1.2)$$

where  $k \in \mathbb{N}_0$ . Eq. (1.2) produces the harmonics  $\nu = [1, -5, +7, -11, +13, \dots]$  for the winding current linkage ordinals. In this case (12-slot 10-pole), the machine operates at the fifth harmonic  $\nu = -5$ . As a result, the fundamental  $\nu = +1$  rotates at a speed five times the speed of the fifth harmonic and in an opposite direction thus resulting in a rotor surface speed six times the rated electrical speed of the rotor. As the fundamental has a considerable amplitude, it is capable of inducing large rotor losses if the rotor has some conductivity. It is, of course, possible to build machines carrying multiple 12-10 base machines. For example 24-20 and 36-30 machines are possible, the former consisting of two base machines and the latter of three base machines. Each of these works, however, with the fifth harmonic of the base machine.

According to a more general approach the ordinals  $\nu$  of an  $m$ -phase concentrated winding base machine can be calculated by equation (Ede et al. 2002, Amara et al. 2005, Nakano et al. 2006)

$$\nu = 1 \pm km, \quad (1.3)$$

where  $k \in \mathbb{N}_0$ . Equation (1.3) produces the harmonics  $\nu = [1, -2, +4, -5, +7, \dots]$  for the winding current linkage ordinals of the three-phase machine. The machine always operates at the  $p^{\text{th}}$  harmonic of the base machine. For example in 12-10 or 12-14 machines, however, the even harmonics are cancelled because both the stator and rotor of the base machine can be symmetrically divided into two 180-degree sectors.

The winding factors will be observed next. The working harmonic winding factor  $k_{\text{wh}}$  of the machine has to be high and other harmonics should have low winding factors. The winding factor can be defined by a voltage vector graph (Pyrhönen, Jokinen, Hrabovcova 2008), or in simple cases, it can be solved from analytical equations. In general, the winding factor can be solved from

$$k_{\text{w}\nu} = k_{\text{p}\nu} \cdot k_{\text{d}\nu} \cdot k_{\text{sq}\nu}, \quad (1.4)$$

where  $k_{\text{p}\nu}$  is the pitch factor,  $k_{\text{d}\nu}$  is the distribution factor and  $k_{\text{sq}\nu}$  is the skewing factor for the harmonic  $\nu$ . In concentrated windings, obviously, the distribution factor  $k_{\text{d}\nu}$  cannot be simply defined for fractional slot windings with concentrated coils. The pitch factor  $k_{\text{p}\nu}$ , however, is defined in general as (Pyrhönen, Jokinen, Hrabovcova 2008)

$$k_{\text{p}\nu} = \sin\left(\nu \frac{W \pi}{\tau_p 2}\right) = \sin\left(\nu \frac{y \pi}{y_Q 2}\right) \quad (1.5)$$

where  $W$  is the coil width,  $y$  the winding step and  $y_Q$  the full step. For a concentrated base winding  $y = 1$  and  $2y_Q = Q$ . Hence, in such a case

$$k_{\text{p}\nu} = \sin\left(\frac{\nu\pi}{Q}\right). \quad (1.6)$$

This pitch factor is enough for single layer 12-10-machines and gives the winding factor for the working harmonic  $k_{\text{wh}} = 0.966$ . In double layer 12-10 machines, also the distribution factor is needed.

The skewing factor can be solved from the equation (Pyrhönen, Jokinen Hrabovcova 2008)

$$k_{sqv} = \frac{\sin\left(v \frac{s_{sq}}{\tau_p} \frac{\pi}{2}\right)}{v \frac{s_{sq}}{\tau_p} \frac{\pi}{2}}, \quad (1.7)$$

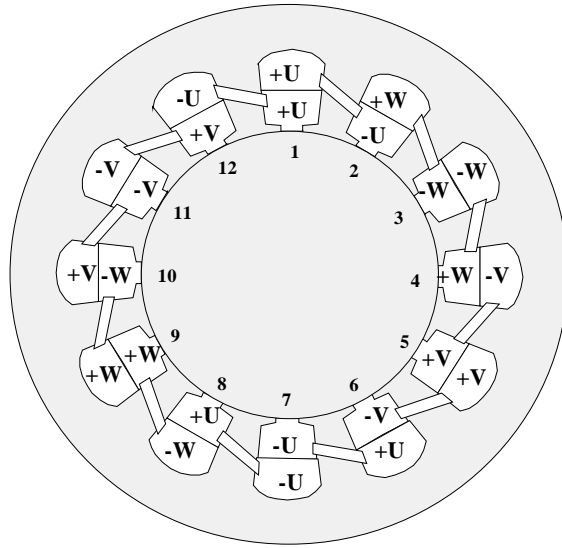
where  $s_{sq}/\tau_p$  is the skewing pitch ratio to the pole pitch. Skewing is used to minimize torque ripple.

As the definition of the distribution factor is not clear, we use the voltage phasor graph in solving the winding factors for the 12-10 two layer machine, Fig.1.4. As we now assume that – despite the five-pole-pair rotor – the winding produces a two pole fundamental wave, the machine has to be originally treated as a  $p = 1$  machine. The angle between the voltage phasors in the adjacent slots is given by expression

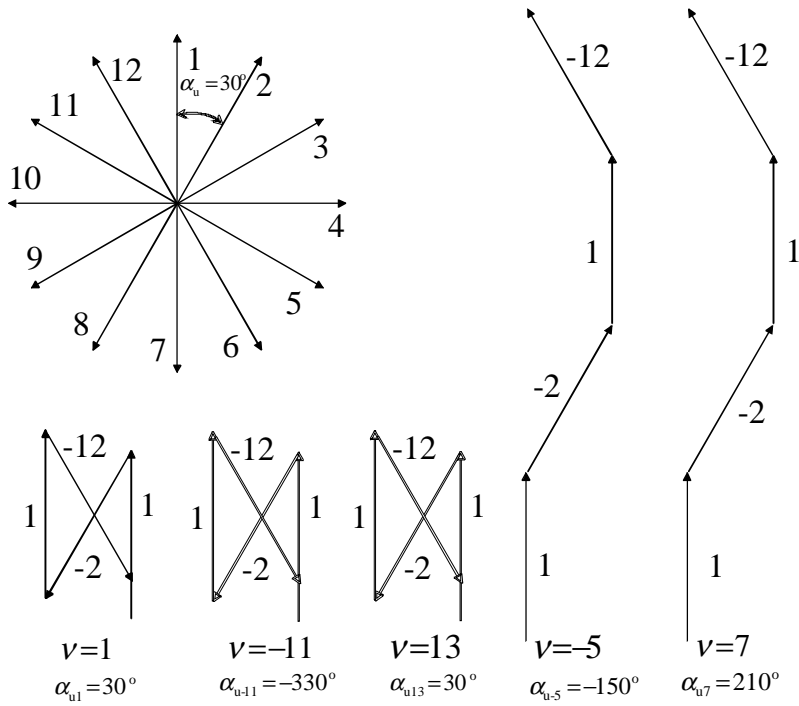
$$\alpha_u = \frac{v 360^\circ p}{Q}. \quad (1.8)$$

For the fundamental  $v = 1$  ( $p = 1$ ) the slot angle is

$$\alpha_u = \frac{1 \cdot 360^\circ \cdot 1}{12} = 30^\circ \quad (1.9)$$



a)



b)

Fig. 1.4. a) Winding arrangement of a 12-10-machine. b) Voltage phasor graph for the fundamental and sum phasors for different harmonics of the 12-10-two-layer winding for phase U located in slots 12-1 and 1-2.

The winding factors of the 12-10-machine are now found with the sum phasor graphs  $k_{w1} = (1 + 1 - \cos 30^\circ - \cos 30^\circ)/4 = 0.067$ ,  $k_{w-5} = 0.933$ ,  $k_{w7} = 0.933$ ,  $k_{w-11} = 0.069$ ,  $k_{w13} = 0.067$ ,  $k_{w-17} = 0.933$  etc. In this machine  $k_{w-5} = k_{wh}$ , which is the working harmonic of the machine.

As the pitch factors are in this case  $k_{p1} = 0.259$ ,  $k_{p-5} = -0.966$ ,  $k_{p7} = 0.966$ ,  $k_{w-11} = 0.259$ ,  $k_{w13} = 0.067$ ,  $k_{w-17} = 0.933$  and so on, the distribution factors should have the same values to produce the winding factor of the double-layer 12/10 machine windings.

Both forward- and backward-rotating harmonic current linkages that do not rotate in synchronism with the rotor may induce significant rotor eddy current losses. This is especially important in concentrated winding machines. To avoid the negative effects caused by the harmonics, the rotor should, in principle, have no conductivity at all – the rotor materials should be perfect insulators. The present-day sintered permanent magnets are far from insulators. NdFeB magnets have a resistivity varying between  $100\text{--}200 \times 10^{-8} \Omega\text{m}$  (Neorem 2009). Such resistivity values, being only from four to eight times the resistivity of normal construction steel, let large eddy currents run in bulky magnets, and hence, significant eddy current losses may take place in the magnets if no special efforts are made to prohibit the eddy currents from running.

The stator current linkage harmonics and the spatial harmonics caused by the stator slotting (permeance variations) cause variations of the magnetic field in the magnets. The permeance-harmonics-caused components of the rotor eddy-current losses depend on the width of the slot openings (Toda et al. 2004).

As in all normal three-phase motors, the multiples of the third harmonic field do not induce any back electromotive force (emf) harmonics in the line-to-line voltages of a three-phase machine, and hence, the third harmonic may be present in the phase voltage of the machine without causing adverse effects.

## 1.2 Scope of the work and outline of the thesis

This work done in Lappeenranta University of Technology is a follow-up to the research series concentrating on permanent magnet machines. Tanja Heikkilä (2002) studied multiple-pole buried V-magnets in radial flux machines and noticed that the torque density calculated with the machine outer dimensions can be considerably increased compared with a four-pole induction machine in the same frame. Panu Kurronen (2003) investigated torque quality and minimization of torque ripple in axial flux machines. Pia Salminen's work (2004) provided new information about the behaviour and characteristics of fractional slot radial flux machines. Asko Parviainen (2005) made a similar

study on different axial flux machines concentrating also on the thermal design of axial flux single rotor double stator machine. Janne Kinnunen (2007) examined damping properties and realization of damper windings in axial flux machines.

This work includes a number of main tasks related to the application of permanent magnets concentrated winding open slot machines. Suitable analytical methods are required for the first design calculations for a new machine. Concentrated winding machines differ from normal integral slot winding machines in such a way that adapted calculation methods are needed. To this end, a simple analytical model for calculating the concentrated winding axial flux machines is provided in this work. Determination of the magnetizing and leakage inductances for a concentrated winding machine differs slightly from traditional calculation methods. Torque production capability of concentrated winding machines with different pole pair numbers and compared with integral slot winding machines is studied in detail to show the potential of the machine type for different applications. The magnetic length of rotor surface magnet machines is studied and it is shown that the traditional methods have to be modified also in this respect. The results of this study are valid for all rotor surface permanent magnet machines without cooling ducts. An important topic in this study has been evaluating and minimizing the rotor permanent magnet Joule losses using segmented magnets in the calculations and experiments. On the other hand, a concentrated winding produces a large amount of harmonics – even sub-harmonics depending on the determination of the harmonic system. Such a winding is, in practice, suitable only for the permanent magnet synchronous machines because the rotor conductivity should be as low as possible – preferably zero (Magnussen and Lendenmann 2007, Pyrhönen, Jokinen, Hrabovcova 2008).

In this work, a prototype AFPM machine with concentrated windings, two stators and a single rotor is designed and measured. Four different prototype versions were used in the measurements: 1) a rotor with no magnets, 2) a rotor with bulky magnets, 3) a rotor with radially segmented magnets and 4) a rotor with tangentially segmented magnets (Figure 1.5). The two-stator-one-rotor design balances, in principle, the axial magnetic forces acting between the stators and the rotor.

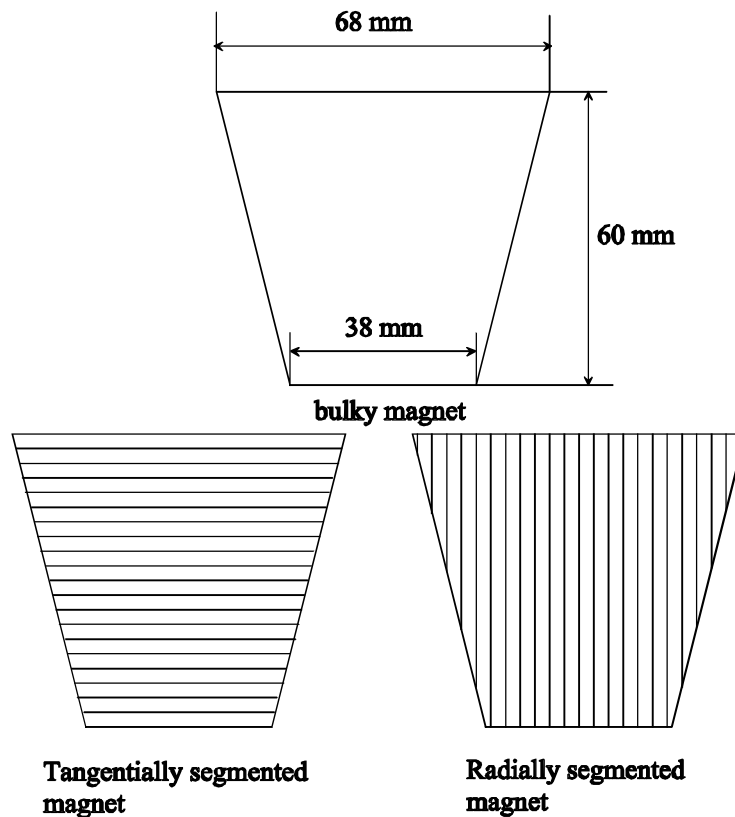


Fig. 1.5. Magnet versions, slicing directions.

- Chapter 2** The chapter introduces the equations to analytically calculate the correct mean radius and magnetic length of the axial flux concentrated winding machine. This is done to solve the inherently 3D axial flux machine problem as a two-dimensional flux problem. Air gap flux density, back-emf, magnetizing and leakage inductances, especially air gap leakage inductance, and rotor Joule losses are analyzed. 2D and 3D Finite Element Analysis (FEA) results are compared with each other and their analytical counterparts are verified.
- Chapter 3** The torque production capability of a concentrated winding machine with different slot-pole combinations is analyzed. A comparison between the pull-out torques of concentrated winding and integral slot winding machines is made and reported in detail.

- Chapter 4     The results determined by a 2D analytical approximation are compared with the 2D and 3D Finite Element Analysis (FEA) and measurements on different rotor topologies.
- Chapter 5     The final chapter summarizes the contributions of the work.

### 1.3 Scientific contributions of the work

The thesis has the following objectives:

1. Introduction of analytic equations and methods to design a 12-slot 10-pole axial-flux machine (or its multiple) with rotor-surface-mounted magnets.
2. Determination of the correct magnetic length of a PMSM with rotor surface magnets.
3. Determination of the stator leakage inductance, in particular the air gap leakage inductance in concentrated winding machines.
4. Comparison of the torque production capabilities of concentrated winding and integral slot winding machines.
5. Evaluation of the permanent magnet Joule losses in an axial flux PMSM with open slots.
6. Introduction of a new practical permanent magnet motor type for industrial use. The special features of the machine are due to the possibility of using concentrated winding and open slot winding constructions of PMSM at the normal speed range of industrial motors, for instance up to  $3000 \text{ min}^{-1}$ , without excessive rotor losses.

### 1.4 Most relevant scientific publications

The rated rotational speeds for the analyzed motors vary from  $400 \text{ min}^{-1}$  to  $3000 \text{ min}^{-1}$ . Concentrated winding radial and axial flux machines are used in calculations. Different slot-pole combinations are analyzed, the emphasis being on 12-slot 10-pole machines, which are investigated in detail. The most relevant publications are listed below.

Various low-speed high-torque permanent magnet synchronous motors with concentrated windings and with different slot and pole combinations were calculated analytically and by applying the finite element method (Flux2D™ by Cedrat) in publications P1–P6. All the calculated motors were radial flux machines with the same frame size of 225, air gap diameter, air gap length and the same amount of permanent magnet material. A speed of  $400 \text{ min}^{-1}$  and an output power of 45 kW were used. Comparisons of the torque ripple and the cogging torque, losses and pull-out torques were carried out. In publications

P4–P5, also the motor losses and torque capabilities in either open or semi-closed stator slots were compared. The differences of rotor surface magnets and embedded magnets were analyzed in publication P6. Publications P1 and P3 have been written by the author of this doctoral dissertation. In publication P1, Hanne Jussila essentially contributed to determination of the iron losses and stator inductances. In publication P3, Hanne Jussila played a key role in presenting the requirements that are usually set for desirable machine constructions and determination of the stator inductances of the machines. Publication P2 has been written by Pia Lindh (formerly Salminen). In this publication, Hanne Jussila contributed to the determination of the cogging torque values by analytical cogging torque equations. Publication P4 has been written by Pia Lindh. In this publication, Hanne Jussila contributed in particular to the analysis of Joule losses of permanent magnets. The publication P5 and P6 has also been written by Pia Lindh. In these publications, Hanne Jussila essentially contributed to determination of the losses.

**P1** Jussila, H., Salminen, P., Niemelä, M. and Pyrhönen, J. 2006. “Comparing Different Slot-Pole Combinations of a Concentrated-Winding Fractional-Slot Permanent-Magnet Machine.” In *Proceedings of the Nordic Workshop on Power and Industrial Electronics, NORPIE 2006*. Lund, Sweden. CD.

**P2** Salminen, P., Jussila, H., Niemelä, M. and Pyrhönen, J. 2006. “Torque Ripple and Cogging Torque of Surface Mounted PM Machines with Concentrated Windings.” In *Proceedings of the XVII International Conference on Electrical Machines, ICEM 2006*. Chania, Crete Island, Greece. CD.

**P3** Jussila, H., Salminen, P., Niemelä, M. and Pyrhönen, J. 2007. “Guidelines for Designing Concentrated Winding Fractional Slot Permanent Magnet Machines.” *International Conference on Power Engineering, Energy and Electrical Drives, POWERENG 2007*. Setúbal, Portugal. CD.

**P4** Salminen, P., Jussila, H., Niemelä, M. and Pyrhönen, J. 2008. “Concentrated Wound Permanent Magnet Motors with Different Pole Pair Numbers.” *IOS Press – Studies in Applied Electromagnetics and Mechanics*, Vol. 30, 2008, pp. 253–258.

**P5** Lindh, P., Pyrhönen, J., Parviainen, A., Jussila, H. and Niemelä, M. “Concentrated Wound PM Motors with Semiclosed Slots and with Open Slots.” *IEEE Energy Conversion*. Forthcoming.

**P6** Lindh, P., Jussila, H., Niemelä, M., Parviainen, A. and Pyrhönen, J. 2009. “Comparison of Concentrated Winding Permanent Magnet Motors with Embedded Magnets and Surface-Mounted Magnets.” *IEEE Transactions on Magnetics*. Vol. 45, Issue 5, May 2009, pp. 2085–2089.

Publication P7 addresses concentrated winding permanent magnet motors and their ability to produce torque. Further, torque comparisons for integral slot winding machines were made. The inductances and the maximum available torque of a concentrated winding PM machine were examined as the pole pair number and the number of slots per pole and phase  $q$  were varied within compatible constraints. The machines under study had a 45 kW output power and a speed of  $400 \text{ min}^{-1}$ . The results show that as  $q$  increases from 0.25 to 0.5, the pull-out torque of the concentrated winding machine increases, obtaining the highest values when  $q$  equals to 0.5. However, as  $q$  increases further and integral slot windings ( $q = 1$ ,  $q = 2$ ) are used, the torque development will be higher when the same rotor main dimensions are maintained. This indicates that the selection of a concentrated winding construction must have other relevant reasons than maximizing the rotor torque per volume ratio. Finite element analysis (Flux2D/3D™ by Cedrat) and analytical equations were used in calculations. The author of this doctoral dissertation has been the first author in this publication. Hanne Jussila contributed in particular to determination of the stator inductances and the maximum available torques of the machines.

**P7** Jussila, H., Salminen, P., Niemelä, M., Parviainen, A. and Pyrhönen, J. 2007. “Torque and Inductances of Concentrated Wound Permanent Magnet Machines.” *International Review of Electrical Engineering (I.R.E.E.)*. Vol. 2, No. 5, September–October 2007, pp. 704–710.

Publications P8–P10 focus on the iron losses and the eddy-current losses of the magnets in concentrated winding PM machines. Publication P8 deals with loss calculations of low-speed,  $400 \text{ min}^{-1}$ , 45 kW permanent magnet synchronous motors with concentrated windings. The eddy-current losses in permanent magnets of  $3000 \text{ min}^{-1}$ , 18.5 kW radial flux permanent magnet synchronous motors with concentrated windings are reported in publication P9. Different geometries and materials, such as open and semi-closed slots, different air gap lengths, sintered and plastic-bonded Neo-magnets were evaluated. In addition, the effects of a semi-magnetic slot wedge on the losses were analyzed. The eddy-current losses in the magnets of a  $2500 \text{ min}^{-1} / 3000 \text{ min}^{-1}$ , 37 kW axial flux permanent magnet synchronous motor with concentrated windings are reported in publication P10. Different magnet materials, such as plastic-bonded Neo-magnets and sintered segmented NdFeB-magnets were evaluated.

Analytical Matlab™ and finite-element-method-based (Flux2D/3D™ by Cedrat) programs were used in the calculations. The author of this doctoral dissertation has been the first author in all the publications below. Hanne Jussila has essentially contributed to determination the eddy-current losses in permanent magnets.

**P8** Jussila, H., Salminen, P. and Pyrhönen, J. 2006. “Losses of a Permanent Magnet Synchronous Motor with Concentrated Windings.” In *Proceedings of the 3<sup>rd</sup> International Conference on Power Electronics, Machines and Drives, PEMD 2006*. Dublin, Ireland, pp. 207–211.

**P9** Jussila, H., Salminen, P., Pyrhönen J. and Parviainen, A. 2007. “Permanent Magnet Eddy-current losses in concentrated winding 12-slot-10-pole machines.” In *Proceedings of International Symposium on Electromagnetic Fields in Mechatronics, Electrical and Electronic Engineering, ISEF 2007*. Prague, Czech Republic. CD.

**P10** Jussila, H., Salminen, P., Parviainen, P., Nerg, J. and Pyrhönen, J. 2008. “Concentrated Winding Axial Flux Permanent Magnet Motor with Plastic Bonded Magnets and Sintered Segmented Magnets.” In *Proceedings of the XVIII International Conference on Electrical Machines, ICEM 2008*. Vilamoura, Portugal. CD.

## 2 ANALYTICAL METHODS FOR CALCULATION OF AXIAL FLUX CONCENTRATED WINDING PM MACHINES

This chapter addresses the analytical design method of concentrated winding axial flux permanent magnet machines. First, the air gap flux density, with a special emphasis on slot effects, is analyzed. Secondly, the torque production capability of the machine as a part of the synchronous inductance  $L_d$  calculation is addressed. The last main object is to analyze some calculation methods for losses of the concentrated winding multiphase PM machine, with a special reference to Joule losses of PMs.

Analytical methods are used in everyday basic machine design because they are fast and easily produce the first practical dimensions of the desired machine. Each design type, however, has its special features, and hence, new analytical machine design tools are frequently needed. For example, in this case, the target is to analyze concentrated winding multiphase machines, which call for a different approach compared with traditional machine design. Numerical methods are used together with analytical ones to refine the design.

In the calculations and measurements, a 37 kW, 2400 min<sup>-1</sup>, 12-slot 10-pole prototype axial flux motor is used as a base reference (Machine 1). The prototype machine has two stator stacks with one internal, ironless rotor disc, two-layer concentrated windings (two coil sides share each slot vertically) and rotor surface magnets. In the two-layer winding, the slots are divided vertically because it minimizes the length of the end windings (Salminen 2004). Other reference machines for calculation are concentrated winding radial flux machines with an output power of 45 kW and a speed of 400 min<sup>-1</sup> (Machine 2; Salminen 2004). In order to verify the analytical results obtained by the calculation, 2D and 3D FEA are performed. The finite element analysis program used in the computations is a Flux2D/3D version 10.2.4 by Cedrat. Finally, a comparison of the experimental results for a prototype machine is presented in Chapter 4. The main parameters of the machines are presented in Table 2.1.

Table 2.1. Main parameters.

Parameter	Machine 1	Machine 2
Machine type	axial flux; two stator, one rotor	radial flux; inner rotor
Output power $P_{out}$	37 kW	45 kW
Rotational speed $n_s$	2400 min <sup>-1</sup>	400 min <sup>-1</sup>
Stator outer diameter $D_o$	274 mm	364 mm
Stator inner diameter $D_i$	154 mm	254 mm
Length of stator stack $l_{Fe}$	75 mm	270 mm
Air gap length $\delta$	2 mm	1.2 mm
Number of stator slots $Q$	12	12, 18, 24, 36
Number of rotor poles $2p$	10	8–84

## 2.1 Modelling of concentrated winding axial flux machines

Analytical methods are needed for the base calculations of the machines, while 2D or 3D FEA are required for more accurate calculation. In particular, in concentrated winding axial flux machines, the base calculation should be accurate, because concentrated winding machines do not necessarily have a similar magnetic symmetry as integral slot winding machines, and therefore, 2D or 3D finite element modelling and calculation are time consuming. Because of the magnetic similarity of every pole, it is possible to model integral slot winding machines by modelling only one pole or one pole pair. In concentrated winding machines, the possible symmetrical parts depend on slot and pole combinations as it is shown in Table 2.2.

Table 2.2. Some slot-pole combination and symmetries for concentrated winding machines.

Slots/Poles	Smallest slots/poles combination	Symmetry parts
9/8	-	1
12/8	3/2	4
12/10	6/5	2
12/14	6/7	2
12/16	3/4	4
21/20	-	1
24/16	3/2	8
24/20	6/5	4
24/22	12/11	2
24/26	12/13	2
24/28	6/7	8

Table 2.2 shows that there are machines that have to be modelled entirely or at least half of the machine has to be modelled by the FEA. Figure 2.1 illustrates the flux routes that display the symmetry of a radial flux 12-slot 10-pole machine.

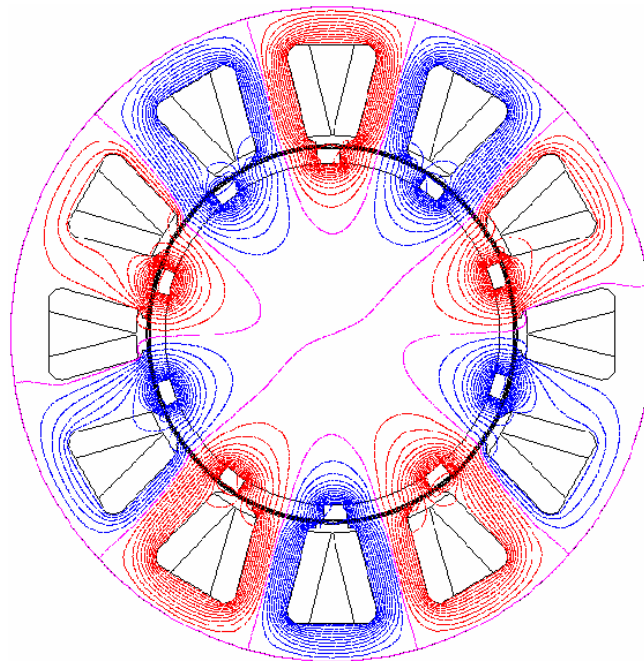


Fig. 2.1. Flux paths of a 12-slot 10-pole radial flux machine. The machine can be divided only into two magnetically symmetric parts. It means that there are five different flux paths in different poles.

The axial flux machine can be calculated analytically or by 2D FEA tools using the geometric mean radius (Valtonen 2007) or the arithmetic mean radius (Gieras et al. 2008) as a design plane. The 2D modelling of the machine can be carried out by introducing a radial cutting plane at the geometric or arithmetic mean radius, which is then developed into a 2D radial flux machine (or linear machine) model. Either a geometric or arithmetic mean radius is used in different references (Valtonen 2007, Gieras et al. 2008). The geometric mean radius  $r_{\text{geom, mean}}$  can be calculated as

$$r_{\text{geom, mean}} = \sqrt{r_{\text{o, axial}} r_{\text{i, axial}}} , \quad (2.1)$$

where  $r_{\text{o, axial}}$  is the outer radius and  $r_{\text{i, axial}}$  the inner radius of the axial flux machine. In the literature, the arithmetic mean of the air gap radius is also used as a design plane. For example Gieras et al. (2008) recommend the use of arithmetic mean  $r_{\text{av, mean}}$

$$r_{\text{av, mean}} = \frac{r_{\text{o, axial}} + r_{\text{i, axial}}}{2} \quad (2.2)$$

in the calculation. If the geometric or arithmetic mean radius is used, the magnet width to pole pitch ratio in an axial flux machine should be constant at different radii and the stator should not be skewed. These methods are suitable for power, voltage and cogging torque calculation, but they are not accurate enough for iron losses calculation, and at least Quasi-3D is required (Parviainen 2005).

In principle, the rotor torque could be calculated using Fig. 2.2.

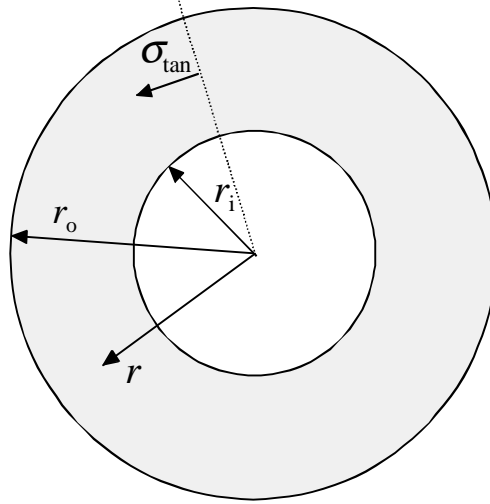


Fig. 2.2. Calculating the disk rotor torque.

The tangential force producing torque can be described if we assume the same average tangential stress  $\sigma_{\tan}$  at a certain radius  $r$

$$F_{\tan} = \sigma_{\tan} 2\pi r dr. \quad (2.3)$$

If we use the working components of the linear current density  $A_{\text{wh}}$  and the air gap flux density  $B_{\text{n,wh}}$ , the tangential stress is found for  $\cos\varphi = 1$  (overlapping  $B$  and  $A$  components) as given by (Pyrhönen, Jokinen, Hrabovcová 2008)

$$\sigma_{\tan}(x) = \hat{B}_{\text{n,wh}} \sin(x) \hat{A}_{\text{wh}} \sin(x), \quad (2.4)$$

and the average tangential stress becomes

$$\bar{\sigma}_{\tan}(x) = 0.5 \hat{B}_{\text{n,wh}} \hat{A}_{\text{wh}} \quad (2.5)$$

In axial flux machines, however, the linear current density depends on the radius and decreases as the radius increases.

In principle, the peak value of the linear current working component density is obtained by dividing the peak value of the slot current by the slot pitch, also taking into account the winding factor  $k_{\text{w,wh}}$  of the working harmonic. If the number of slots per pole and phase is  $q$ , the number of coil turns is  $N_s$ , the

number of phases is  $m = 3$ , and the number of slots is  $Q$ , we obtain the effective peak current of the slot from the equation

$$\hat{i}_u = \frac{k_{w,wh} N_s \hat{i}_s}{q}, \quad (2.6)$$

where  $i_s$  is stator current. The slot pitch is

$$\tau_u = \frac{2\tau_p}{Q/p}. \quad (2.7)$$

Since in a three-phase machine, there is a connection between the number of slots per pole and phase  $q$  and the number of slots  $Q$

$$Q = m2pq = 6pq, \quad (2.8)$$

based on the dimensions of the winding, we obtain for the linear current density

$$\hat{A}_{wh} = \frac{3k_{w,wh} N_s \hat{i}_s}{p\tau_p}. \quad (2.9)$$

As the pole pitch is

$$\tau_p = \frac{2\pi r}{2p}, \quad (2.10)$$

we see that the linear current density is inversely proportional to the radius  $r$ .

$$\hat{A}_{wh} = \frac{3k_{w,wh} N_s \hat{i}_s}{\pi r}. \quad (2.11)$$

If we assume the working component of the flux density to be independent of the radius, we can write for the torque producing tangential stress

$$\bar{\sigma}_{\tan}(x) = 0.5\hat{B}_{n,wh}\hat{A}_{wh} = 0.5\hat{B}_{n,wh}\frac{3k_{w,wh}N_s\hat{i}_s}{\pi r} \quad (2.12)$$

We now get for the torque

$$dT = F_{\tan} r = \sigma_{\tan} 2\pi r^2 dr =$$

$$= 0.5\hat{B}_{n,wh} \frac{3k_{w,wh} N_s \hat{i}_s}{\pi r} 2\pi r^2 dr = \hat{B}_{n,wh} 3k_{w,wh} N_s \hat{i}_s r dr \quad (2.13)$$

The total torque of the disk side is

$$T = \int_{r_i}^{r_o} \hat{B}_{n,wh} 3k_{w,wh} N_s \hat{i}_s r dr = \hat{B}_{n,wh} \frac{3}{2} k_{w,wh} N_s \hat{i}_s (r_{o,axial}^2 - r_{i,axial}^2) \quad (2.14)$$

In the case of two stators, the torque found by Eq. (2.14) must be multiplied by 2.

The linear current density at the arithmetic mean radius is

$$\hat{A}_{wh,ar,mean} = \frac{3k_{w,wh} N_s \hat{i}_s}{\pi \frac{r_{i,axial} + r_{o,axial}}{2}}, \quad (2.15)$$

and at the geometric mean radius, the linear current density is

$$\hat{A}_{wh,geom,mean} = \frac{3k_{w,wh} N_s \hat{i}_s}{\pi \sqrt{r_{i,axial} r_{o,axial}}}. \quad (2.16)$$

Now we get for the average stresses

$$\bar{\sigma}_{tan,ar,mean} = 0.5\hat{B}_{n,wh} \hat{A}_{wh,ar,mean} = 0.5\hat{B}_{n,wh} \frac{3k_{w,wh} N_s \hat{i}_s}{\pi \frac{r_{i,axial} + r_{o,axial}}{2}} \quad (2.17)$$

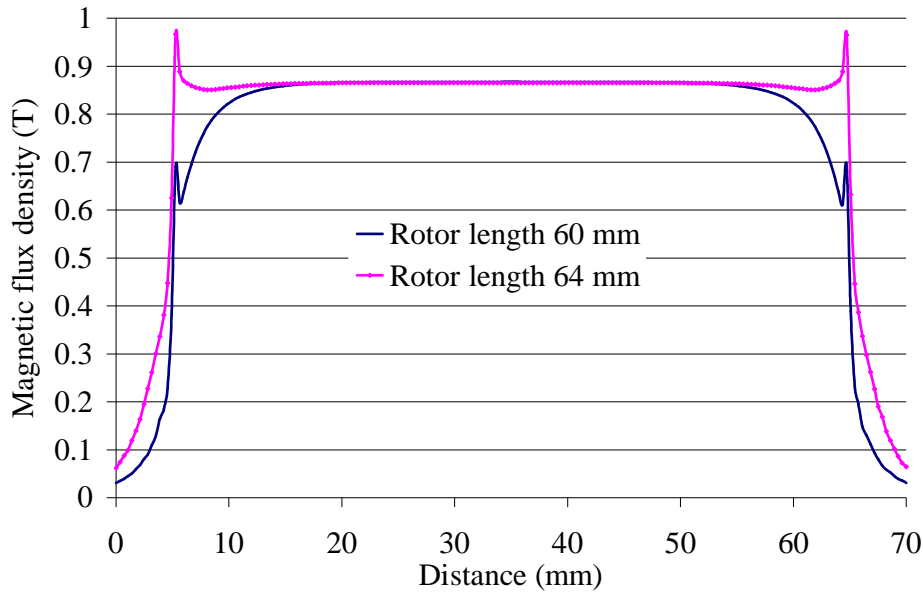
$$\bar{\sigma}_{tan,geom,mean} = 0.5\hat{B}_{n,wh} \hat{A}_{wh,geom,mean} = 0.5\hat{B}_{n,wh} \frac{3k_{w,wh} N_s \hat{i}_s}{\pi \sqrt{r_{i,axial} r_{o,axial}}} \quad (2.18)$$

The corresponding torque values, if  $S$  is used for the disk surface, become

$$T_{ar,mean} = r_{ar,mean} S \bar{\sigma}_{tan,ar,mean} \quad (2.19)$$

or





e)

Fig. 2.3. Flux behaviour produced by the rotor and the stator in PM machines. a) Principal permanent magnet flux behaviour when the magnet and the rotor iron are of equal length with the stator stack. The PM leakage flux is significant at the motor ends. b) The magnets and the possible rotor stack are made longer than the stator stack, and significantly more flux is obtained in the stator. c) Flux generated by the armature; there is some armature leakage at the ends. The armature flux at the ends of the motor bypassing the magnets does not produce torque in a rotor surface magnet machine with no reluctance differences and may, hence, be regarded as leakage flux. This flux can be regarded as leakage flux as the permanent magnet current linkage does not reach beyond the rotor ends. d) The armature leakage is minimized when the magnets are long and more torque is produced. e) 2D FEA-calculated permanent magnet normal flux density behaviour on the stator surface in the test machine with different magnet lengths. In In Fig. 2.3e the flux density produced by the permanent magnet in the middle of the stator length (35 mm) remains the same in the case of a long magnet compared with a short magnet. The flux density integral is larger with long magnets.

In case 2.3a, the stator and permanent magnet lengths are equal (60 mm), and in case 2.3b, the rotor PM lengths are selected to be  $l_{Fe} + 2\delta = 64$  mm. The effective 2D FEA-calculated electrical length from the viewpoint of the permanent magnet flux is 57.9 mm in the first case (96.5 % of the stator length), and in case 2.3b 61.4 mm (102.3 % of the stator length). The stator lamination is located between 5 mm and 65 mm and its length is, hence, 60 mm. This result corresponds well to the results found by the 3D finite element analysis. When comparing the measurement results and the 3D FEA results, it seems that in analytic calculation, for security, one could select for the effective rotor length only  $l' = l_{Fe} - 2\delta$ . This value does not give too optimistic results to the torque

and back-emf. The practical measurements in this case confirm that the analytic calculations give the best results when  $l' = l_{Fe} - 2\delta = 56$  mm is selected for the rotor length.

The traditional advice of calculating the effective length  $l' = l_{Fe} + 2\delta$  is given for instance in (Pyrhönen, Jokinen, Hrabovcová 2008). This equation is valid for machines having stator and rotor current linkages longer than the lamination stacks. It is, however, not valid for rotor surface permanent magnet machines unless the permanent magnets are considerably longer than the stator stack. This can be easily understood as in traditional machines the stator and rotor current linkages reach beyond the stator and rotor stacks as the windings have to travel straight towards the end windings. In the case of permanent magnet excitation and equally long PM and  $l_{Fe}$ , the PM and armature leakages make the machine rotor current linkage look shorter as it was shown above. In the case of the test machine studied in this thesis, the traditional equation  $l' = l_{Fe} + 2\delta$  could be used if the rotor and permanent magnet lengths were  $l_{Fe} + 4\delta$ , which in this case would mean that the rotor should be 68 mm long while the stator lamination is 60 mm long and the air gap is 2 mm. The observation of the PM machine rotor length is important as it gives practical guidelines for motor designers in selecting the permanent magnet dimensions.

The above observation also shows a new source for the stator leakage. When calculating the stator magnetizing inductance,  $l' = l_{Fe} + 2\delta$  can be used, but the flux in the end areas of the stator does not effectively participate in the energy conversion, and should hence be regarded as leakage flux, Fig. 2.3c. Thus, the length of the magnets affects the leakage of the machine at least in principle, because lengths of about  $1.5\delta$  (Fig. 2.3e) at both ends of the stator (subtracted from the traditional effective length  $l' = l_{Fe} + 2\delta$ ) do not take part in the torque production but carry flux, which is traditionally considered the main flux but changes here to leakage. Hence, the magnetizing inductance should be calculated by  $l' = l_{Fe} - 2\delta$ .

When both the stator lamination stack and the rotor permanent magnets have an equal length of 60 mm, the rotor magnets are seen as 56 mm long. Thus, when calculating the stator magnetizing inductance, the value of 56 mm should be used. By applying  $l' = l_{Fe} + 2\delta$  in the calculation of the stator magnetizing inductance, the proportion  $l_{Fe} + 2\delta - (l_{Fe} - 2\delta) = 4\delta$  of the magnetic length of the traditional stator length produces leakage instead of magnetizing inductance.

In analytical calculation, it seems that when calculating with the geometric mean radius, the errors made in the calculation of the length when using  $l_{Fe}$

compensate each other and a good result for the torque is found. This, however, is somewhat an erroneous method as the above study has shown. The correct way of performing the analytical calculation could be to use the arithmetic mean radius and take the PM leakage into account by shortening the effective stack length in the case of magnets of equal length. If the magnets are made longer than the stator stack, it is possible to directly apply the arithmetic mean radius and the real length of the stack in the calculation or to increase the effective lamination length even further if the magnets are long compared with the stator stack.

Figure 2.4 shows the comparison between the 2D and 3D FEA induced voltage over one pole pitch. The 2D FEA calculation uses either the geometric or arithmetic mean radius as a design plane.  $l_{Fe}$  is used as the length of the stator stack.

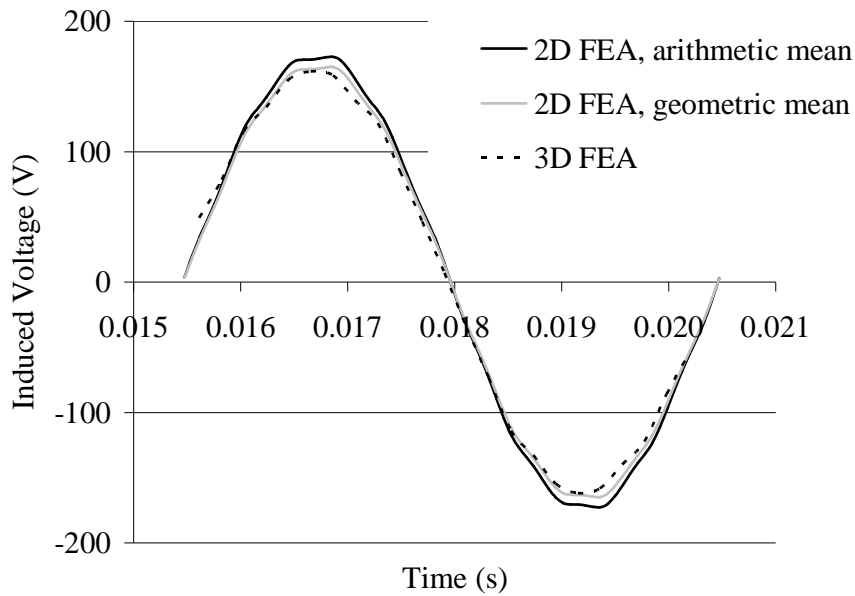


Fig. 2.4. Induced back-emf voltage over one pole pitch with the geometric mean radius (2D FEA using  $l' = l_{Fe}$ ), the arithmetic mean radius (2D FEA) and the 3D FEA.

In this case, using the geometric mean radius seems to compensate the error made in the flux leakage at the ends of the rotor, and the calculation results of 3D and 2D calculations will be the same.

We can see in Fig. 2.4 that the 2D FEA result using the geometric mean radius and  $l_{Fe}$  as the stator length has a good agreement with the 3D FEA result. The

arithmetic mean radius with the 2D FEA and  $l' = l_{Fe}$  results in a greater flux than the geometric radius with 2D or 3D. In this study, the arithmetic mean radius is used as a design plane from now on, and the effective length of the stator stack seen from the rotor is reduced according to the previous study  $l' = l_{Fe} - 2\delta$ . The arithmetic mean radius can be used, because the magnet width to the pole pitch ratio in the axial flux machine studied is kept constant at different radii. The induced back electromagnetic forces seem to be in good agreement with radial and axial flux machines when using the arithmetic mean radius as a design plane in 2D and the reduced effective stack length (Fig. 2.5).

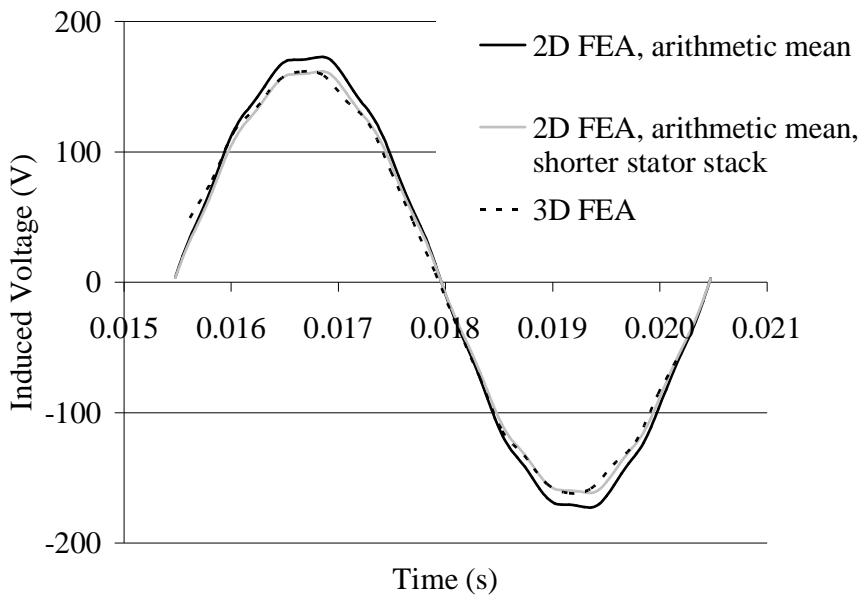


Fig. 2.5. Induced back-emf voltage over one pole pitch with the arithmetic mean radius (2D FEA using  $l' = l_{Fe}$ ), the arithmetic mean radius (2D FEA using  $l' = l_{Fe} - 2\delta$ ) and the 3D FEA.

Axial flux machines could also be calculated applying analytical or 2D tools by replacing the actual 3D analysis by a number of 2D analyses as Parviainen (2005) and Kurronen (2003) did. From the quasi-3D modelling point of view, the axial flux PM machine can be considered to be composed of several linear machines (without end effects) connected in parallel. The overall performance of the axial flux machine is obtained by summing the performance of individual linear machines. The approach allows taking into account different magnet shapes and variation of tooth width in the direction of the machine radius (Parviainen 2005).

## 2.2 Analytical calculation of the magnetic flux density in the air gap

The air gap magnetic field distribution of rotor surface magnet axial-flux permanent magnet motors can be analyzed using Zhu et al. (2002) analytical solution. The model presented by Zhu et al. (2002) is an improved model of the analytical solution by Zhu et al. (1993). The solution is made for concentrated winding radial flux PM machines for a non-slotted stator applying 2D polar coordinate technique. The model is simplified using the following assumptions (Zhu et al. 2002): 1) Permanent magnets have a linear demagnetization characteristic, and are fully magnetized in the direction of magnetization. 2) End-effects are neglected. 3) The stator and rotor back-irons are infinitely permeable. The open-circuit air gap flux density distribution for a PM motor equipped with radially or parallel magnetized magnets is presented as

$$B_{\text{PM}}(r, \theta) = \sum_{v=1,3,5,\dots}^{\infty} \frac{\mu_0 M_v}{2\mu_{\text{r,PM}}} \frac{vp}{(vp)^2 - 1} \cdot \left[ \frac{(A_{3v} - 1) + 2\left(\frac{r_r}{r_{\text{PM}}}\right)^{vp+1} - (A_{3v} + 1)\left(\frac{r_r}{r_{\text{PM}}}\right)^{2vp}}{\frac{(\mu_{\text{r,PM}} + 1)\left[1 - \left(\frac{r_r}{r_i}\right)^{2vp}\right] - (\mu_{\text{r,PM}} - 1)\left[\left(\frac{r_{\text{PM}}}{r_i}\right)^{2vp} - \left(\frac{r_r}{r_{\text{PM}}}\right)^{2vp}\right]}{\mu_{\text{r,PM}}}} \right] \cdot \left[ \left(\frac{r_\delta}{r_i}\right)^{vp-1} \left(\frac{r_{\text{PM}}}{r_i}\right)^{vp+1} + \left(\frac{r_{\text{PM}}}{r_\delta}\right)^{vp+1} \right] \cos(vp\theta). \quad (2.21)$$

$$M_v = \begin{cases} \frac{B_r}{\mu_0} \alpha_{\text{PM}} (A_{1v} + A_{2v}) + vp \frac{B_r}{\mu_0} \alpha_{\text{PM}} (A_{1v} - A_{2v}) \\ \text{for parallel magnetization,} \\ 2 \frac{B_r}{\mu_0} \alpha_{\text{PM}} \frac{\sin\left(\frac{v\pi\alpha_{\text{PM}}}{2}\right)}{\frac{v\pi\alpha_{\text{PM}}}{2}} \\ \text{for radial magnetization.} \end{cases} \quad (2.22)$$

$$A_{1v} = \frac{\sin\left[(vp+1)\alpha_{PM}\frac{\pi}{2p}\right]}{(vp+1)\alpha_{PM}\frac{\pi}{2p}}, \quad (2.23)$$

$$A_{2v} = \frac{\sin\left[(vp-1)\alpha_{PM}\frac{\pi}{2p}\right]}{(vp-1)\alpha_{PM}\frac{\pi}{2p}}, \quad (2.24)$$

$$A_{3v} = \begin{cases} \left(vp - \frac{1}{vp}\right) \frac{M_{rv}}{M_v} + \frac{1}{vp} & \text{for parallel,} \\ vp & \text{for radial,} \end{cases} \quad (2.25)$$

$$M_{rv} = \begin{cases} \frac{B_r}{\mu_0} \alpha_{PM} (A_{1v} + A_{2v}) & \text{for parallel,} \\ 2 \frac{B_r}{\mu_0} \alpha_{PM} \frac{\sin\left(\frac{v\pi\alpha_{PM}}{2}\right)}{\frac{v\pi\alpha_{PM}}{2}} & \text{for radial,} \end{cases} \quad (2.26)$$

$$\alpha_{PM} = \frac{b_{PM}}{\tau_p}, \quad (2.27)$$

where  $B_r$  is the remanent magnet flux density,  $\mu_{r,PM}$  is the permanent magnet relative permeability,  $\alpha_{PM}$  is the ratio of the magnet width to the pole pitch and  $\delta$  is the physical air gap length,  $r_i$  is the stator inner radius,  $r_r$  the rotor radius,  $r_{PM}$  the magnet radius and  $r_\delta$  the air gap radius. Figure 2.6 shows the comparison of the air gap flux densities applying the analytical method and 2D FEA.

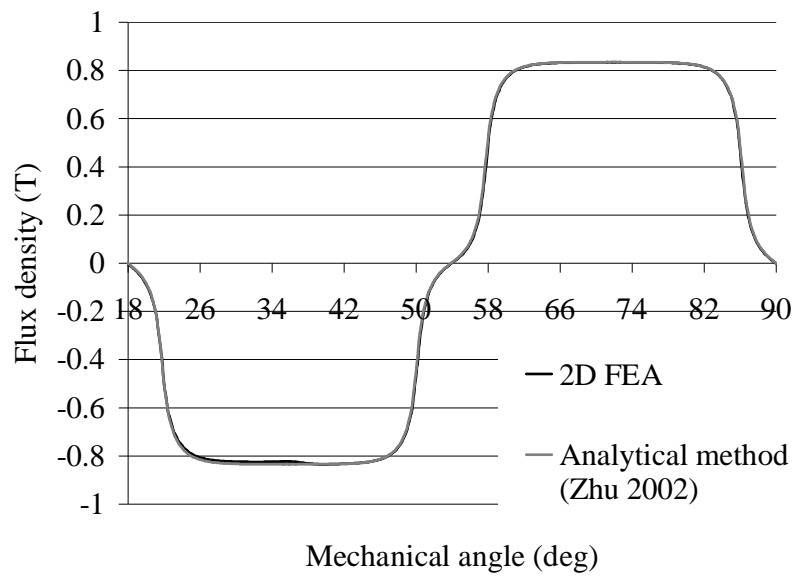


Fig. 2.6. Comparison of the air gap flux densities using the analytical method (Zhu et al. 2002) and 2D FEA. A good match is seen.

Similar comparison is made for the air gap flux densities calculated by the 2D and 3D FEA, Fig. 2.7.

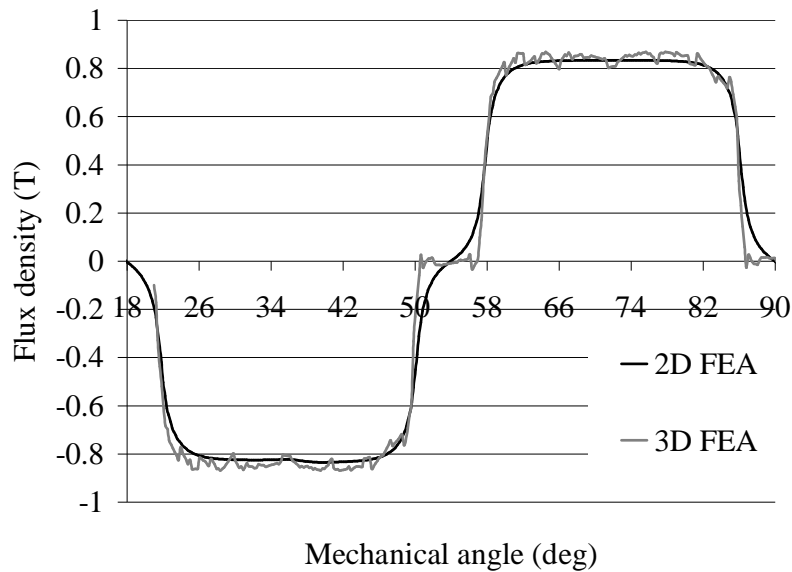


Fig. 2.7. Comparison of the air gap flux densities by the 2D and 3D FEA. The coarse form of the 3D result is a consequence of sparse elements.

Figures 2.6 and 2.7 show that the presented analytical estimation and the 2D FEA give quite a good estimation for the air gap flux density of a concentrated winding axial flux machine with a smooth air gap.

### 2.2.1 Slotting effect

The effect of the stator slots on no-load magnetic field distribution is investigated. The air gap flux density always drops at stator slot openings, and this effect has a significant influence on the values of the flux and the induced voltage in the analytical calculation. For this reason, it is important to accurately model the air gap flux density. Accurate calculation of the stator slotting effect is also needed for calculating the possible cogging torque, Joule losses in PMs, vibration, noise and forces affecting the windings, teeth and the yoke.

In 1993, Zhu and Howe introduced two-dimensional relative permeance functions, which take into account the effects of stator slotting in the air gap flux density. The equation is based on the relative permeance function presented by Heller and Hamata (1977). The specific slot permeance variation due to the stator slots and a smooth rotor is written according to Zhu and Howe (1993) as

$$\lambda(\alpha, r) = \begin{cases} A_0 \left[ 1 - \beta(r) - \beta(r) \cos\left(\frac{\pi}{0.8\alpha_0} \alpha\right) \right] & \text{for } 0 \leq \alpha \leq 0.8\alpha_0 \\ A_0 & \text{for } 0.8\alpha_0 \leq \alpha \leq \alpha_t/2 \end{cases} \quad (2.28)$$

where the air gap flux density is assumed to vary with the circumferential coordinate  $\alpha$ ,  $A_0 = \mu_0 / \delta_{\text{PM}}$ ,  $\alpha_0 = b_1/r_i$ ,  $\alpha_t = \tau_u/r_i$ , where  $b_1$  is slot opening width. The air gap is defined here as

$$\delta_{\text{PM}} = \delta + \frac{h_{\text{PM}}}{\mu_{r,\text{PM}}}, \quad (2.29)$$

where  $h_{\text{PM}}$  is the height of permanent magnet. The function  $\beta(r)$  is defined at the axis of a stator slot, and it depends on the radial position. The function  $\beta(r)$  using the Schwarz–Christoffel (SC) conformal mapping technique is defined as

$$\beta(r) = \frac{1}{2} \left[ 1 - \frac{1}{\sqrt{1 + \left(\frac{b_1}{2\delta_{\text{PM}}}\right)^2 (1 + v^2)}} \right]. \quad (2.30)$$

The coefficient  $v$  is iterated from

$$\frac{1}{2} \ln \frac{\sqrt{a^2 + v^2} + v}{\sqrt{a^2 + v^2} - v} + \frac{2\delta_{\text{PM}}}{b_1} \arctan \frac{2\delta_{\text{PM}}}{b_1} \frac{v}{\sqrt{a^2 + v^2}} = y \frac{\pi}{b_1}, \quad (2.31)$$

where

$$a^2 = 1 + \left(\frac{2\delta_{\text{PM}}}{b_1}\right)^2 \quad (2.32)$$

and  $y$  is given as

$$y = r - r_i + \delta_{\text{PM}} \quad (2.33)$$

Figs. 2.8 and 2.9 show the results of the analytical model and the 2D FEA.

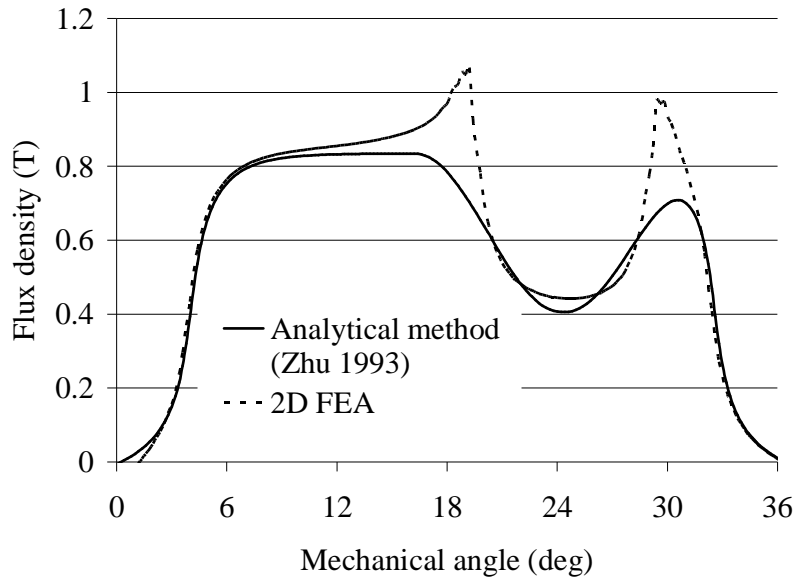


Fig. 2.8. Slotting effect applying the Zhu and Howe method (1993) and the 2D FEA.

The analytical solution has quite a good agreement with the FEA. However, inaccuracies occur at the bottom of the slot and the boundary of the tooth and the slot edge. The effect, which causes an increase in the flux density at the tooth tips, is not taken into account in the analytical models. The no-load air gap flux density is computed by the 2D and 3D FEA. The air gap flux density distribution waveforms obtained by the 2D and 3D analyses have been plotted in Fig. 2.9.

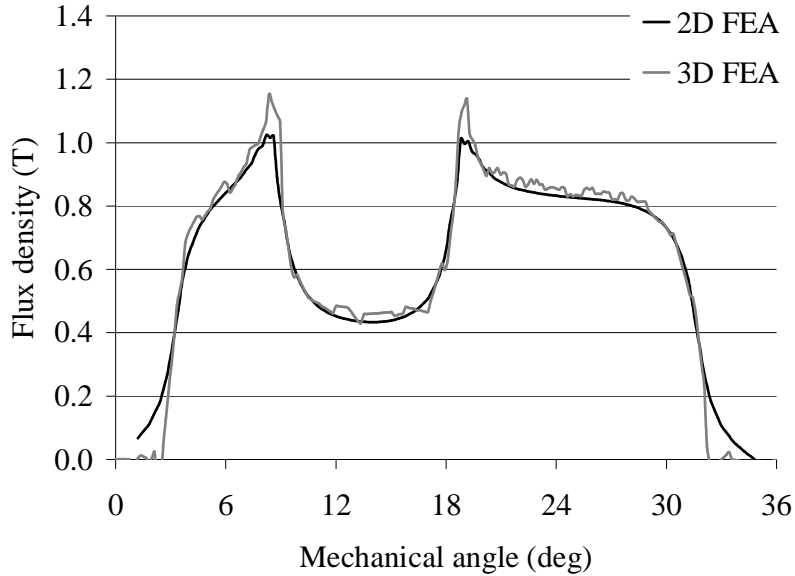


Fig. 2.9. Axial flux motor air gap flux density waveforms: the 2D and 3D analyses along one pole pitch. In 3D, the ripple is caused by the FEA net quality. Bad elements are always present in 3D. Their amount is typically in the range of 4 %. Local mistakes are emphasized but for example the flux integral is usually fairly accurate.

In the literature, many other improved methods for the slotting effect are presented, for instance by Zarko et al. (2006), Liu and Li (2007) and Dupas and Espanet (2009). Nevertheless, the computation procedures presented in Zarko et al. (2006), Liu and Li (2007) and Dupas and Espanet (2009) are more complicated compared with the methods introduced in Zhu and Howe (1993), and in this study, Zhu and Howe's two-dimensional model is found sufficient to model the slotting effect as the flux integral, voltage and torque calculations match well enough with the measured results.

The flux of the machine phase can be calculated from the analytic flux density solution seen in Fig. 2.10. As the working harmonic in this case is the fifth one, the windings of a certain phase are located only at certain teeth, in Fig 2.10 on the teeth 12, 1, 7 and 8. The maximum flux of a certain pole can be found when a permanent magnet is located so that the centre lines of the magnets and the centre lines of the teeth are in the same positions. Integrating the positive flux pulse under the tooth gives the maximum flux for the pole  $\hat{\Phi}$ . The flux linkage of the whole winding is calculated by  $\hat{\Psi} = k_{w,wh} N_s \hat{\Phi}$ . The induced voltage is then  $\hat{e} = \omega_s \hat{\Psi}$ .

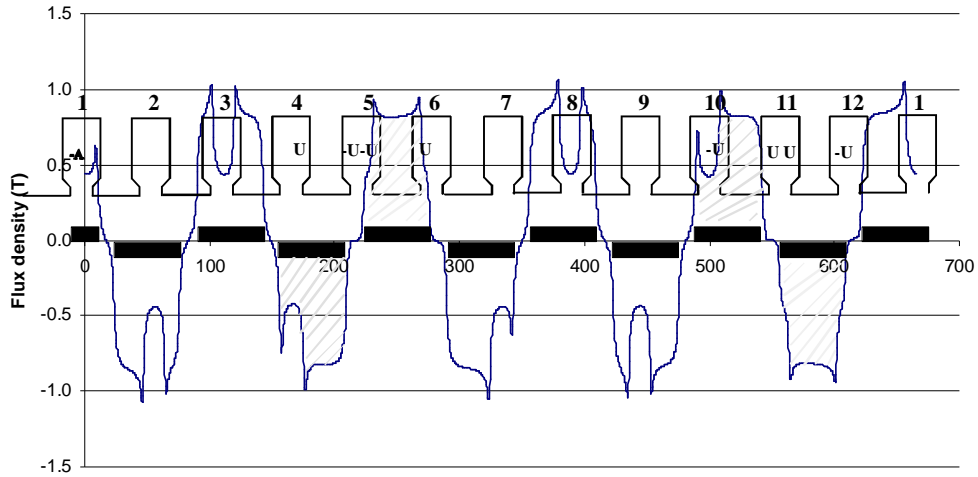


Fig 2.10 Air gap flux density and the permanent magnet positions of a radial flux machine or an axial flux machine at a certain radius. The x-axis co-ordinate is given in mm for the machine observed. Calculating the maximum flux of a pole can be done in such a pole where the magnet and the tooth observed are aligned (in this case between 200 mm and 300 mm).

In radial flux machines the width of the skewed magnets and in axial flux machines the flux linkage and the voltage are calculated from the flux density distribution and the winding arrangements are solved slice-wise (Kurronen 2003). In radial flux machines with no skewing the flux can be calculated simply in one plane.

### 2.3 Torque and inductances

In a rotor surface magnet machine, the direct- and quadrature-axis magnetizing inductances ( $L_{md}$ ,  $L_{mq}$ ) and the stator leakage inductance  $L_{s\sigma}$  form together the synchronous inductances  $L_d$  and  $L_q$ , which can be used in the evaluation of the machine torque production capabilities in analytical calculations (Gieras and Wing 1997, Hendershot and Miller 1994). The torque capability is inversely proportional to the inductances

$$T = \frac{mp}{\omega_s^2} \left[ \frac{E_{PM} U_s}{L_d} \sin(\delta) + \frac{U_s^2}{2} \left( \frac{1}{L_q} - \frac{1}{L_d} \right) \sin(2\delta) \right], \quad (2.34)$$

where  $\omega_s$  is the stator angular frequency,  $\delta$  is the load angle,  $E_{PM}$  electromagnetic force and  $U_s$  the supply line phase voltage. The torque is divided into two parts: excitation torque and reluctance torque. The excitation torque (the first term in 2.34) developed is generated by the interaction between the magnets and the current, and represents usually most of the total steady-state torque available. The reluctance torque is additional torque and results from the saliency (the second term in 2.34 – inductance difference). Despite the slight permeability deviation of the permanent magnet from the permeability of vacuum ( $\mu_{PM} \approx 1.05\mu_0$ ) for rotor-surface-mounted magnets, the direct- and quadrature axis inductances ( $L_d, L_q$ ) can, in practice, be supposed to be equal without making a major mistake, and hence, no saliency is assumed. In practice, there may be inductance differences caused by the saturation of iron parts (Parviainen 2005). It is assumed also in this study that the two series-connected stators are equal measured by the magnetic parameters. In practice, there could be differences caused by the construction, assembly problems and so on (Parviainen 2005).

For small machines, where the per unit stator resistance is larger than 0.01, the stator resistance should be taken into account in the torque equation (Gieras and Wing (1997)).

The equivalent air gap is defined as (Pyrhönen, Jokinen, Hrabovcová 2008)

$$\delta'_{PM} = k_C \left( \delta + \frac{h_{PM}}{\mu_{r,PM}} \right), \quad (2.35)$$

and the effective air gap length taking also the average effects of iron of the magnetic circuit into account

$$\delta_{ef} = k_C \left( \delta + \frac{h_{PM}}{\mu_{r,PM}} \right) + \frac{l_{mf}}{\mu_{r,Fe,ave}} \quad (2.36)$$

where  $k_C$  is the Carter factor and  $l_{mf}$  main flux path length.

$$\kappa = \frac{2}{\pi} \left[ \arctan \frac{b_1}{2\delta} - \frac{2\delta}{b_1} \ln \sqrt{1 + \left( \frac{b_1}{2\delta} \right)^2} \right] \quad (2.37)$$

$$k_C = \frac{\tau_u}{\tau_u - \kappa b_1}, \quad (2.38)$$

where  $\kappa$  is the factor for reduction of slot opening.

### Magnetizing inductance

Magnetizing inductance for an integral slot winding multiphase machine according to (Pyrhönen, Jokinen, Hrabovcová 2008) is solved as

$$L_{\text{md}} = \frac{2m\mu_0}{\pi} \frac{\tau_p}{p\pi\delta_{\text{ef}}} l' (k_{w1} N_s)^2, \quad (2.39)$$

where  $\mu_0$  is the permeability of air,  $\tau_p$  is the pole pitch and  $l'$  is the effective length of the stator core depending on the rotor construction as discussed above. In a 12-10-machine, the mutual coupling is established in a different way compared with an integral slot winding machine, but the coupling still exists. However, using the pole pitch width  $\tau_p$  in the calculation of the magnetizing inductance of a concentrated winding machine may lead to too large an inductance value. Equation (2.39) assumes sinusoidal flux distribution along the whole pole pitch. This, however, is not the case in concentrated winding machines, where the flux is concentrated mainly on the tooth area in the air gap. We may here refer to Fig. 1.2 in Chapter 1; it helps to understand the main flux behaviour of concentrated winding machines, even though the figure shows mainly the PM flux. In concentrated winding machines, the air gap area through which the flux travels to produce flux linkage is the area spanned by the coils  $Q/m$  through the area  $\tau_u l'$ , as illustrated in Fig. 3.5. By taking such an approach, the magnetizing inductance for a three-phase machine can be solved as (Hanselmann (2003) and Salminen (2004))

$$L_{\text{md}} = \frac{2m\mu_0}{\pi} \frac{\tau_u}{\frac{Q}{m}\pi\delta_{\text{ef}}} l' (k_{w,\text{wh}} N_s)^2, \quad (2.40)$$

which is proposed for concentrated winding machines instead of Eq. (2.39). The effective air gap is defined by (2.36).

### Leakage inductances

In this work, modified leakage inductance equations are given for a concentrated winding machine based on Vogt (1996) and Richter (1954, 1963, 1967). The leakage inductance  $L_{s\sigma}$  can be divided into five components, which are according to Richter (1954) air gap leakage inductance, slot leakage inductance, end winding leakage inductance, tooth tip leakage inductance and

skew leakage inductance. The skew leakage inductance is not considered in this study.

### Air gap leakage inductance

The air gap leakage flux differs from the other leakage fluxes. The air gap leakage flux is crossing the air gap while the other leakage fluxes do not (Pyrhönen, Jokinen, Hrabovcová 2008). The other leakage fluxes are illustrated in Fig. 2.10.

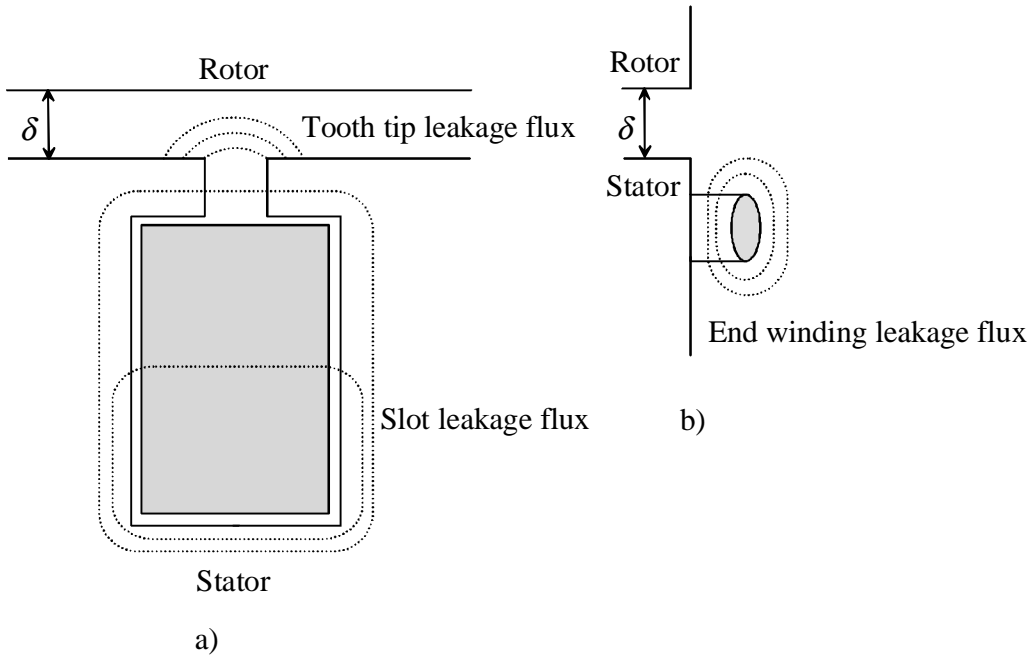


Fig. 2.10. Leakage flux components. a) Slot and tooth tip leakage flux and b) end winding leakage flux.

Air gap leakage inductance could be presented as

$$L_{\delta} = L_{\text{md}} \sigma_{\delta}, \quad (2.41)$$

where the factor  $\sigma_{\delta}$  can be modified from the winding harmonics content presented by Richter (1954)

$$\sigma_{\delta} = \sum_{\substack{v=-\infty \\ v \neq \text{wh}}^{v=+\infty}} \left( \frac{k_{\text{wv}}}{vk_{\text{w,wh}}} \right)^2, \quad (2.42)$$

where the  $\nu$  is the ordinal of the harmonic,  $k_{w\nu}$  is the winding factor of the harmonic and  $k_{w,wh}$  is the winding factor of the working harmonic. In a 12-slot 10-pole machine, the working harmonic is the 5<sup>th</sup>, and the leakage factor is calculated using the 1<sup>st</sup>, 7<sup>th</sup>, 11<sup>th</sup>, 13<sup>th</sup> harmonics (etc.) according to Eq. (2.42). Often in practical concentrated winding multiphase machines, the fundamental harmonic 1<sup>st</sup> is part of the leakage factor, because it is not the working harmonic of the machine. In this work, this system for the harmonics was partly selected as Eq. (2.42) can be directly applied to the leakage calculation. With the subharmonic presentation, Eq. (2.42) should be modified accordingly.

### Slot leakage inductance

A magnetic field crossing from one side of a slot to the other side links the coil sides in a somewhat different way when there is a two-layer winding in the slot, and the slot is divided horizontally instead of vertical division. However, in this study, horizontal and vertical divisions of the slot are assumed equal. According to Richter (1954), the slot leakage inductance can be defined as

$$L_u = \frac{4m}{Q} \mu_0 l' N_s^2 \lambda_u, \quad (2.43)$$

where the slot leakage factor  $\lambda_u$  depends on the slot geometry and the winding construction. Different slot shapes and equations for the slot leakage factor are given in Vogt (1996), Richter (1954) and Jokinen (1973). The slot leakage factor for a two-layer winding according to Richter

$$\lambda_u = k_1 \frac{h_4 - h'}{3b_4} + k_2 \left( \frac{h_3}{b_4} + \frac{h_1}{b_1} + \frac{h_2}{b_4 - b_1} \ln \frac{b_4}{b_1} \right) + \frac{h'}{4b_4}, \quad (2.44)$$

where the dimensions  $b_1$ ,  $b_4$ ,  $h_1 - h_4$  are illustrated in Fig. 2.11.  $h'$  is the possible insulator thickness between the upper and lower conductors in a double-layer winding.

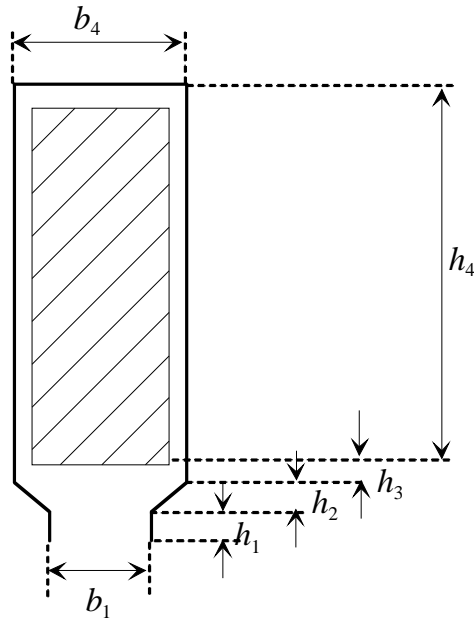


Fig. 2.11. Slot dimensions.

The factors  $k_1$  and  $k_2$  can be calculated as

$$k_1 = \frac{5 + 3g}{8} \quad (2.45)$$

$$k_2 = \frac{1 + g}{2}. \quad (2.46)$$

According to Richter (1967), a “two-layer” factor, which multiplies the permeance between the coils in the slot, to take into account the difference of the phase shift of two coils in the same slot, can be found as

$$g = \frac{1}{2q} \sum_{n=1}^{2q} \cos \gamma_n. \quad (2.47)$$

The angle  $\gamma_n$  is the temporal phase shift between the currents of the coil sides. The summation includes all coil sides of one phase. The slot leakage inductance is calculated independently for each slot connected in the winding section under observation. Equation (2.47) has to be modified so that it suits a concentrated winding. This can be done by comparing the winding construction of the 12-slot 10-pole machine with an integral slot winding with  $q = 2$  with short-pitching

$W/\tau_p = 5/6$ , where  $W$  is the coil width. Figure 2.12 illustrates the phase (A) winding constructions of these two machines ( $q = 0.4$  and  $q = 2$   $W = 5/6$ ).

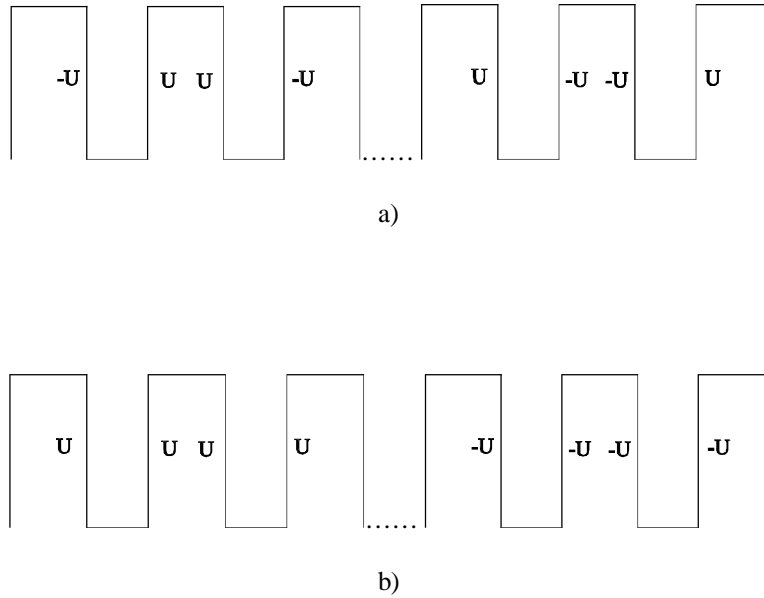


Fig. 2.12. a) All coils in one phase (U) for a concentrated winding  $q = 0.4$  and b) All coils in one phase (U) for an integral slot winding  $q = 2$ ,  $W/\tau_p = 5/6$ .

We modify Eq. (2.47) into

$$g = \frac{1}{\frac{Q}{m}} \sum_{n=1}^{\frac{Q}{m}} \cos \gamma_n \quad (2.48)$$

If semi-magnetic slot wedges of a width  $b_{\text{wedge}} = b_1$  are used, the slot opening width  $b_1$  can be calculated as  $b_1 = b_{\text{wedge}}/\mu_{r, \text{wedge}}$ .

### End winding leakage inductance

The end winding leakage flux is created by the magnetic field that surrounds a coil after it leaves one slot and before it enters another slot. The end winding of the prototype machine is illustrated in Fig. 2.13.



Fig. 2.13. End winding of a double-layer concentrated winding.

The end winding inductance can be defined as (Richter, 1963)

$$L_w = \frac{4m}{Q} \mu_0 N_s^2 q l_w \lambda_w, \quad (2.49)$$

where the average length  $l_w$  of the end winding leakage factor  $\lambda_w$  is defined as

$$l_w \lambda_w = 2l_{ew} \lambda_{lew} + W_{ew} \lambda_w \quad (2.50)$$

The factor  $l_{ew}$  is the height and  $W_{ew}$  is the width of the end winding. The reactance factors for the end windings  $\lambda_{lew}$  and  $\lambda_w$  depend on many parameters, such as the structure of the winding and the order of end winding layers. There are several methods available to estimate the values for these factors, as for instance given by Richter (1954, 1963, 1967) and Jokinen (1973). In this study, the reactance factors  $\lambda_{lew} = 0.518$  and  $\lambda_w = 0.138$  were used; they are defined for synchronous machines by Richter (1963). The width of the end winding of the concentrated winding arrangement is the same as the slot pitch  $\tau_u$  (Salminen 2004).

In axial flux machines, the inner and outer end windings are of different sizes. The division direction of the slot either vertically or horizontally also produces a small difference, which is, however, ignored here as the calculation of the end winding leakage is based on empirical knowledge in any case. Gieras et al. (2008) present different estimations for the permeance factor of the end connections of the axial flux machine. For double-layer, low-voltage, small-

and medium-power machines, the permeance factors of the inner and outer connections according to Gieras et al. (2008) are

$$\lambda_{w,in} \approx 0.17 \left( 1 - \frac{2 w_{c,in}}{\pi l_{ew,in}} \right) \quad (2.51)$$

$$\lambda_{w,out} \approx 0.17 \left( 1 - \frac{2 w_{c,out}}{\pi l_{ew,out}} \right) \quad (2.52)$$

where  $l_{ew,in}$  is the length of the inner end connection and  $l_{ew,out}$  the length of the outer end connection,  $w_{c,in}$  the inner coil span and  $w_{c,out}$  the outer coil span. The total permeance factor is the sum of Eqs. (2.51) and (2.52)

$$\lambda_w = \lambda_{w,in} + \lambda_{w,out} \quad (2.53)$$

Both Eqs. (2.50) and (2.53) lead to quite similar results in the prototype machine.

### Tooth-tip leakage inductance

Tooth-tip leakage inductance is produced by the leakage flux penetrating via the air gap to the next tooth. The tooth tip inductance of the phase coil is by Richter (1967)

$$L_z = \frac{4m}{Q} \mu_0 l' N_s^2 \lambda_z. \quad (2.54)$$

According to Richter, the leakage inductance factor can be defined by

$$\lambda_z = k_2 \frac{5 \left( \frac{\delta'_{PM}}{b_1} \right)}{5 + 4 \left( \frac{\delta'_{PM}}{b_1} \right)}, \quad (2.55)$$

where  $\delta'_{PM}$  is defined according to Eq. (2.35). In a two-layer winding, some coil sides in a slot belong to two different phases, and thus, there occur different currents in the same slot. The factor  $k_2$ , which takes this into account, is calculated as presented in the slot leakage inductance section of this work.

## 2.4 Joule losses of permanent magnets

Eddy current losses in the rotor permanent magnets are caused by three different reasons (Sahin et al. 2001, Arrilaga and Watson 2003, Nerg et al. 2002). First, a concentrated winding stator produces a large amount of current linkage harmonics generated flux densities travelling across the permanent magnets, thereby causing eddy currents. These are called winding harmonics. Secondly, the large slot openings cause flux density variations that induce eddy currents in the permanent magnets. These are called permeance harmonics. Finally, frequency-converter-caused time harmonics in the stator current waveform cause extra losses in the rotor. In this study, however, frequency-converter-caused time harmonics are not analyzed. In general, present day industrial frequency converters use switching frequencies in the range of 3–4 kHz. Such a switching frequency often produces an overall efficiency maximum to an industrial variable speed drive as the sum of losses in the converter and the motor is minimized (Slaets et al. 2000). In industrial induction motors the frequency-converter-caused losses are concentrated, especially, on the rotor surface. Some increase in the stator copper and iron losses can also be observed.

In a permanent magnet machine with no damper winding and with segmented magnets, the transient inductance is quite large – in the range of synchronous inductance – and hence, the motor current remains fairly sinusoidal.

Significant eddy-current losses in the PMs will not only affect the machine efficiency, but may also result in excessive heating, which could lead to irreversible deterioration in the machine performance, for instance demagnetization of the magnets. Eddy current losses may occur also in the rotor under the magnets. In this study, this is not considered, and non-conducting rotor material is used in the calculations. This is justified because in the prototype machine there is no iron in the rotor at all.

For practical reasons, in the following, the winding-harmonics-caused and permeance-harmonics-caused losses will be studied separately even though such an approach may lead to a somewhat erroneous result because the winding-harmonic-caused and the permeance-harmonic-caused flux components can either strengthen or cancel each other in the air gap, which, because of the nonlinearity of materials, can prevent the superposition of the loss components (Jokinen 1973).

Figure 2.14 illustrates permeance-harmonic-caused (no load,  $B_r = 1.03$ ) and winding-harmonic-caused (rated load,  $B_r = 0$ ) PM Joule losses calculated by the

2D FEA compared with the total harmonic-caused (rated load,  $B_r = 1.03$ ) PM Joule losses calculated by the 2D FEA for a 12-slot-10-pole machine.

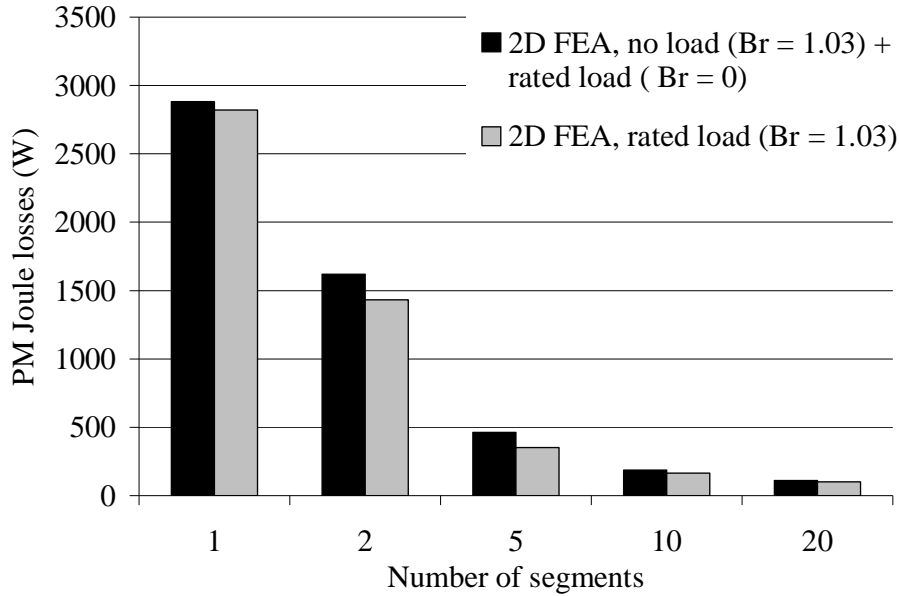


Fig. 2.14. Permeance-harmonic-caused (no load,  $B_r = 1.03$ ) and winding-harmonic-caused (rated load,  $B_r = 0$ ) PM Joule losses calculated by the 2D FEA compared with the total harmonic-caused (rated load,  $B_r = 1.03$ ) PM Joule losses calculated by the 2D FEA for a 12-slot-10-pole- machine. One magnet is segmented into 20 pieces at maximum.

#### 2.4.1 Joule losses caused by winding harmonics

Some analytical models on calculating the eddy-current loss in the rotor of a radial flux permanent magnet machine have been presented in the literature. In most of the publications, it is assumed that the magnet losses in a radial flux permanent magnet machine caused by the space harmonics of the stator windings and the stator slotting are negligible. Polinder and Hoeijmakers (1999) give a model for the magnet losses caused by the time harmonics of the stator currents. In this study, the same model is applied to calculate the magnet losses caused by the space harmonics of the stator windings. In the model, the stator current linkage is represented by an equivalent current sheet on the surface of the magnets. There is a restriction that the magnet width has to be small enough, because the magnet flux density is assumed constant over the magnet width. The eddy-current losses per unit of magnet volume are calculated as:

$$k_{PM} = \frac{1}{b_{PM}} \int_{-\frac{b_{PM}}{2}}^{\frac{b_{PM}}{2}} \rho_{PM} J_{PM}^2(x) dx = \frac{b_{PM}^2}{12\rho_{PM}} \left( \frac{dB}{dt} \right)^2, \quad (2.56)$$

where  $b_{PM}$  is the magnet width,  $\rho_{PM}$  the permanent magnet resistivity and  $J_{PM}$  the current density. Equation (2.56) is comparable with the eddy-current losses in laminated iron.

The analytical model for Joule loss prediction in permanent magnets in Cartesian co-ordinates is based on a cross-section of a two-pole PM machine (Polinder and Hoeijmakers 1997, 1999, 2000) shown in Figure 2.15. The magnets are numbered from 1 to  $N_{PM}$ .

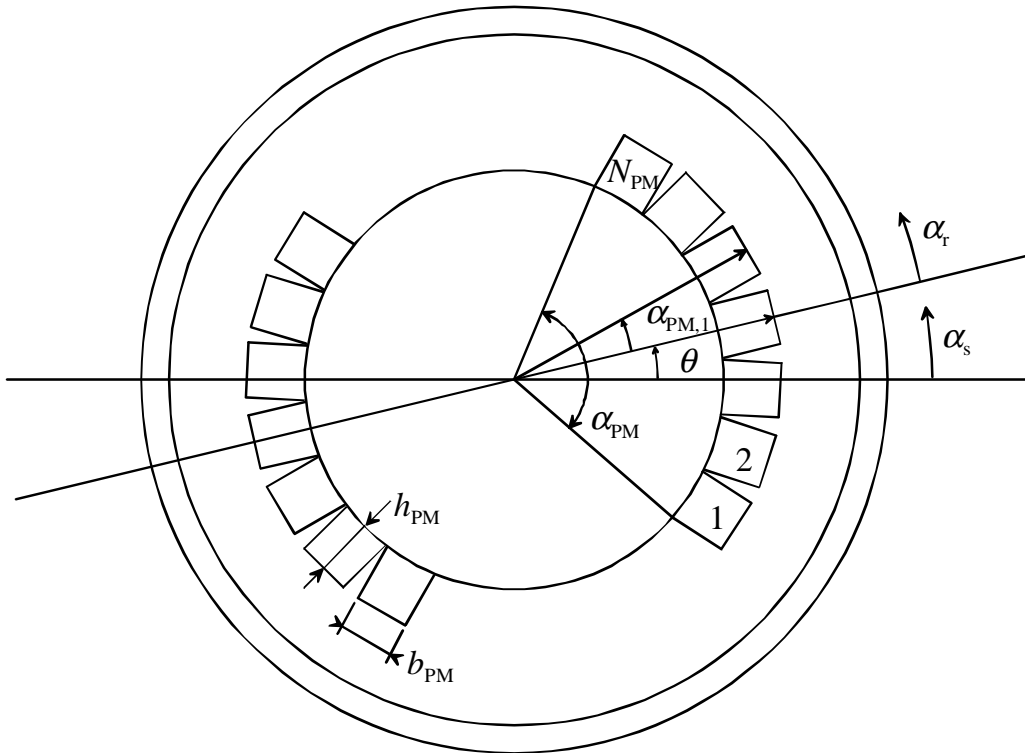


Fig. 2.15. Cross-section of the two-pole PM machine (Polinder and Hoeijmakers 1999).

The total magnet losses are defined as

$$\begin{aligned}
 P_{\text{PM,ec}} &\approx 2pr_{\delta}l_{\text{Fe}}h_{\text{PM}}\frac{b_{\text{PM}}^2}{12\rho_{\text{PM}}}\int_{-\frac{\alpha_{\text{PM}}}{2}}^{\frac{\alpha_{\text{PM}}}{2}}\left(\frac{d}{dt}(\hat{B}\cos(p(\alpha_r-\beta)))\right)^2d\alpha_r \\
 &= \frac{r_{\delta}l_{\text{Fe}}h_{\text{PM}}b_{\text{PM}}^2}{12\rho_{\text{PM}}}\left[\begin{aligned} &(p\alpha_{\text{PM}}+\sin(p\alpha_{\text{PM}}))\left(\frac{d}{dt}(\hat{B}\cos(p\beta))\right)^2 \\ &+(p\alpha_{\text{PM}}-\sin(p\alpha_{\text{PM}}))\left(\frac{d}{dt}(\hat{B}\sin(p\beta))\right)^2 \end{aligned}\right], \quad (2.57)
 \end{aligned}$$

where  $N_{\text{PM}}$  is the number of magnet segments per pole and  $\beta$  is the spatial angle between the stator and magnet field.

Further, at least the eddy-current losses in the magnets can be estimated similarly as the eddy current losses in the iron if the depth of penetration is higher than the magnet segment height  $h_{\text{PM}}$ . The length of the magnet is substantially larger than the magnet width  $b_{\text{PM}}$ . Also the end effects are negligible.

$$P_{\text{PM,ec}} \approx \frac{V_{\text{PM}}b_{\text{PM}}^2\hat{B}^2\omega^2}{12\rho_{\text{PM}}}, \quad (2.58)$$

where  $V_{\text{PM}}$  is the magnet volume. The angular frequency  $\omega$ , is calculated for the phenomenon under study, and it is different for each harmonic,  $\rho_{\text{PM}}$  is the resistivity of the magnet material, and the magnetic flux density  $B$  is found by the flux analysis.

The method introduced by Atallah et al. (2000) is also based on representing the stator current linkage distribution by an equivalent current sheet. Only the losses caused by the stator current linkage space harmonics are analyzed. Analytical models also assume that in an actual machine the skin depths associated with most of the dominant stator space harmonics are usually greater than the magnet dimensions, and therefore the induced eddy currents are resistance limited so that their influence on the inducing magnetic field distribution is negligible. The eddy current loss per unit axial length in one magnet is given by

$$P_{\text{PM,ec}} = \frac{\Omega}{2\pi} \int_0^{2\pi/\Omega r_{\text{PM}}} \int_{r_r}^{\alpha_{\text{PM}}/2} \rho_{\text{PM}} J_{\text{PM}}^2 r dr d\theta_r dt \quad (\text{W/m}) \quad (2.59)$$

$$P_{\text{PM,ec}} = \sum_{\nu=1}^{\infty} (P_{\text{cv}} + P_{\text{av}}) \quad (\text{W/m}) \quad (2.60)$$

where

$$P_{\text{cv}} = \frac{m^2 \mu_0^2 \alpha_{\text{PM}} J_{\text{PM}\nu}^2}{8 \rho_{\text{PM}} \nu^2 p_s^2} (\nu p_s m p_r)^2 \Omega^2$$

$$\cdot \left[ \left( \frac{r_{\text{PM}}}{r_i} \right)^{2\nu p_s} \frac{r_i^2 r_{\text{PM}}^2}{(2\nu p_s + 2)} \left( 1 - \left( \frac{r_r}{r_{\text{PM}}} \right)^{2\nu p_s + 2} \right) \right. \quad (2.61)$$

$$\left. + \left( \frac{r_r}{r_i} \right)^{2\nu p_s} r_i^2 r_r^2 F_\nu + \left( \frac{r_r}{r_i} \right)^{2\nu p_s} r_i^2 (r_{\text{PM}}^2 - r_r^2) \right] /$$

$$\left[ 1 - \left( \frac{r_r}{r_i} \right)^{2\nu p_s} \right]^2$$

and

$$F_\nu = \begin{cases} \frac{\left[ \left( \frac{r_{\text{PM}}}{r_r} \right)^{-2\nu p_s + 2} - 1 \right]}{(-2\nu p_s + 2)} & \text{for } \nu p_s \neq 1 \\ \ln \left( \frac{r_{\text{PM}}}{r_r} \right) & \text{for } \nu p_s = 1 \end{cases} \quad (2.62)$$

and

$$\begin{aligned}
P_{av} = & -\frac{m^2 \mu_0^2}{\alpha_{PM} \rho_{PM}} \frac{J_{PMv}^2}{v^4 p_s^4} (vp_s \mp p_r)^2 \Omega^2 \\
& \cdot \left[ \left( \frac{r_{PM}}{r_i} \right)^{vp_s} \frac{r_i r_{PM}^2}{(vp_s + 2)} \left( 1 - \left( \frac{r_r}{r_{PM}} \right)^{vp_s + 2} \right) \right. \\
& \left. + \left( \frac{r_r}{r_i} \right)^{vp_s} r_i r_r^2 G_v \right]^2 \cdot \frac{\sin^2 \left( vp_s \frac{\alpha_{PM}}{2} \right)}{\left( r_{PM}^2 - r_r^2 \right) \left[ 1 - \left( \frac{r_r}{r_i} \right)^{2vp_s} \right]^2}
\end{aligned} \tag{2.63}$$

and

$$G_v = \begin{cases} \frac{\left[ \left( \frac{r_{PM}}{r_r} \right)^{-vp_s + 2} - 1 \right]}{(-vp_s + 2)} & \text{for } vp_s \neq 2 \\ \ln \left( \frac{r_{PM}}{r_r} \right) & \text{for } vp_s = 2 \end{cases} . \tag{2.64}$$

Here, the - sign applies to  $v = 3k + m$  and + sign to  $v = 3k - m$ . The value for  $m = \pm 1$  is dependent on the winding configuration (Toda et al. 2004). For the 12-slot-10-pole machine  $m = -1$ . The space harmonic order is  $v$ ,  $p_s$  and  $p_r$  are the fundamental numbers of pole pairs associated with the stator winding and the rotor,  $\Omega$  is the rotor angular velocity and

$$J_{PMv} = \frac{2N_s \hat{i}_s}{\pi r_i} k_{wv} . \tag{2.65}$$

In a 12/10 machine  $p_s = 1$ . Because the machine produces the harmonics +1, -5, +7 (and so on) and works with the fifth harmonic, Eqs. (2.61) and (2.63) contain the relative speeds of the harmonics bypassing the magnet. The fifth harmonic does not produce travelling stator harmonics in the magnets.

Ede et al. (2002) present a computationally efficient 3D technique to determine the influence of the axial segmenting of the permanent magnets on the rotor eddy-current loss in concentrated winding PM machines. Axial segmenting of the permanent magnets of a surface-mounted magnet rotor has been shown to

be effective in reducing the rotor eddy-current loss in concentrated winding radial flux machines.

Ishak et al. (2005) extend the model presented in Atallah et al. (2000) by considering time harmonics in the stator current linkage distribution. The phase current waveforms are calculated from the analytical simulation models.

### Prototype

In concentrated winding multiphase machines, the fundamental and other than the working current linkage harmonics cause high rotor eddy currents if the rotor has conductivity. In a 12-10-machine, the working harmonic that produces torque is the 5<sup>th</sup> harmonic, and the main reason for rotor eddy current losses is the behaviour of the fundamental and the 7<sup>th</sup> harmonic, which travel in a different direction compared with the rotor. The stator supply frequency is 200 Hz and harmonics and their frequencies with respect to the rotor are given in Table 2.3. The 3<sup>rd</sup> and its multiples are not included in the observation.

Table 2.3. Space harmonics of the 12-slot-10-pole machines and the frequencies caused by these harmonics at the rotor surface, when the stator supply frequency is 200 Hz.

Space harmonic order	Frequency (Hz)
1	240
-5	0
7	68.6
-11	21.8
13	55.4
-17	28.2
19	50.5

In this study, the results given by the models by Polinder and Hoeijmakers (1999) and Atallah et al. (2000) are compared with the time-stepping finite element analysis (2D FEA) calculations for a 12-slot-10-pole machine with different magnet segments, when the supply frequency is 200 Hz. FEA calculations are done with electrically conducting non-magnetized permanent magnets under a typical stator phase current with a rated load. Figures 2.16–2.17 show a comparison of PM Joule losses calculated by both analytical models and the 2D FEA.

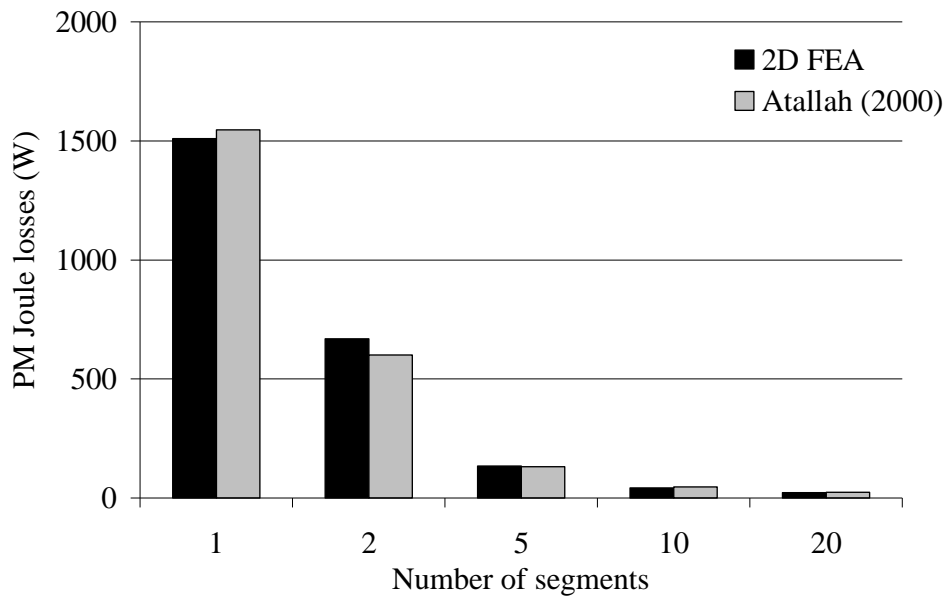


Fig. 2.16. Stator-harmonic-caused PM Joule losses calculated analytically by the Atallah et al. (2000) method and the 2D FEA for a 12-slot-10-pole machine. One magnet is segmented into 20 pieces at maximum.

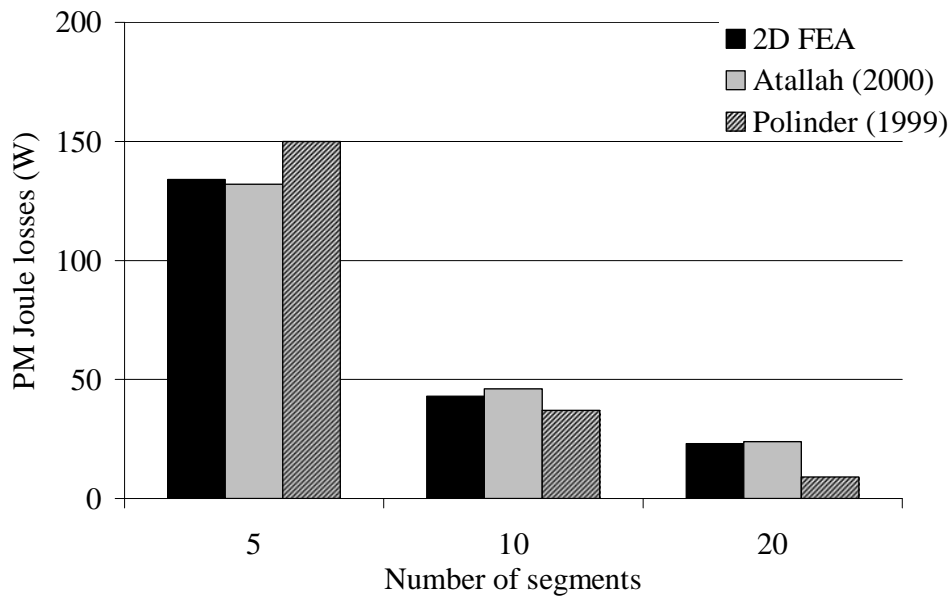


Fig. 2.17. Same results as in the previous figure calculated analytically by the methods by Atallah et al. (2000) and Polinder and Hoeijmakers (1999) and the 2D FEA for a 12-slot-10-pole machine. One magnet is segmented into 20 pieces at maximum.

Figures 2.16 and 2.17 show that the model by Atallah et al. (2000) is appropriate to analyze the PM Joule losses caused by space harmonics for all different size segments. The model by Polinder and Hoeijmakers (1999) is appropriate when the magnet segments are so small that the magnetic flux density can be considered constant over the magnet width, which is mentioned as a restriction in their publication (Polinder and Hoeijmakers 1999). Radial segmentation of the permanent magnets of a surface-mounted magnet rotor has been shown to be effective in reducing the rotor eddy-current loss as Atallah et al. (2000) and Polinder and Hoeijmakers (1999) have presented. In this work, the influence of the segmentation direction was also studied; tangentially and radially segmented magnets were investigated by practical measurements.

#### 2.4.2 Joule losses caused by permeance harmonics

Joule losses generated in PMs because of stator slotting have been studied in some publications. Especially in concentrated winding machines with open slots, the air gap flux density pulsations owing to the slot openings are high, and the Joule losses in the magnets caused by permeance harmonics have to be taken into account (Ishak et al. 2005, Reichert 2004, Deak et al. 2006, Deak et al. 2008). An analytical calculation model is presented by Markovic and Perriard (2008). In the Markovic and Perriard model it is assumed that only the slot opening influences the air gap magnetic field regardless of whether the teeth have crowns or not, in other words, the rest of the slot has no influence. Therefore, the slots can be treated as infinitely deep. The influence of slotting may be taken into account by introducing a 2D permeance function that modulates the air gap flux density calculated by Zhu's and Howe's method (1993) in the analytical calculation. The permeance function is based on a Fourier series presentation of the flux density under the slot opening. The mean loss of one magnet is obtained from a simple form:

$$P_{PM,ec} = \frac{l_{Fe} h_{PM} \hat{B}^2 v_r^2 b_{PM}}{2\rho_{PM}} \sum_n K_n^2 \left[ 1 - \left( \frac{\tau_u}{\pi n b_{PM}} \sin\left( \frac{\pi n b_{PM}}{\tau_u} \right) \right)^2 \right] \quad (2.66)$$

which includes

$$MOD = \sum_n K_n^2 \left[ 1 - \left( \frac{\tau_u}{\pi n b_{PM}} \sin\left( \frac{\pi n b_{PM}}{\tau_u} \right) \right)^2 \right] \quad (2.67)$$

where  $v_r$  is the rotor surface speed and  $K_n$  the coefficients obtained from the 2D modulation function.  $MOD$  describes the proportion of losses caused by the

permeance variations. Figure 2.18 illustrates the modulation function. The modulation function describes the changes in the air gap flux density caused by the slot opening permeance variation. The permeance function is assumed a continuous function, and hence, it can be described with a Fourier series. Figure 2.18 shows an example of the permeance function, and the caption gives the coefficients presented by Zhu and Howe (1993). An analogous approach is given in Pyrhönen (1991, p. 61).

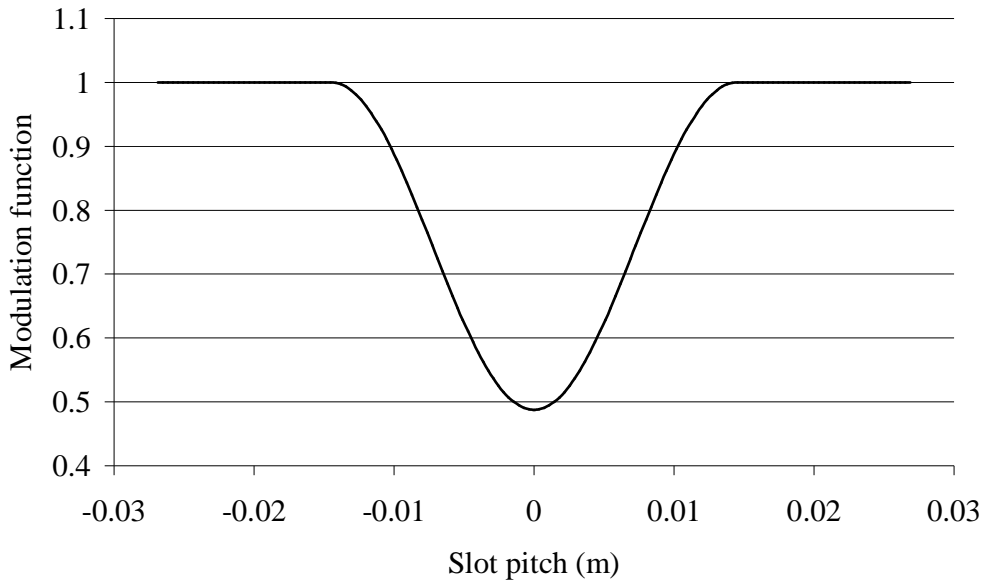


Fig. 2.18. Modulation function according to Zhu and Howe (1993) and the corresponding Fourier-series-based factors for the prototype machine are  $K_0 = 0.8618$ ,  $K_1 = -0.2282$ ,  $K_2 = -0.1219$ ,  $K_3 = -0.0312$ ,  $K_4 = 0.0052$ ,  $K_5 = 0.0042$ .

In this study, Eq. (2.66) is also provided for segmented magnets by substituting  $b_{PM}$  by  $b_{PM,segment}$  to get some estimation of losses for segmented magnets. There is also one restriction in the publication: The skin depth in the magnet should be higher than the dimensions  $h_{PM}$  and  $b_{PM}$  of the magnet pieces (Markovic and Perriard 2008).

The stator slot openings cause a variation of the magnetic field in the magnets, this component of rotor eddy-current loss being dependent on the width of the slot openings and the pole/slot number combination. For the 12-slot-10-pole machine, the supply frequency is 200 Hz, the rotor is rotating  $40 \text{ s}^{-1}$ , and one magnet passes 12 slots in one revolution. The first slot harmonic frequency causing eddy current in the magnets is then 480 Hz. Slot harmonic frequencies are presented in Table 2.4.

Table 2.4. Slot harmonic ordinals and frequencies of the 12-slot-10-pole machine, supply frequency 200 Hz.

Slot harmonic order	Frequency on rotor surface (Hz)
1	480
2	960
3	1440
4	1920
5	2400
6	2880
7	3360
8	3840
9	4320

The results from the analytical calculations have to be compared with the time-stepping finite element analysis calculations with electrically conducting and magnetized permanent magnets under no-load situation (Fig. 2.19). The FEAs take into account only the induced eddy-current component that results from the variation of the magnet working point caused by the stator slotting.

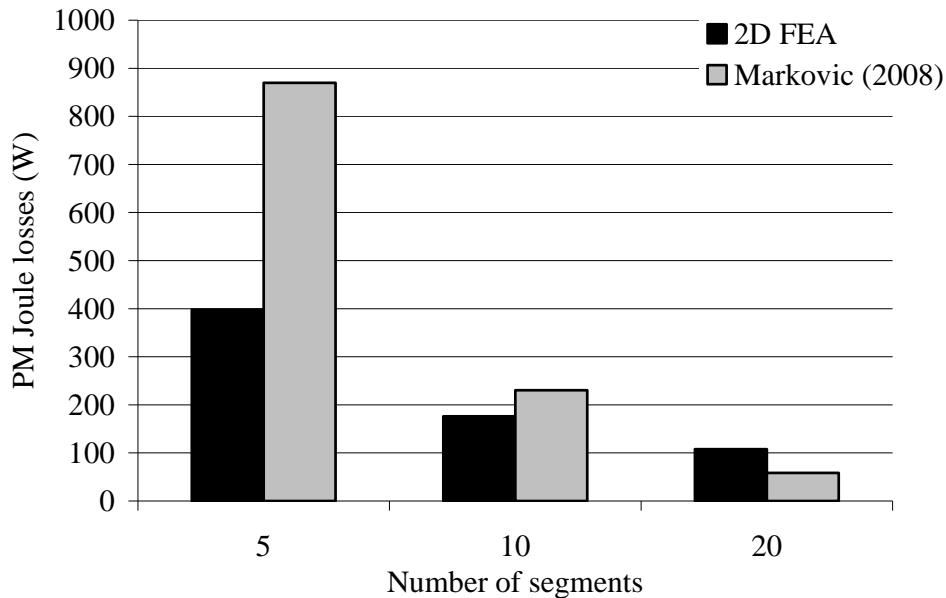


Fig. 2.19. Permeance-harmonic-caused PM Joule losses calculated analytically by the Markovic and Perriard method (2008) and by the 2D FEA for a 12-slot-10-pole machine. One magnet is segmented into 20 pieces at maximum.

We can see that the iteration is not valid when the magnet width is not relative small. In the calculated machines, the skin depth of the first slot harmonic is

$$\delta = \sqrt{\frac{2\rho_{\text{PM}}}{2\pi f \mu_{r,\text{PM}} \mu_0}} = \sqrt{\frac{2 \cdot 1.5 \cdot 10^{-6}}{2\pi \cdot 480 \cdot 1.05 \cdot 4\pi 10^{-7}}} \text{ m} = 0.027 \text{ m}, \quad (2.68)$$

where  $f$  is the slot harmonic frequency. The Joule losses results of 10 and 20 segments are only at an acceptable level, in which the skin depth is clearly higher than the PM dimension  $h_{\text{PM}}$  and  $b_{\text{PM}}$ . (Markovic and Perriard 2008).

Figure 2.20 shows the proportion of losses (obtained by the 2D FEA) caused by the space harmonics resulting from the winding distribution and the space harmonics caused by the stator slotting. These results were obtained calculating the losses at no-load and load conditions. At no load, there are no stator harmonics present, but the permeance harmonics remain.

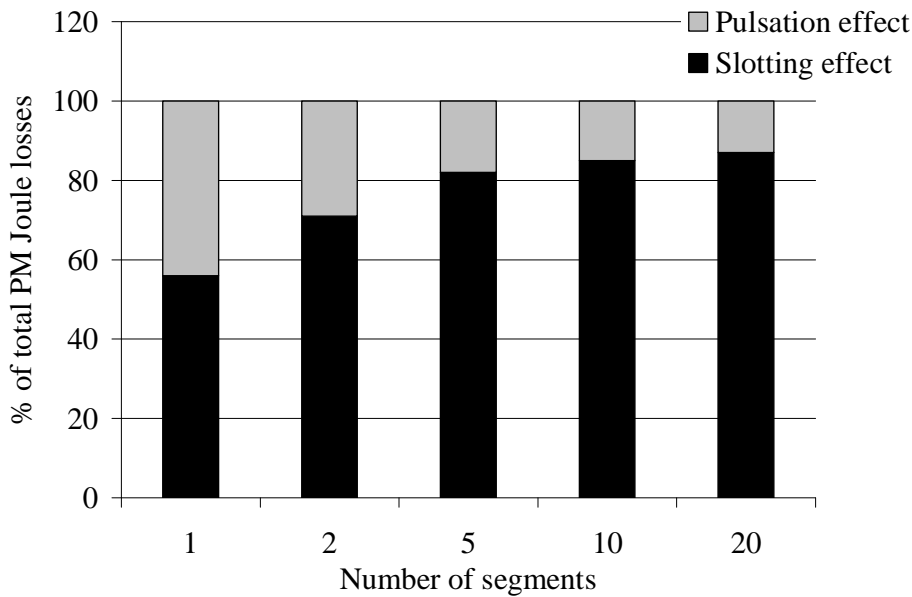


Fig. 2.20. Proportions of PM Joule losses caused by the winding and permeance harmonics calculated by the 2D FEA for a 12-slot-10-pole machine.

Figure 2.20 shows that the eddy current losses of the permanent magnet in the concentrated winding motor with open slots are mainly produced by the stator slot openings, especially, when segmented magnets are used. Tables 2.3 and 2.4 show that the frequencies of the stator harmonics are low compared with the frequencies of the permeance harmonics. The amplitudes of the permeance

harmonics are also large compared with the stator harmonics. These facts explain why the proportion of the slotting effect increases as the amount of slices is increasing.

The amplitude of the permeance-harmonic-caused flux pulsation is large compared with the amplitudes of the stator harmonics because the magnetizing inductance is low. Even the working harmonic armature reaction ( $L_{md,p.u.} = 0.3$ ) is small and, especially, other armature-harmonics-caused flux densities are considerably weaker than the permanent magnet density changes caused by the slot openings above the magnets, because the winding factors of the harmonics are usually low.

## 2.5 Other losses

### Winding losses

$$P_{Cu} = 3R_s I_s^2, \quad (2.69)$$

where  $R_s$  is the alternating current (AC) resistance for one phase winding and  $I_s$  is the phase current (RMS). When the current frequency is high and the conductor cross-section is large enough, eddy-current losses are induced in the copper as a result of skin and proximity effects.

### Stator core losses

The losses include the hysteresis losses, the Joule losses and the excess losses. The iron losses are defined in the periodic state (time stepping magnetic applications over one complete period); Cedrat's Flux2D is employed in finite element computations (Bertotti et al. 1991, Cedrat 2009). The iron losses are calculated in a magnetic region during the analysis.

$$\frac{1}{T} \int_0^T P_{Fe}(t) dt = k_h \hat{B}^2 f k_f + \frac{1}{T} \int_0^T k_f \left[ \sigma_{Fe} \frac{d^2}{12} \left( \frac{dB(t)}{dt} \right)^2 + k_e \left( \frac{dB(t)}{dt} \right)^{1.5} \right] dt, \quad (2.70)$$

where  $\hat{B}$  is the maximum flux density in the element concerned,  $f$  the frequency,  $\sigma_{Fe}$  the conductivity,  $d$  the lamination sheet thickness,  $k_h$  the coefficient of hysteresis loss,  $k_e$  the coefficient of excess loss and  $k_f$  is the filling factor. The factors depend on the steel material applied.

The analytical equation for iron losses presented by Deng (1999) includes the harmonic effect of the flux densities

$$P_{\text{Fe}} = k_{\text{eh}} k_{\text{h}} f \hat{B}^\alpha + \frac{k_{\text{e}}}{2\pi^2} \left( \frac{dB}{dt} \right)_{\text{RMS}}^2 + \frac{k_{\text{exe}}}{(2\pi^2)^{\frac{3}{4}}} \left( \frac{dB}{dt} \right)_{\text{RMS}}^{1.5}, \quad (2.71)$$

where  $f$  and  $\hat{B}$  are the frequency and peak value of the flux density,  $k_{\text{h}}$ ,  $k_{\text{e}}$ ,  $k_{\text{exe}}$  and  $\alpha$  are constants determined by the loss data provided by the manufacturer. An empirical correction factor  $k_{\text{eh}}$  is applied to take into account the effect of minor hysteresis loops on the hysteresis loss.  $\left( \frac{dB}{dt} \right)_{\text{RMS}}$  is the RMS value of the rate of change of the flux density with respect to time in an AC cycle.

A different analytical equation for iron losses is presented by Pyrhönen, Jokinen, Hrabovcová (2008). Hysteresis losses can be written as

$$P_{\text{Hy}} = fVb_{\text{Hy}}. \quad (2.72)$$

Empirical equations yield an approximation for the hysteresis loss

$$P_{\text{Hy}} = \eta Vf \hat{B}^n. \quad (2.73)$$

where the exponent  $n$  varies typically between [1.5, 2.5],  $\eta$  being an empirical constant.

Joule losses

$$P_{\text{Fe,ec}} = \frac{bh\pi^2 f^2 d^3 \hat{B}^2}{6\rho_{\text{Fe}}} = \frac{V \cdot \pi^2 f^2 d^2 \hat{B}^2}{6\rho_{\text{Fe}}}. \quad (2.74)$$

or

$$P_{\text{Fe},n} = P_{15} \left( \frac{\hat{B}_n}{1.5 \text{ T}} \right)^2 m_{\text{Fe},n}. \quad (2.75)$$

Further, hysteresis and Joule losses together in the stator yoke and teeth

$$P_{\text{Feys}} = k_{\text{Feys}} P_{15} \left( \frac{B_{\text{ys}}}{1.5} \right)^2 m_{\text{ys}} \left( \frac{f}{50} \right)^{\frac{3}{2}} \quad (2.76)$$

$$P_{\text{Fets}} = k_{\text{Fets}} P_{15} \left( \frac{B_{\text{ts}}}{1.5} \right)^2 m_{\text{ts}} \left( \frac{f}{50} \right)^{\frac{3}{2}} \quad (2.77)$$

The hysteresis losses are roughly proportional to the square of the flux density, and the Joule losses are proportional to the square of the flux density. It is determined that both losses are proportional to the square of the flux density. Further, a compromise is made with the power of the frequency. The hysteresis losses are, in principle, directly proportional to the frequency, and Joule losses are proportional to the square of the frequency; thus, together the losses are about proportional to  $f^{3/2}$ . The iron coefficients are found by a curve-fitting approach of the material data from the manufacturer.

The iron losses calculated by Eq. (2.77) give the following values for the test machine, Table 2.5. The remanent flux density of the PM at 20 °C is  $B_{r20C} = 1.1$  T in the no load situation and at 80 °C,  $B_{r80C} = 1.03$  T in the rated load situation.

Table 2.5. Analytically calculated iron losses of the 12-slot-10-pole machines in no-load and rated load situations, the coefficients  $k_{\text{Feys}}=1.5$  and  $k_{\text{Fets}}=1.7$  for yokes and teeth were selected according to Müller et al. (2008). One magnet is segmented into 1 or 20 pieces.

Rotor equipped with	$P_{\text{Feys}}/\text{W}$	$P_{\text{Fets}}/\text{W}$	Single stator iron losses/W	Double stator iron losses/W
No load; bulky magnets	80	230	310	630
No load; radially segmented magnets	80	220	290	580
Rated load; bulky magnets	70	200	280	550
Rated load; radially segmented magnets	70	190	250	510

### Additional losses

Additional losses are usually losses caused by the flux harmonics and other core losses except stator eddy and hysteresis losses of the working harmonic. These losses vary significantly for different machines and various operating conditions. The additional losses can be calculated by (Gieras and Wing 1997)

$$P_{\text{ad}} = k_{\text{ad}} P_{\text{out}} , \quad (2.78)$$

where the additional loss coefficient for PM machines  $k_{ad} = 0.03...0.05$  for small machines up to 10 kW,  $k_{ad} = 0.005...0.01$  for medium-speed machines up to 100 000 kW and  $k_{ad} = 0.003...0.005$  for large-power machines. The PM machine type also has an effect on the coefficient.

Mechanical losses can be calculated by the equation

$$P_p = k_p D_r (l_r + 0.6 \tau_p) v_r^2 \quad (2.79)$$

found for instance in (Pyrhönen, Jokinen, Hrabovcová 2008).  $k_p = 15 \text{ W s}^2/\text{m}^4$  for totally enclosed fan-cooled small machines.

When the average diameter is used for  $D_{ro}$  and the length 0.06 m, we obtain 220 W.

## 2.6 Summary

Basic guidelines for the analytical calculation of axial flux concentrated winding PM machines were introduced. It was shown that an axial flux PM machine can be modelled as a radial flux PM machine by applying the arithmetic mean radius as a design plane. The analytical calculation of the air gap magnetic flux density for a non-slotted and slotted stator was presented. Equations for magnetizing inductance and different leakage inductance components were presented. Special attention was paid to the evaluation of permanent magnet Joule losses. It was shown that a major part of the permanent magnet Joule losses are due to the stator slotting when the motor is supplied by sinusoidal current. The frequency-converter-caused time harmonics are not analyzed in this study. The analytical calculation results were verified by comparing them with the numerical results obtained from the 2D and 3D FEA.

### 3 TORQUE CAPABILITIES OF DIFFERENT WINDING CONSTRUCTIONS

There is discussion whether concentrated winding or integral slot winding PM machines should be used for a certain application; this question is discussed in this chapter with examples of machines having the number of slots per pole and phase varying from  $q = 0.25$  to  $q = 2$  and fixed motor outer dimensions. In the following study, the mass of PM material, back emf and the stator outer dimensions are kept constant.

The end windings in a concentrated winding with  $q \leq 0.5$  are notably smaller than in integral slot winding machines, which provides an opportunity of using a large rotor and producing large torque in predetermined machine overall dimensions. The short end windings also guarantee low copper losses. With careful design, a very good torque quality of a concentrated winding machine can be achieved.

This study, however, indicates that the torque production capability of integral slot windings is good compared with concentrated winding machines. There may also be problems with the rotor losses in concentrated winding machines as the permanent magnet material flux density pulsates heavily in concentrated winding machines, especially in open slot machines. Hence, the machine designer must be aware of all the factors and find a good design compromise. It seems that because of high rotor magnet losses, concentrated machines suit best for low-speed high-torque applications if permanent magnet losses cannot be limited to a tolerable level at higher speeds.

This chapter addresses the behaviour of inductances and the maximum available pull-out torques of concentrated winding machines with  $q \leq 0.5$  compared with integral slot winding machines. All the motors studied have rotor-surface-mounted magnets. Inductances and pull-out torques are calculated for concentrated winding machines  $q = 0.25$ ,  $q = 0.29$ ,  $q = 0.4$  and  $q = 0.5$  and integral slot winding machines  $q = 1$  and  $q = 2$ . The equations applied in inductance calculation were given in Chapter 2. The pull-out torques of some machines are also verified by FEA calculations using Flux2D™ by CEDRAT (Salminen 2004). Tables 3.1 and 3.2 summarize the machines under study.

Table 3.1. Slot numbers  $Q$  of concentrated winding machines studied in the work.

$q/p$	4	5	6	7	8	10	11	12	13	14	15	16	21	24
0.25					12			18				24		36
0.29				12						24			36	
0.4		12				24					36			
0.5	12		18		24			36						

Table 3.2. Slot numbers  $Q$  of integral slot winding machines studied in the work.

$q/p$	2	3	4	5	6	7	8	9	10	11	12
1	12	18	24	30	36	42	48	54	60	66	72
2	24	36	48	60	72	84	96	108	120	132	144

### 3.1 Machine parameters

All analyzed machines have the same frame size 225. This frame size is usually used in 50 Hz network-driven industrial induction machines with the rated output torque of 150–400 Nm (ABB 2007) depending on the number of poles. With a higher amount of poles, the rotor in the same frame size, and correspondingly the torque, can be larger than in machines with two magnetic poles. The frame size specifies the outer diameter and overall length of the motor. The machine magnetic length and the air gap diameter were selected to be constant parameters to keep the rotor volume equal for all the machines. Such an approach will indicate the torque capability differences between different constructions. The torque and volume dependence is presented as (Pyrhönen, Jokinen, Hrabovcová 2008)

$$T = kD_r^2l_r \quad (3.1)$$

where  $k$  is a machine type dependent constant,  $D_r$  is the rotor diameter and  $l_r$  is the rotor length. The equation shows that the torque is proportional to the rotor diameter squared and directly proportional to the rotor length, that is, the volume of the rotor. The constant values used in the comparison are given in Table 3.3.

Table 3.3. Machine constant parameters.

Stator stack length, $l_{Fe}$	270 mm
Stator stack outer diameter, $D_o$	364 mm
Stator stack inner diameter, $D_i$	254 mm
Air gap length, $\delta$	1.2 mm
The amount of the permanent magnet material, $m_{PM}$	10.3 kg
Rated output power, $P_{out}$	45 kW
Rated speed, $n_s$	400 min <sup>-1</sup>

Also the back-emf is used as a fixed parameter. It is set equal to or higher than 0.9 of the supply voltage. To achieve the same back-emf for all the machines, in machines with  $q = 0.5$  and  $0.25$ , more winding turns are required than in machines with  $q = 0.4$  and  $0.29$  because of the lower winding factor. When using such fixed parameters, all the machines do not have an optimal design as for instance the stator yoke flux density can be low in some designs; nevertheless, indication of the torque producing capability is found. The flux densities in the stator teeth and yoke were selected to be about 1.8 T and 1.6 T, respectively.

### 3.2 Inductances and torques of concentrated winding machines and integral slot winding machines in the case of semi-closed slot openings

Inductances and the maximum pull-out torque developed by concentrated winding machines equipped with different number of slots and poles are analyzed. Semi-closed slots are used; the relative slot opening width ( $b_1/\tau_u$ ) varies between 0.08 and 0.09. The magnetizing inductance equation for concentrated winding machines was given in Chapter 2. The per-unit (p.u.) magnetizing inductance value trends with different numbers of slots per pole and phase are shown in Fig.3.1.

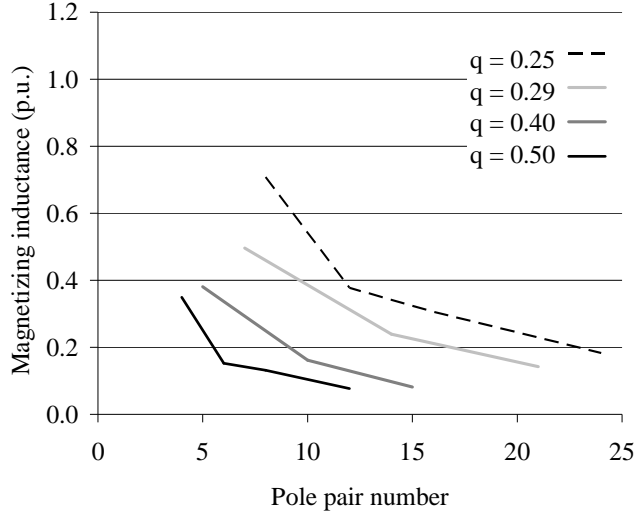


Fig. 3.1. Per unit magnetizing inductances of concentrated winding machines with numbers of slots per pole and phase  $q = 0.25, 0.29, 0.4$  and  $0.5$  (Jussila et al. 2007).

Figure 3.1 shows that for a constant value of  $q$ , the magnetizing inductance (p.u.) decreases as the number of pole pairs increases. This may be expected, because the magnetizing inductance is inversely proportional to the square of the pole pair number  $p$ , Eq. (2.40), where  $Q = 2pqm$ . Also the slot pitch  $\tau_u$  decreases when  $p$  decreases with a certain  $q$  value.

The equations for the leakage inductances for concentrated winding PM machines are described in Chapter 2. By reorganizing the leakage inductance components applying  $Q = 2pqm$  and  $\tau_u = \frac{\pi D_\delta}{Q}$ , the leakage inductance can be written as

$$L_{\delta\sigma} = m\mu_0 N_s^2 l' \left[ \begin{array}{l} \frac{2D_\delta k_{wv}^2}{m} \sigma_\delta + \dots \\ \frac{Q^2}{m} \pi \delta_{ef} \\ \frac{2}{pmq} \left( \lambda_u + \lambda_z + q \frac{l_w \lambda_w}{l'} \right) \end{array} \right] \quad (3.2)$$

Figure 3.2 presents the leakage inductances of concentrated winding machines.

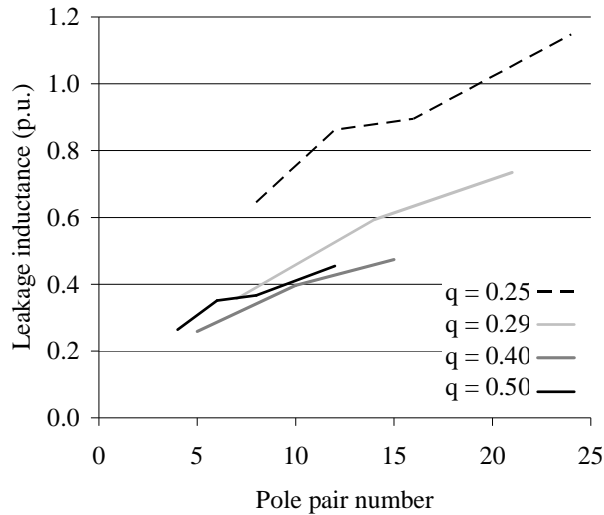


Fig. 3.2. Leakage inductances of concentrated winding machines with numbers of slots per pole and phase  $q = 0.25, 0.29, 0.4$  and  $0.5$  (Jussila et al. 2007).

For a constant value of  $q$ , the leakage inductance increases as the number of pole pairs increases. This is due to the fact that the leakage inductance is inversely proportional to  $pq$ . In Eq. (2.19) the factor  $\sigma_{\delta}$  and  $L_{md}$  are small and the main part of leakage inductance is formed by the tooth tip and slot leakages, which both depend on  $pq$ . The synchronous inductance, however, is the sum of magnetizing and leakage inductances, of which one component increases and the other decreases as a function of pole pair number, and therefore, the synchronous inductance will get a minimum value at some  $p$ .

The dependency of torque on the number of slots per pole and phase  $q$  of the concentrated winding machines is studied. Analytically calculated pull-out torques for concentrated winding machines are presented in Fig. 3.3. Pull-out torques are also verified by FEA in (Salminen 2004).

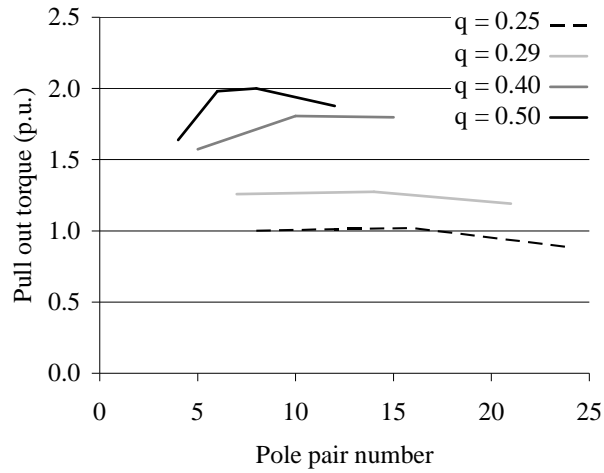
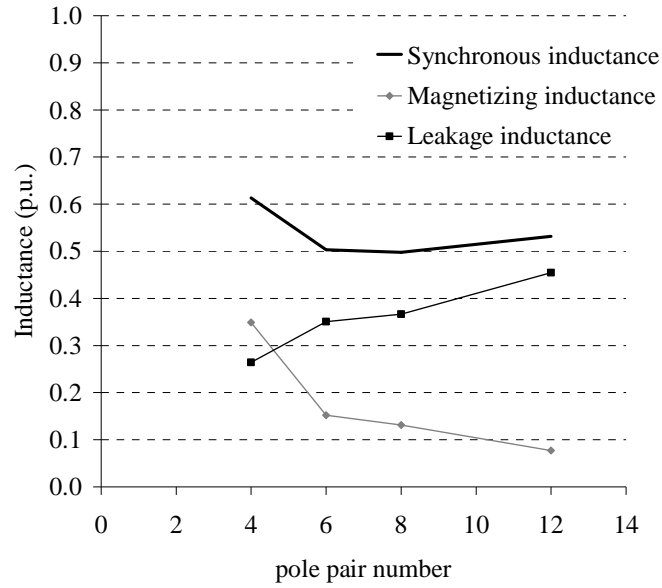


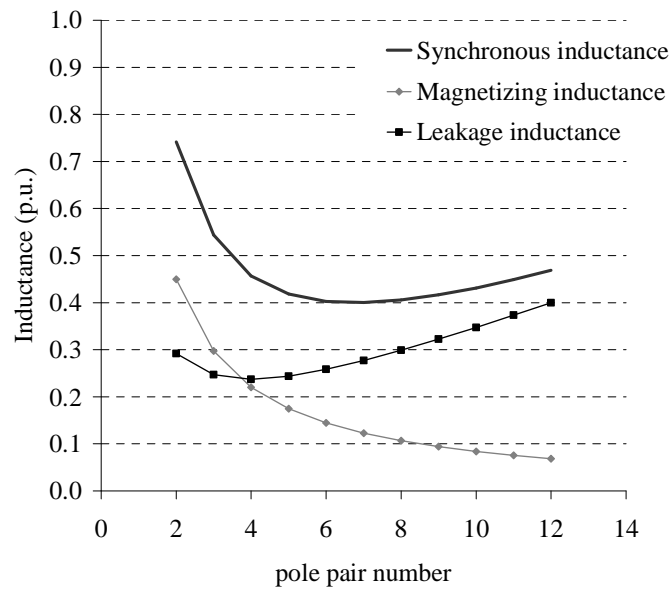
Fig. 3.3. Pull-out torques of concentrated winding machines with  $q = 0.25, 0.29, 0.4$  and  $0.5$  (Jussila et al. 2007).

It can be seen that machines having  $q = 0.25$  give the smallest pull-out torques. A higher torque was produced when  $q$  was increased (Salminen 2004, Salminen et al. 2005, Salminen et al. 2006, Jussila et al. 2007).

The inductances and torques of the integral slot winding machines were compared with the values of concentrated winding machines. Semi-closed slot openings are used. In Fig. 3.4, the magnetizing inductance  $L_{md}$  and the leakage inductance  $L_{s\sigma}$  are calculated analytically for a concentrated winding ( $q = 0.5$ ) and an integral slot winding machine ( $q = 2$ ).



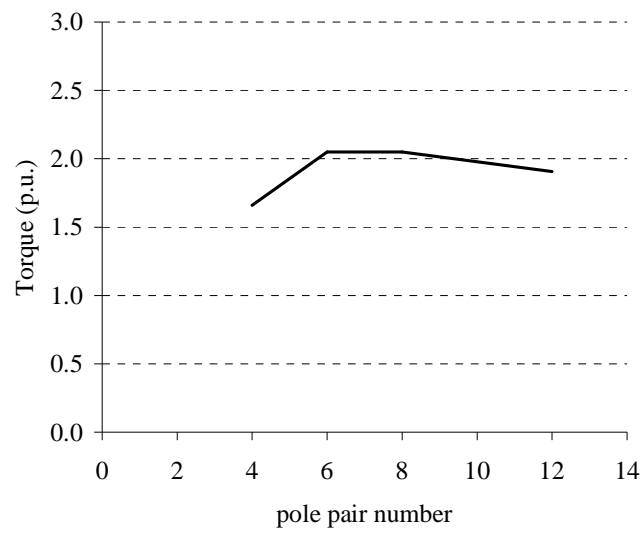
a)



b)

Fig. 3.4. a) Synchronous inductance  $L_d$ , magnetizing inductance  $L_{md}$  and leakage inductance  $L_{\sigma}$  of a concentrated winding ( $q = 0.5$ ) machine as a function of pole pair number. b) Corresponding values of integral slot winding ( $q = 2$ ) machines as a function of pole pair number (Jussila et al. 2007)

Also the pull-out torques are calculated analytically and verified by 2D FEA calculations, Fig. 3.5.



a)

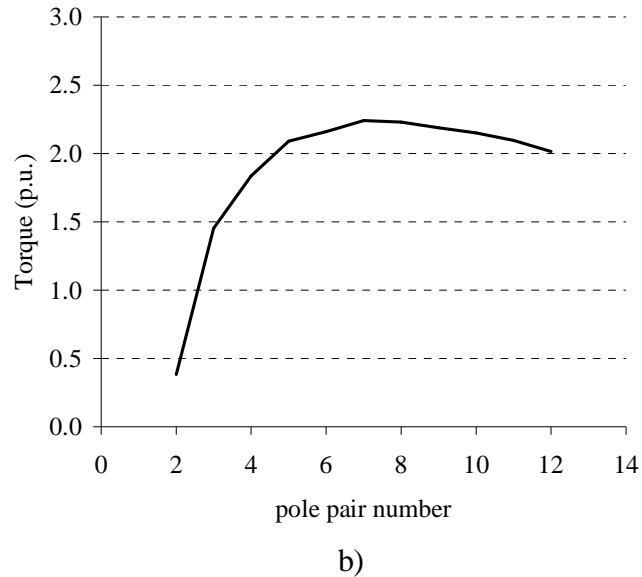


Fig. 3.5. a) Maximum pull-out torque of a concentrated winding ( $q = 0.5$ ) machine as a function of pole pair number. b) Corresponding value of an integral slot winding ( $q = 2$ ) machine as a function of pole pair number (Jussila et al. 2007).

The study shows that for both integral slot winding and concentrated winding machines, it is possible to find optima for  $p$  values with  $q$  as a parameter, at which the pull-out torque is at highest. With high pole pair numbers, the amount of leakage inductance is dominating, while with a low pole pair number, the magnetizing inductance is dominating; consequently, the synchronous inductance will get a minimum value in the area between these extreme values.

Fig. 3.6 shows the pull-out torques as a function of  $p$  and  $q$  for concentrated winding and integral slot winding machines.

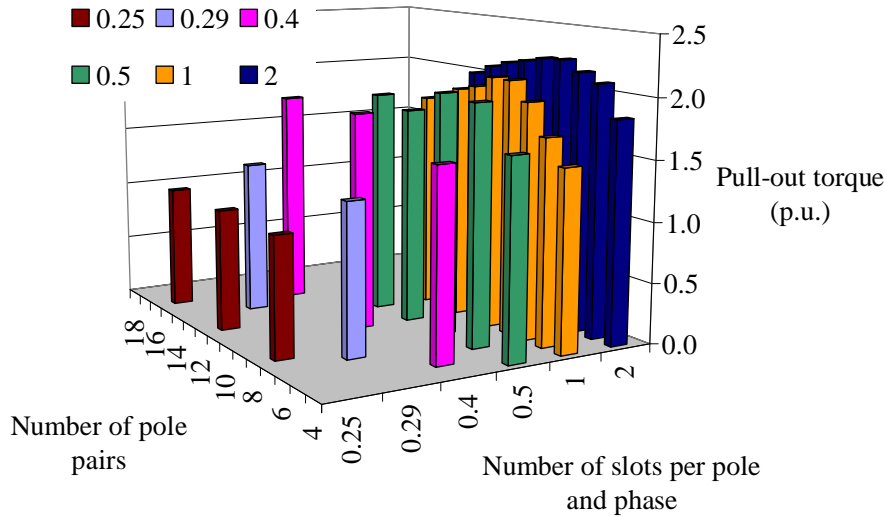


Fig. 3.6. Pull-out torque as a function of  $p$  and  $q$  for concentrated winding and integral slot winding PM machines.

When comparing integral slot winding machines and concentrated winding machines, it is noticeable that the per unit inductances and pull-out torques behave quite similarly as a function of pole pair number. The minima and maxima are located at about the same pole pair numbers. However, integral slot winding machines produce more torque with the same rotor size.

A small synchronous inductance is necessary to obtain a high torque from the permanent magnet motor. The maximum torque is inversely proportional to the synchronous inductance ( $T_{\max} \cong L_d^{-1}$ ). The results show that as  $q$  increases from 0.25 to 0.5, the pull-out torque of the concentrated winding machine increases. However, as  $q$  increases further and integral slot windings ( $q = 1$ ,  $q = 2$ ) are used, the torque development will be higher when the same rotor main dimensions are maintained. This indicates that selecting a concentrated winding construction must have other relevant reasons than maximizing the rotor torque per rotor volume ratio.

It is possible to take an advantage of the short end windings of concentrated windings by inserting a longer stator stack compared with the stack of integer slot wound machines in the same frame size. Consequently, longer active parts will give more torque (Cros and Viarouge 2004, Salminen 2004, Libert and Soulard 2004). Concentrated winding machines also provide an opportunity of using a large number of poles, which leads to a low stator yoke thickness, hence

making it possible to increase the rotor size in the same overall motor volume again. However, the mechanical and manufacturing issues must be taken into account, and hence, the stator yoke cannot be always made as thin as the magnetic calculations should indicate. For example if the stator yoke is welded, typically 5–10 mm of the yoke material is easily lost because of the weld penetration in the yoke.

### 3.3 Inductances and torques of concentrated winding machines in the cases of a semi-closed slot opening and a totally open slot

Inductances are evaluated for concentrated winding machines, when  $q$  varies from 0.5 to 0.25; both open slots and semi-closed slot structures are studied. The pull-out torques for some concentrated winding machines with rotor surface magnets are given in Fig. 3.7 (Salminen 2004, Lindh et al. 2009).

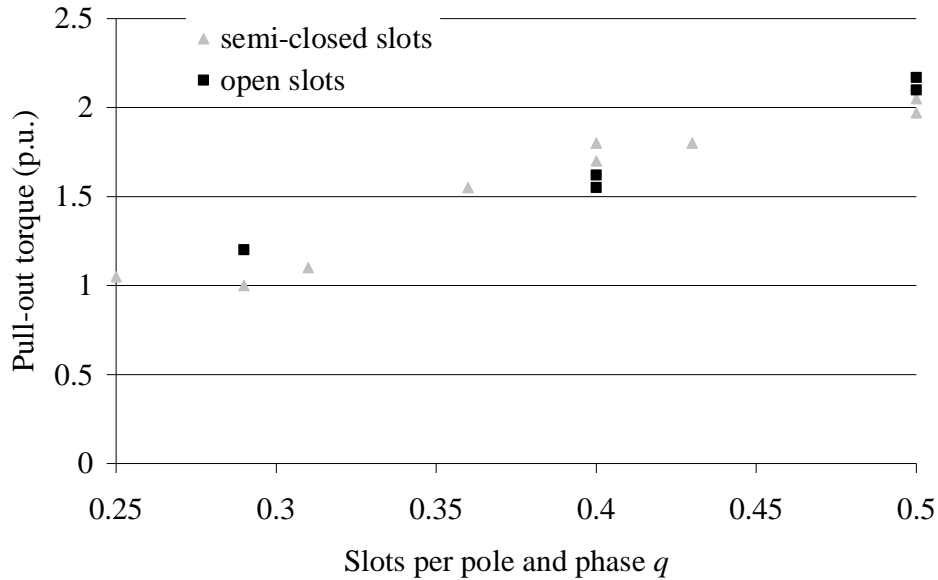


Fig. 3.7. Pull-out torques of some concentrated winding machines with rotor surface magnets (Lindh et al 2009).

With open and semi-closed slots, the machine main flux varies significantly, and hence, the number of turns in series per stator windings varied from 84 to 120 to induce a similar back-emf, which was at least 0.9 of the supply voltage. The induced back electromagnetic force RMS value can be calculated as

$$E_{\text{PM}} = \frac{\omega_s N_s k_{w, \text{wh}} \hat{\Phi}}{\sqrt{2}} \quad (3.3)$$

where  $\omega$  is the electric angular frequency,  $N_s$  the number of turns in series per stator winding,  $k_{w,wh}$  the fundamental or working harmonic winding factor and  $\hat{\Phi}$  the peak value of the flux passing through the magnetic pole.

Machines with open slot structures must have more winding turns compared with machines with semi-closed slot structures to produce the same back-emf. This is because the amount of flux that can flow through the air gap to the stator teeth is higher in the semi-closed structure. In an open slot structure there are narrow teeth facing the air gap, and therefore, the area through which the flux can flow is smaller. Figure 3.8 illustrates the effect of semi-closed and open slots.

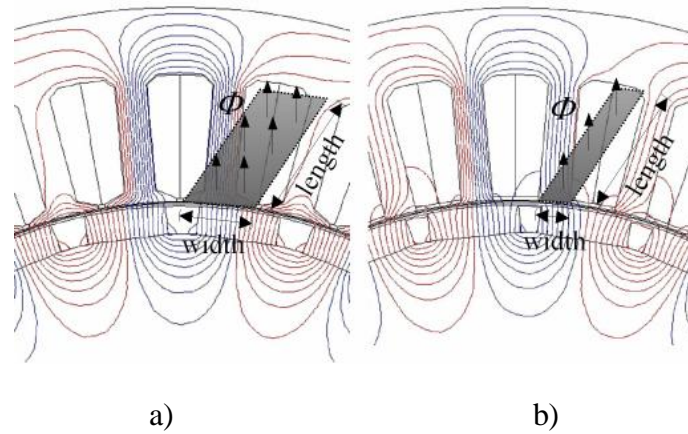


Fig. 3.8. 36-slot-24-pole motor, which has a) semi-closed slot openings with the relative slot opening width of 0.09 of the slot pitch and b) open slots with relative slot opening width of 0.6 of the slot pitch (Lindh et al. “Concentrated Wound PM Motors with Semiclosed Slots and with Open Slots.” *IEEE Energy Conversion* (forthcoming)).

In (Lindh et al. 2009) it was observed that with semi-closed slots the efficiencies of different machines were slightly better. This is, of course a result of the main flux variation and the change of the number of turns.

### 3.4 Summary

Concentrated winding permanent magnet machines with rotor surface magnets give a high torque, when the number of slots per pole and phase  $q$  is chosen to be either 0.4 or 0.5. The concentrated winding machines with  $q = 0.5$  produce the highest pull-out torque values. However, using this number of slots per pole and phase ( $q = 0.5$ ) leads to high sensitivity in selecting the machine dimensions because the torque quality of the machine is strongly dependent on correct mechanical dimensions (Salminen 2004, Salminen et al. 2006). Furthermore, very high torque ripples and cogging torques easily occur in a  $q =$

0.5 machine (Salminen 2004, Salminen et al. 2006). In most studied cases, the concentrated winding machines give a lower pull-out torque than integral slot winding machines with the same rotor dimensions. However, concentrated winding machines provide some benefits such as small copper losses and small end windings in certain applications.

Rotor surface magnet motors with open slot structures give slightly higher pull-out torques, but the efficiencies of the open slot structures remain somewhat lower than in motors with semi-closed slots. This is mainly due the higher stator Joule losses. An attractive solution would be to manufacture machines with totally open slots to have the simplest possible stator structure, which of course also provides a means to reduce production costs. Open slot machines can be wound automatically.

According to the previous study, the 12-slot-10-pole concentrated winding machine is one of the best alternatives when concentrated winding machines, in general, are desired. Its torque producing capability is almost as good as with  $q = 0.5$  machines (Salminen 2004) and not very much lower than in integral slot winding machines. As the winding arrangement provides an opportunity to increase the rotor size in a certain overall size compared with integral slot winding machine rotors, it seems that the 12-10-machine is a good compromise among concentrated winding machines with  $q \leq 0.5$ .

In the following chapter, a new 12-10-axial-flux PMSM construction is introduced for normal industrial speeds. The basic construction was selected because its manufacturing costs are low compared with integral slot winding machines and because it is easy to integrate such a short machine into a working machine construction such as a fan or a compressor. Such machines operate at normal industrial speeds from 1500 to 6000  $\text{min}^{-1}$ . In this speed range, a special problem with concentrated winding and open slot machines is the heavy permeance-harmonics-caused eddy current loss in the permanent magnets, and therefore special effort has been put to find a solution to solve the magnet heating problem in the design.

#### 4 PROTOTYPE MACHINE AND TEST RESULTS

The prototype machine is a two-stator-one-rotor axial flux permanent magnet machine with an ironless rotor. The rotor is regarded here as a surface magnet rotor as the magnets are facing the stators. In the tests, the machine was equipped with different rotors, in particular with different kinds of magnet arrangements. As the rotor is of special construction, there are no iron losses under the magnets; such losses are possible in other types of permanent magnet machines. The magnets define the rotor thickness and are facing both stators. The stator winding is a double-layer concentrated winding, where the number of slots per pole and phase  $q = 0.4$ . The two stators are electrically connected in series to ensure good balance of the machine. The magnet material type is NdFeB 495a by Neorem Magnets, see Fig. 1.2 in the introduction. The construction of NdFeB magnets varied from just one bulky magnet per pole to segmented magnets where there were 20 magnet segments per pole either in radial or tangential direction. The magnet segments are glued together. The thickness of the glue is 0.1 mm in each bond.

The rotor core material is totally nonconductive and made of impregnated glass fibre. The stator material is standard electrical steel sheet 270-35A (Cogent 2009). The rated power of the machine is 37 kW and the rated rotational speed  $2400 \text{ min}^{-1}$ . The winding arrangements are shown in Fig. 4.1. Some main dimensions and mechanical arrangements are illustrated in Fig. 4.2.

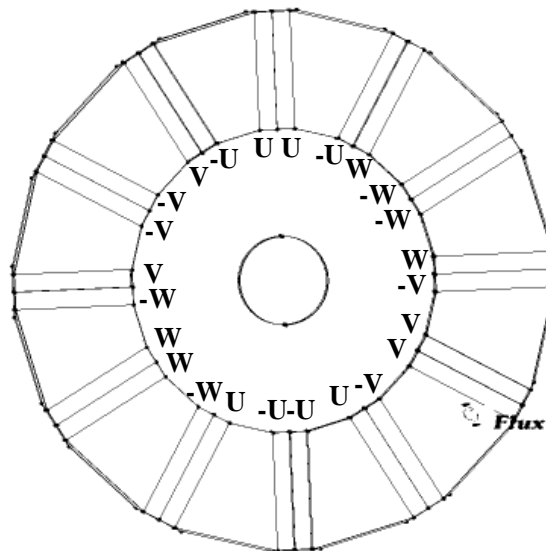


Fig. 4.1. Locations of the stator coil sides in slots

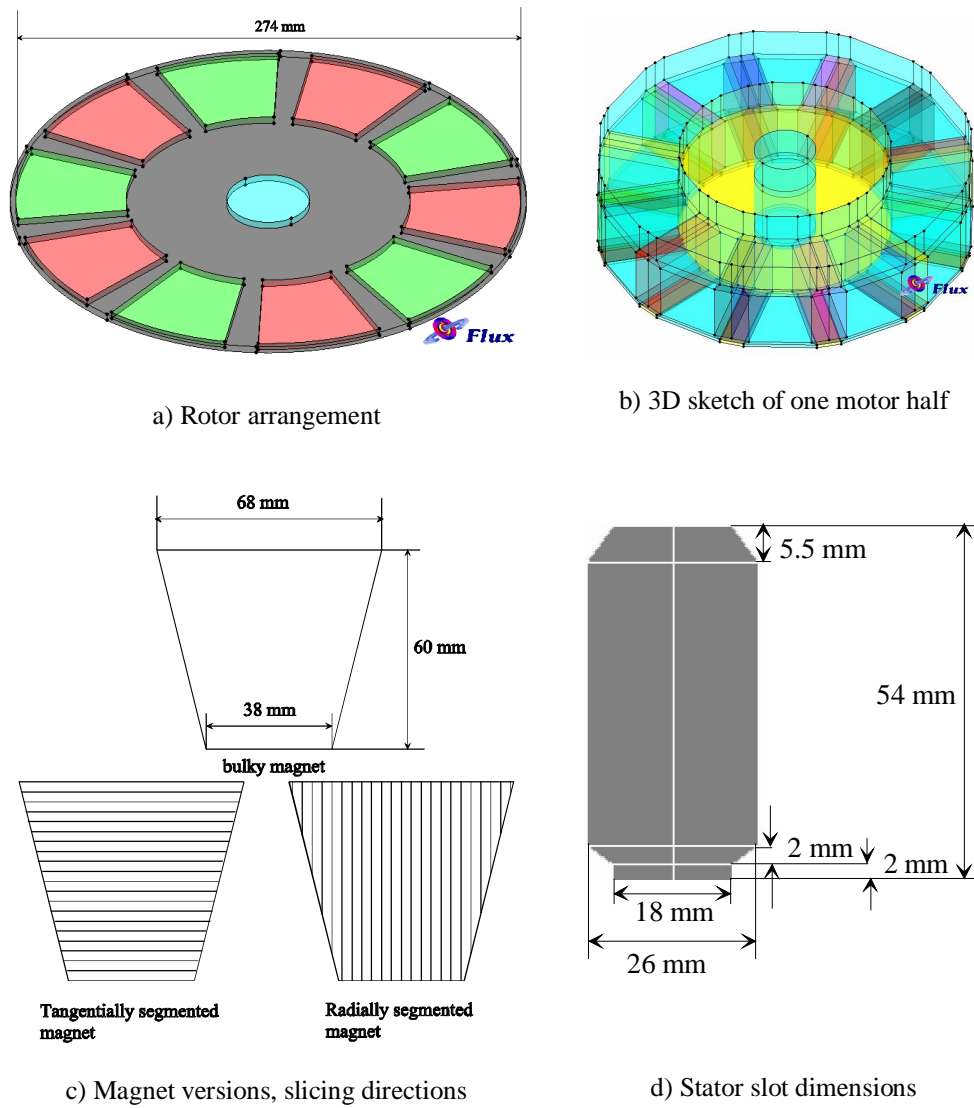
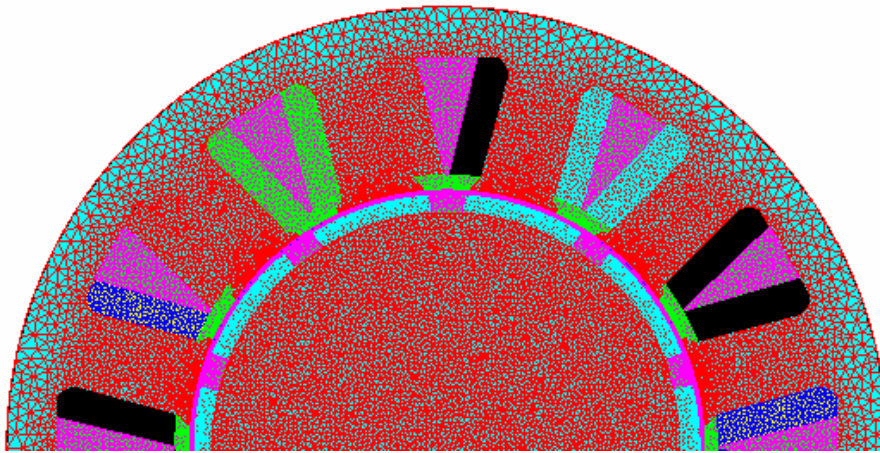
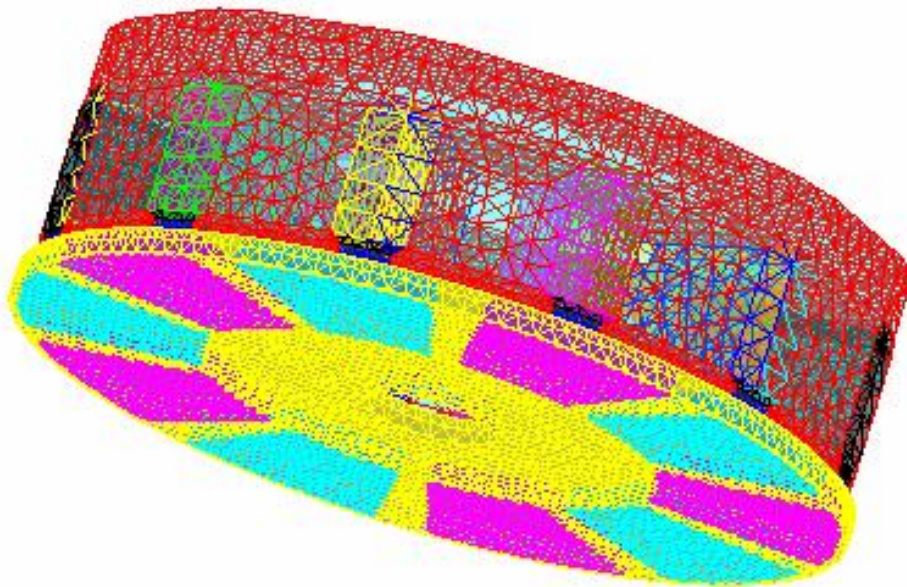


Fig. 4.2. Main dimensions and mechanical arrangements.

Figure 4.3 illustrates the mesh used in the FEA calculations and the time steps applied in the 2D and 3D FEA;  $6.94 \mu\text{s}$  in 2D and  $34.7 \mu\text{s}$  in 3D.



a)



b)

Fig. 4.3. Mesh figures in a) radial flux machine 2D FEA and b) axial flux machine 3D FEA.

Some of the motor parts are shown in Fig. 4.4. Fig. 4.4a shows the stator lamination stack before the windings were inserted. Fig. 4.4b shows one of the stators equipped with the two-layer concentrated winding. Fig. 4.4c illustrates the glass-fibre-made magnet supporting rotor frame and Fig. 4.4d shows the rotor with magnets inserted.

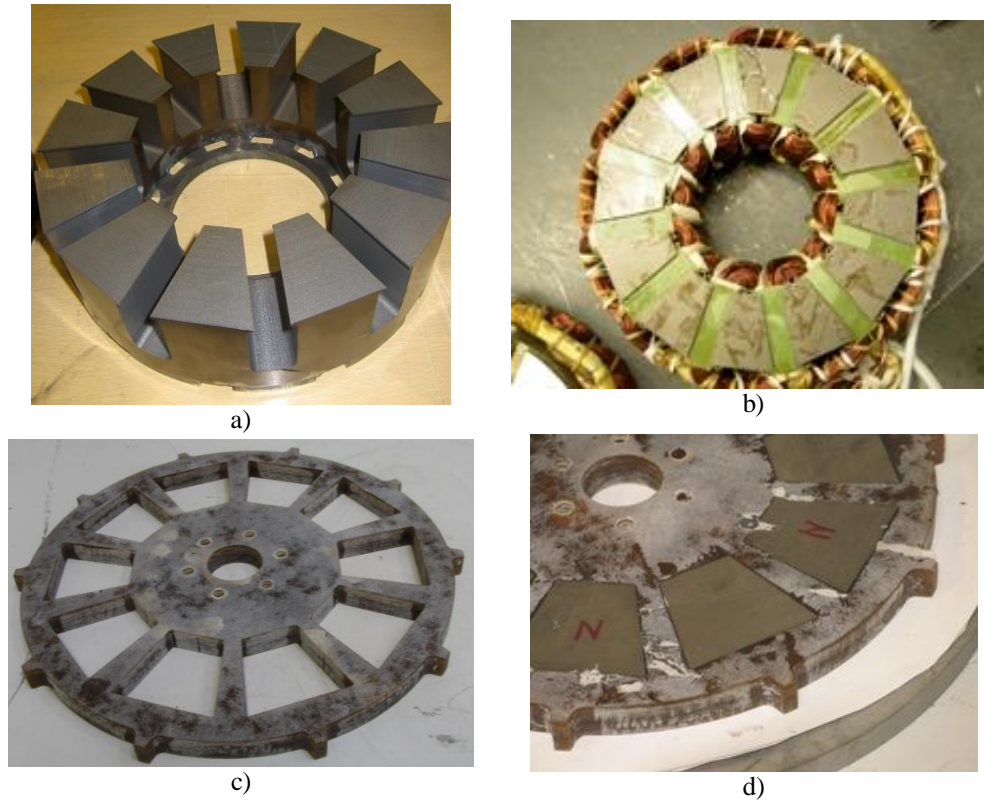


Fig. 4.4. a) Stator lamination stack, b) one stator equipped with windings, c) rotor frame, d) rotor with magnets assembled

As it can be seen in Fig. 4.4a, the stator lamination is not ideal as the teeth do not bend but all the bending takes place in the stator yoke adjacent to the slot area. This causes a radius variation to the stator lamination, which may cause slight extra losses in the motor.

The main parameters of the machine are listed in Table 4.1.

Table 4.1. Main parameters of the prototype machines.

Number of stator slots, $Q$	12
Number of rotor poles, $2p$	10
Winding factor of the fifth harmonic of the stator (the machine operates with the fifth harmonic), $k_{w5}$	0.933
Output power, $P_{out}$	37 kW
Speed, $n_s$	2400 min <sup>-1</sup>
Line-to-line terminal voltage in star connection, $U$	400 V
Winding turns in series per stator winding, $N_s$	64
Rated torque, $T_N$	147 Nm
Rated current, $I_s$	59–61 A
Length of air gap (on both sides of the rotor) $\delta$	2.0 mm
External diameter of the stator stack, $D_{o, axial}$	274 mm
Internal diameter of the stator stack, $D_{i, axial}$	154 mm
Stator yoke height, $h_{ys}$	21 mm
Thickness of PM, $h_{PM}$	16 mm
PM remanent flux density, 20 °C, $B_{r20C}$	1.1 T
PM remanent flux density, 80 °C, $B_{r80C}$	1.03T
Mass of magnets (NdFeB), $m_{PM}$	3.9 kg
PM resistivity $\rho_{PM}$	150 $\mu\Omega\text{cm}$

The machine is totally enclosed and fan cooled. Fig. 4.5 illustrates the motor without and with a fan. The fan motor input power is 350 W.

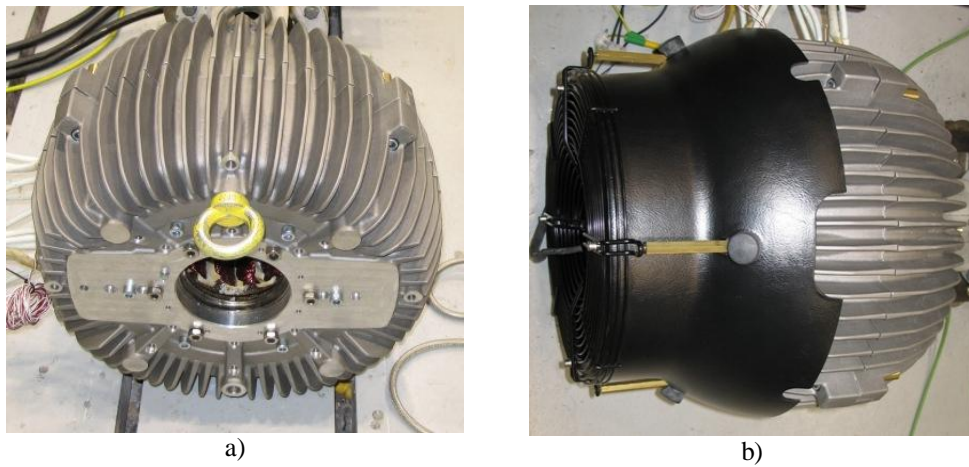


Fig. 4.5. Motor without a fan and with an externally operated fan.

In the measurements, the prototype motor was fed by a variable-speed frequency converter (ABB M1 DTC converter) and rotated or loaded with a direct current (DC) machine drive. The torque of the motor was measured with two different torque transducers; in the load tests, the rated torque of the torque transducer was 200 Nm, and when the rotor mechanical loss and the permanent magnet losses were measured in the DC motor drive, the torque transducer rated torque was selected to be 50 Nm in order to obtain more accurate results for the rotor mechanical loss. The electrical values of the PM machine drive were measured with a Yokogawa PZ4000 power analyzer. Table 4.2 shows the measurement devices and their uncertainties, and Fig. 4.6 illustrates the test setup.

Table 4.2. Measurement devices and their accuracies.

Measurement device	Measurement uncertainty (% of the rated value)
Torque transducer: Vibrometer, Torquemaster TM-214	0.2
Torque transducer: Vibrometer, Torquemaster TM-204	0.2
Reading unit for torque transducer: Vibrometer, DCU 280	0.1
Power analyzer: Yokogawa PZ4000	0.1
Current transducers	0.2
Reading unit for the temperature values: Fluke Hydra 2620A	0.1

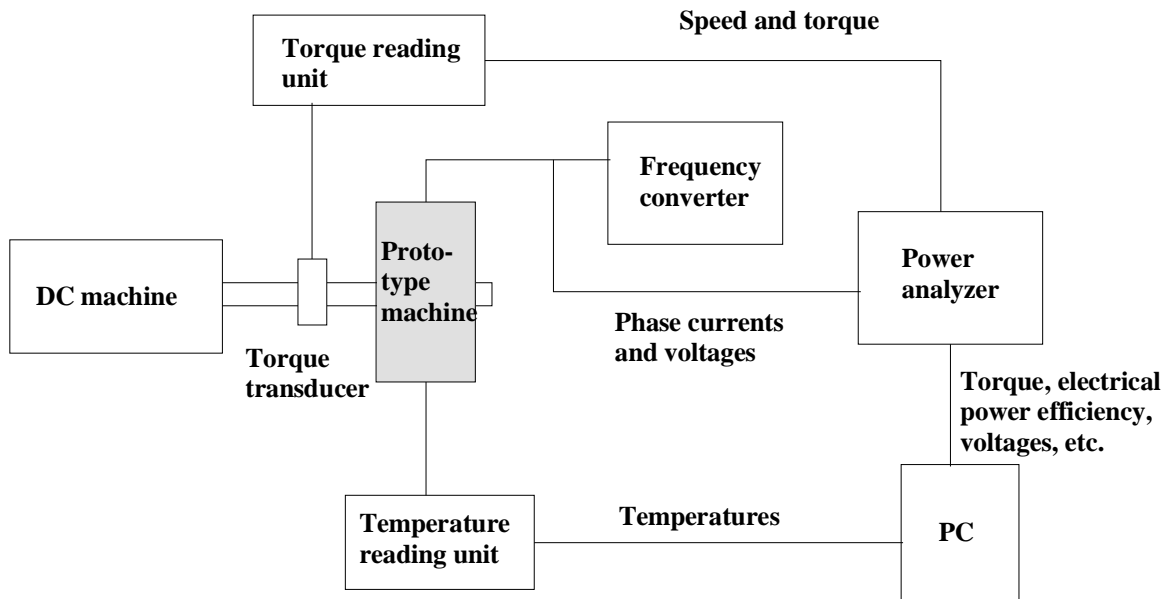


Fig. 4.6. Load test arrangement for the concentrated winding axial flux PM. The measured prototype motor was supplied by a frequency converter. The torque and the rotating speed were measured with a Vibrometer torque transducer. The electric power was measured with a Yokogawa PZ4000 power analyzer equipped with three current transformers. Four thermoelements were mounted in the stator windings and two in both stators for temperature analyses. A Fluke Hydra 2620A measured the temperatures.

The main parameters of the frequency converter are given in Table 4.3.

Table 4.3. ABB M1 DTC converter parameters.

Average switching frequency	4 kHz
Converter rated current	60 A
Converter input voltage	400 V
Motor rated voltage	230 V
Motor rated speed	2400 min <sup>-1</sup>
Motor supply frequency	200 Hz
Motor power	37 kW

#### 4.1 Stator resistance

The stator phase resistance was measured with four wire measurements to be 0.02 mΩ for one stator at room temperature. 0.047 mΩ was measured for the whole motor by using the motor identification run of the ABB M1 frequency

converter. The motor cabling was taken into account in the measurement results by the frequency converter.

### No-load measurements

The no-load tests were performed in the generator mode using the DC machine drive as a prime mover. The no-load test was performed to evaluate the induced back-emf, stator iron losses, the Joule losses of the permanent magnets and the mechanical loss in no-load conditions. The measured no-load voltages of the machine are given in Table 4.4.

Table 4.4. Measured and calculated FEA 2D/3D voltages at no load at  $2400 \text{ min}^{-1}$  in the generator mode.

Rotor equipped with	Measured EPM (V)	2D FEA EPM (V)	3D FEA EPM (V)
radially segmented magnets	220	222	-
tangentially segmented magnets	227	-	-
bulky magnets	220	229	225

The analysis of the voltages given in Table 4.4 is presented in Figs. 4.7 and 4.8. A comparison of no-load voltage waveform between the measurements and the computation results are given in Fig. 4.7, whereas Fig. 4.8 illustrates the effect of segmentation. The figure shows a slight voltage drop, which is proportional to reduction in the magnet volume caused by the glue bonds between the segments.

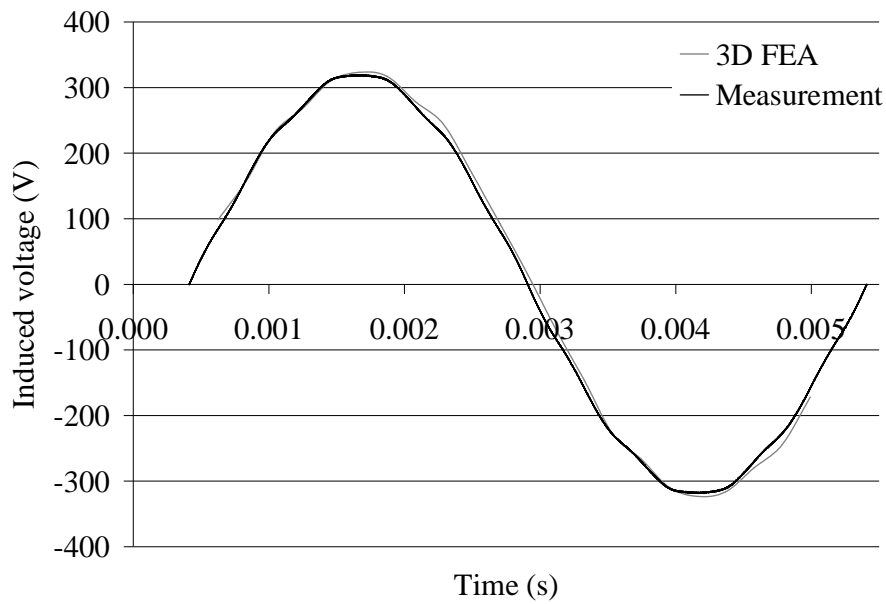


Fig. 4.7. Voltage with the 3D FEA and the measurement. The no-load voltage waveform was measured for the motor equipped with bulky magnets, and it corresponded well with the voltage computed by the 3D FEA.

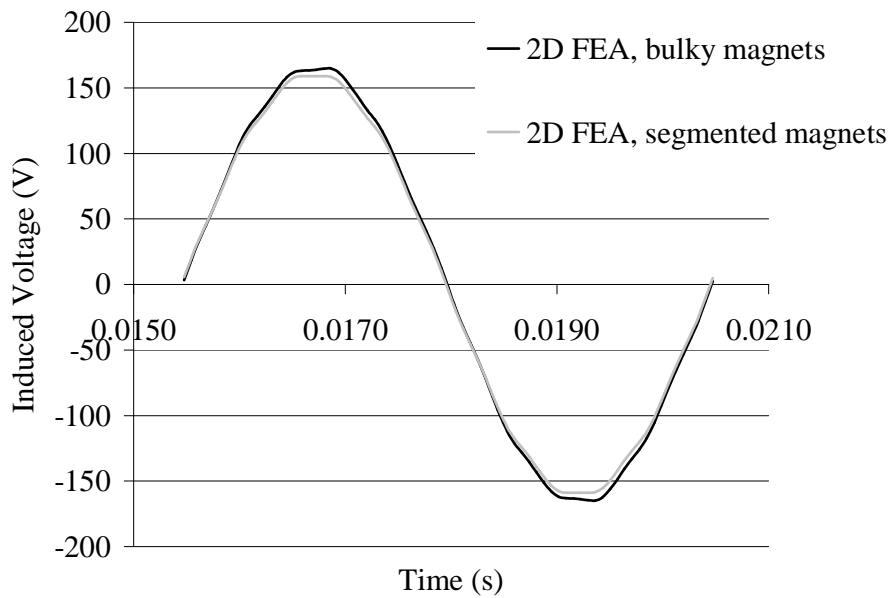


Fig. 4.8. Effect of segmentation. The voltage drop is proportional to the change in volume of the magnet mass when segmented magnets (20) are used. Half of the axial flux machine (one stator) is modelled to the radial flux machine.

One of the most important and interesting results is related to the losses of the permanent magnets. To find the permanent magnet losses, the no-load mechanical loss of the rotor was first measured without magnets. The permanent magnet slot openings were covered during the test to ensure a smooth rotor surface. The loss was measured by using a 50 Nm torque gauge, and the result may be considered reliable. The no-load mechanical loss of the machine was measured to be 170 W. The measured no-load losses of the machine are given in Table 4.5.

Table 4.5. Measured losses at no load at  $2400 \text{ min}^{-1}$  in the generator mode compared with the 2D FEA results.

Rotor equipped with	Measured losses (W)	2D FEA losses (W) + measured mechanical losses (170 W)
radially segmented magnets	630	630
tangentially segmented magnets	680	- (not possible to calculate with 2 D)
bulky magnets	2000	2400
Rotor frame (no magnets)	170	-

There are also some differences in the measurements of the motor equipped with rotors having either radially or tangentially segmented magnets. This is mainly because there were some difficulties in achieving exactly the same air gap lengths in all cases. There was also a voltage drop in the actual measurement, which may partly explain the smaller loss in the case of bulky magnets. The measured loss was smaller than the loss evaluated by the 2D FEA.

To find out the losses in the permanent magnets, the stator no-load iron losses should be known. As the motor flux cannot be varied, definition of the iron losses is difficult. Hence, FEA calculations are used to facilitate the definition of the iron losses at no load. According to the finite element analysis, the iron losses in the stator should be 370 W at  $E_{PM} = 229 \text{ V}$ . With segmented magnets, the iron losses in the stator were calculated to be 350 W at  $E_{PM} = 222 \text{ V}$ . The corresponding losses in the bulky magnets were calculated to be 1900 W, and in the segmented magnets 110 W. Table 4.6 gives an estimation of the loss division at no load.

Table 4.6. Loss division at no load at 2400 min<sup>-1</sup> in the generator mode. No-load losses and mechanical losses are measured, while iron losses and loss in PMs are estimated from the 2D FEA results.

Rotor equipped with	No-load loss (W), meas.	Mechanical loss (W), meas.	Iron loss (W), FEA	Loss in PM (W), FEA	Loss in PM (W) = No-load loss - Mechanical loss - Iron loss
radially segmented magnets	630	170	350	110	110
tangentially segmented magnets	680	170	350 (estimation)	-	160
bulky magnets	2000	170	370	1900	1500

There is a 50 W difference in the loss results of the tangentially and radially segmented magnets. In practice, it is impossible to say which segmentation produces the smallest losses as the difference may result from a measurement uncertainty or it may be caused by differences in the motor assemblies. Nevertheless, the loss in the bulky non-segmented magnet is about 1500 W, which is such a large value that it cannot be accepted. Actually, the non-segmented magnets were slightly demagnetized during the no-load test because of too large a heat stress. This test very clearly indicated that there can be severe losses in NdFeB magnets if harmonic flux density components are present. This motor type emphasizes the losses in bulky magnets, but the motor can be operated with segmented magnets with a good efficiency.

## 4.2 Load measurements

The machine was driven as a motor supplied by an ABB M1 frequency converter and loaded with a DC motor drive to achieve a rated output power of 37 kW. The most important results are given in Table 4.7. The distribution of losses is given in Table 4.8.

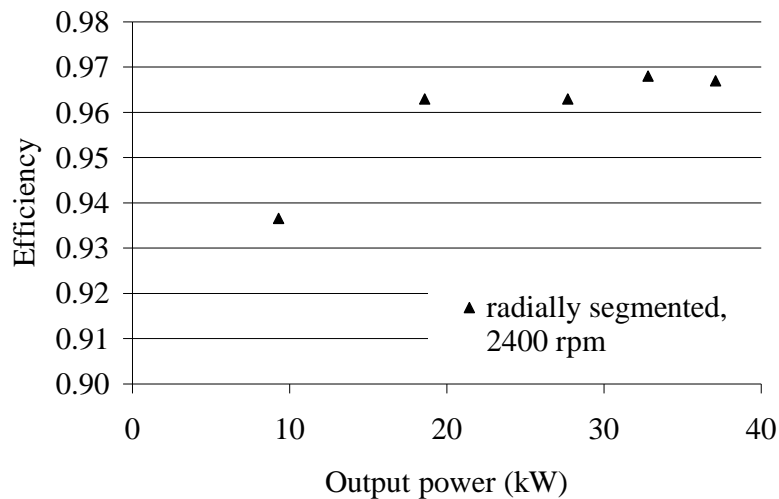
Table 4.7. Measured losses at the rated load at 2400 min<sup>-1</sup> in the motor mode.

Rotor equipped with	Measured total losses (W)
radially segmented magnets	1250
tangentially segmented magnets	1300
bulky magnets	-
no magnets	170

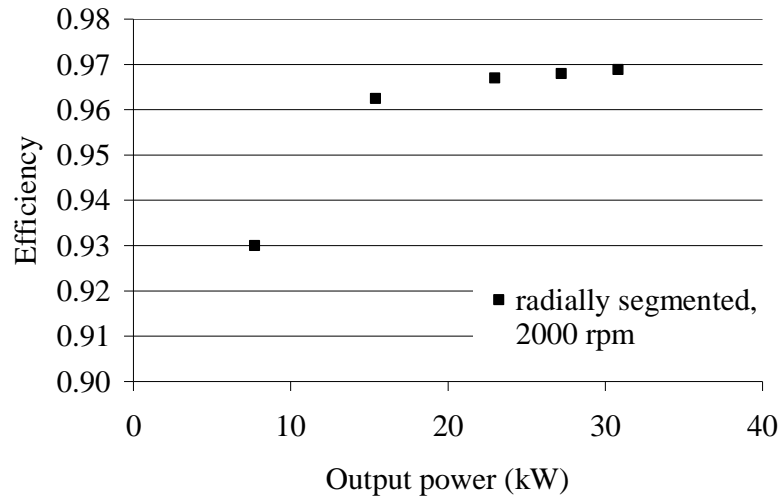
Table 4.8. Loss distribution at load at  $2400 \text{ min}^{-1}$  in the motor mode. The load losses and mechanical losses are measured, while the iron losses, copper losses and loss in the PMs are estimated from the 2D FEA results.

Rotor equipped with	Load loss (W), meas.	Mechanical loss (W), meas.	Iron loss (W), FEA	Copper loss (W), calc.	Loss in PM (W), FEA	Loss in PM (W) (+ additional loss (W)) = Load loss - Mechanical loss - Iron loss - Copper loss
radially segmented magnets	1250	170	330	560	100	190
tangentially segmented magnets	1300	170	330 (estimation)	560	-	240

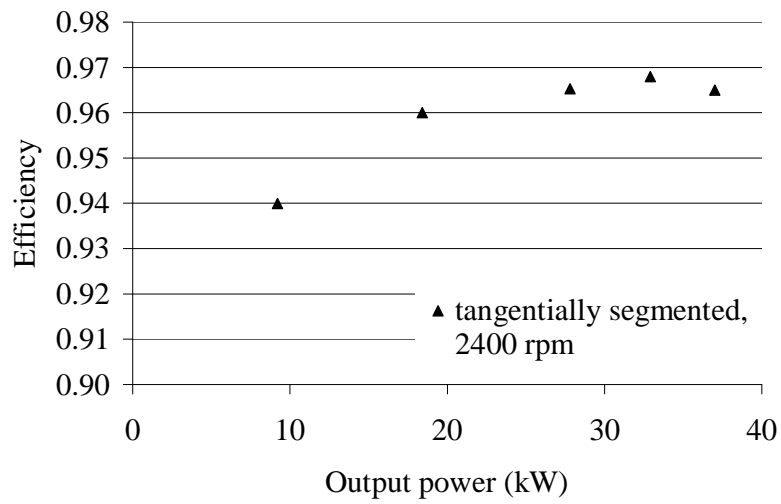
The efficiency of the prototype motor with both segmented magnets at the rated load was measured to be between 0.96–0.97. The measured efficiencies with two different rotational speeds are shown in Fig. 4.9.



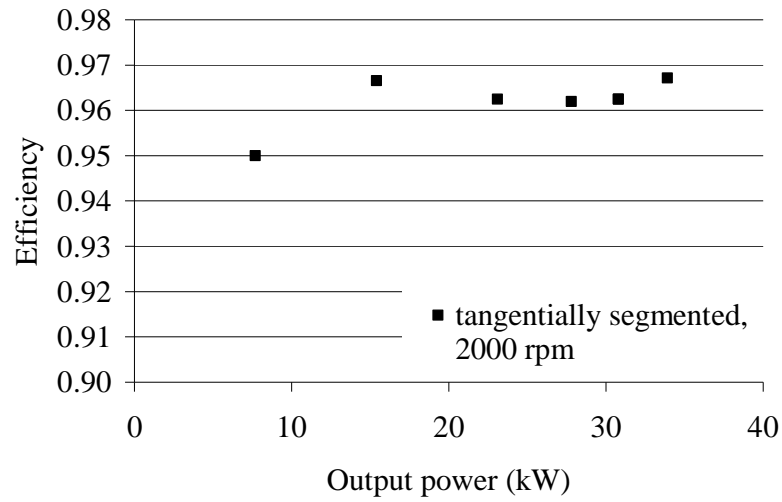
a)



b)



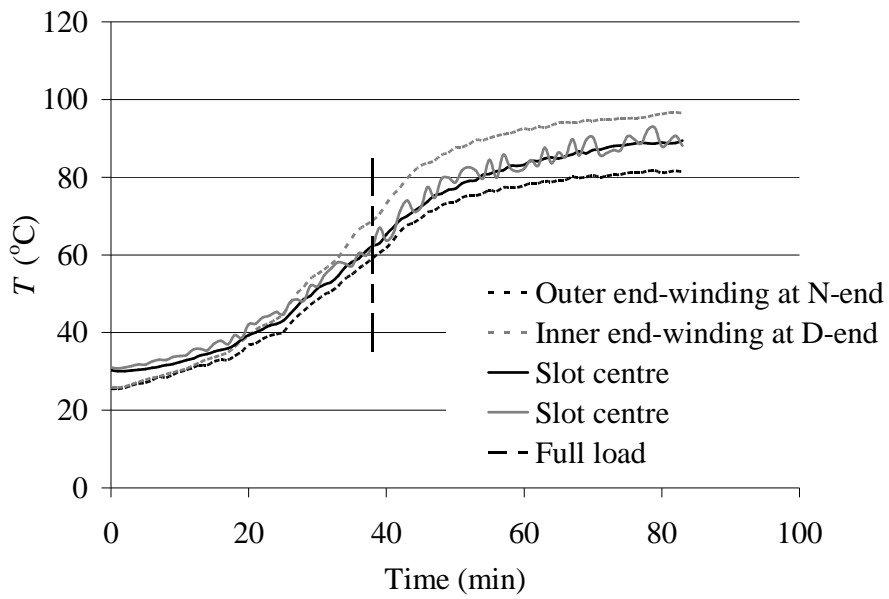
c)



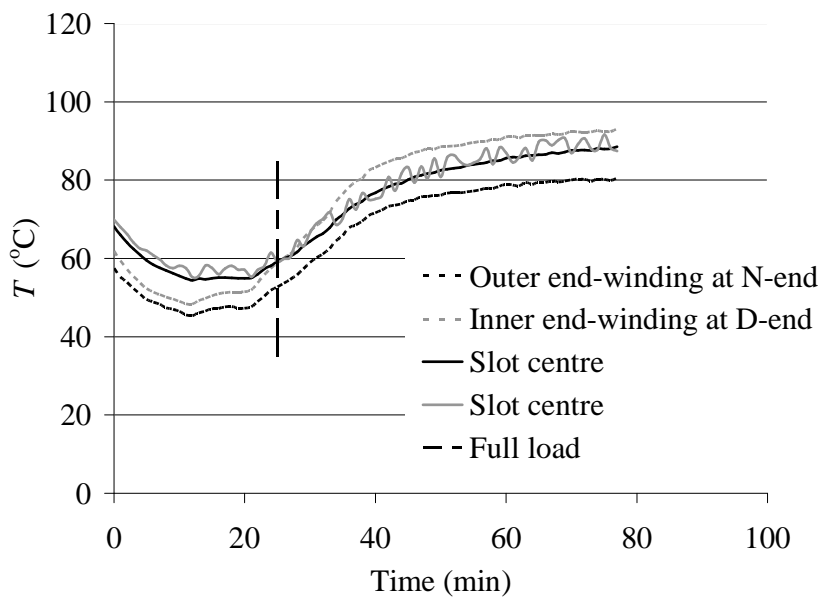
d)

Fig. 4.9. Measured efficiencies with radially and tangentially segmented magnets at 2400 and 2000  $\text{min}^{-1}$ .

The phase winding temperatures with two different rotational speeds are shown in Fig. 4.10.



a)



b)

Fig. 4.10. Temperatures at rated loads. a) Radially segmented and b) tangentially segmented magnets at  $2400 \text{ min}^{-1}$ .

### 4.3 Maximum pull-out torques

The torque as a function of load angle for the bulk and segmented magnet (20 pieces) machines calculated by the 2D are shown in Fig. 4.11 and Fig. 4.12.

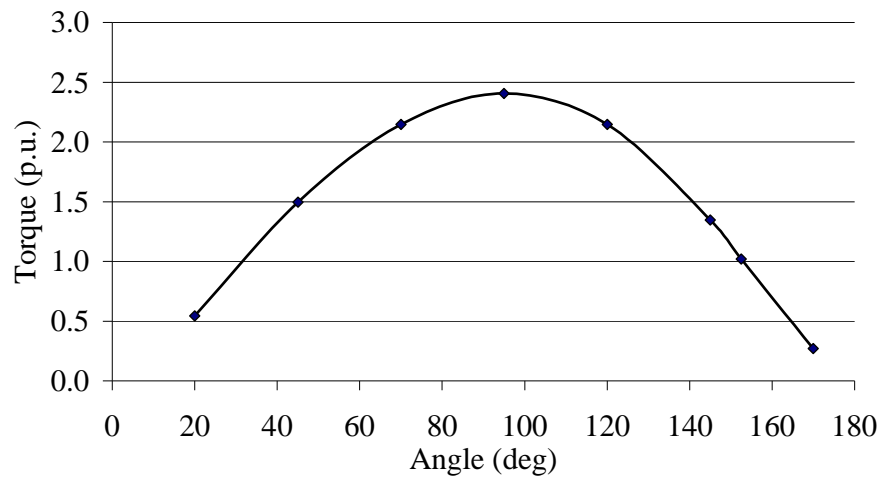


Fig. 4.11. Torque curve as a function of load angle for the bulk magnet machine.

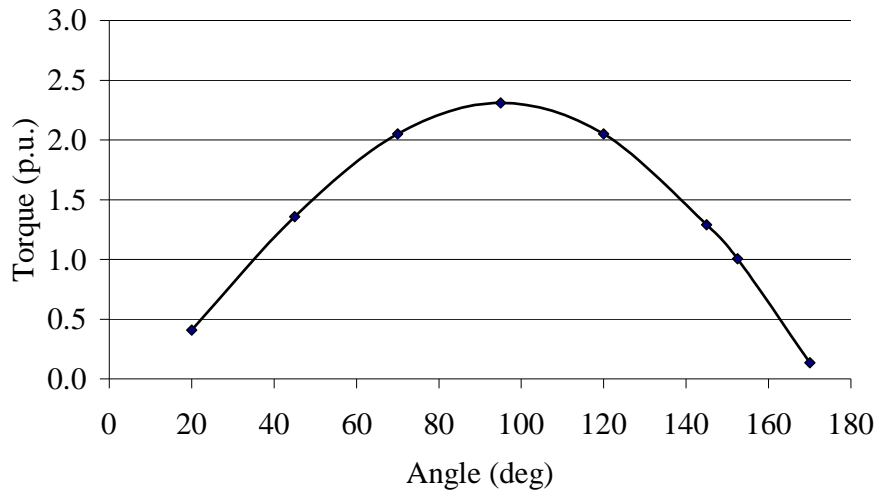


Fig. 4.12. Torque curve as a function of load angle for the segmented (20 pieces) magnet machine.

Figures 4.10 and 4.11 show that the bulk magnets produce more torque than the segmented magnets.

#### 4.4 Cogging torque with the 2D and 3D FEA

The cogging of the motor was calculated both with the 2D and 3D FEA. The cogging of this motor is, however, not very important as the motor is mainly aimed at integrated pump and fan applications, and hence, the cogging torque of the machine was not measured. One may also observe that the cogging torque is not very high, about 3–4 % of the rated torque. The waveform of the cogging torques calculated with the 2D and 3D FEA are shown in Fig. 4.13.

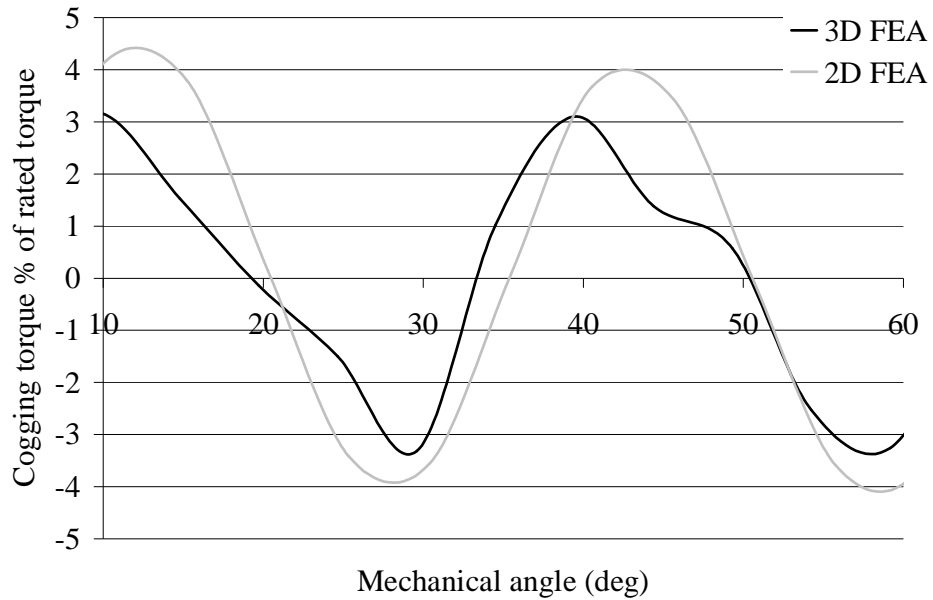


Fig. 4.13. Peak-to-peak values of the cogging torque in (%) of the rated torque with the 2D and 3D FEA.

#### 4.5 Summary

A 37 kW axial flux machine was designed and constructed. A comparison between the theoretical and experimental results with the prototype machine was presented. The analytical, 2D and 3D FEA values together with the measured values show a good agreement.

## 5 CONCLUSION

The work focused on the properties of concentrated winding multiphase permanent magnet machines. Such machines have their benefits and drawbacks; however, their analytical calculation and also the 2D FEA-based analysis will pose some challenges. The 3D FEA is a good design tool, yet too time consuming for practical applications at the moment.

The benefits of the machine type may be regarded as:

- Extremely compact design.
- Low amount of copper needed as the end windings are very short compared with traditional integral slot winding machines.
- Small stator and rotor yokes needed as pole numbers are high.
- Large rotor volume, and hence, large torque per predetermined outer dimensions.
- Suitable construction for, especially, large-torque low-speed applications.
- Good torque quality when properly designed.
- Low manufacturing costs because prefabricated windings can be used, especially, in open slot constructions.

The main drawbacks of the machine type are:

- Difficult to design applying traditional analytical methods.
- High permanent magnet losses as the flux density in the permanent magnets fluctuates heavily because there is no smooth stator surface, but between each tooth there can be large spaces of air that make the permanent magnet material flux density vary considerably causing high losses in sintered materials.
- At higher speeds, more expensive segmented permanent magnets are needed to avoid large Joule losses in the magnets.

In the work, concentrated winding multiphase machines were analyzed numerically by Cedrat's Flux2D/3D version 10.2.4. and by measurements. One

of the objectives of this study was to study the effect of permanent magnet segmentation in a concentrated winding multiphase axial flux machine. Also the effect of the segmentation directions on the motor performance and the PM Joule losses were studied experimentally.

The scientific contributions of this thesis can be listed as:

1. A set of analytic equations and methods were found to design a 12-slot 10-pole axial-flux machine with rotor-surface-mounted magnets.
2. The correct effective length of a PMSM with rotor surface magnets was determined.
3. Stator leakage inductance, especially air gap leakage inductance calculation was clarified.
4. The torque production capabilities of concentrated winding and integral slot winding machines were compared.
5. The permanent magnet Joule losses in an axial flux PMSM with open slots operating at a typical industrial machine speed were evaluated.
6. A new practical permanent magnet motor type for industrial use was introduced.

After having built a prototype with several different rotor constructions, the induced back-emfs of the three different rotor constructions were measured at no load. The analytical results, Cedrat's Flux2D/3D results and the measured results of the no-load voltage were compared. There was quite a good correspondence between the measured, 2D and analytical results of the segmented magnets.

One of the rotors was equipped with bulky permanent magnets. It became obvious already in the no-load tests that bulky magnets cannot be used in these kinds of machines because of excessive Joule losses in the magnets.

The efficiencies of the three different rotor constructions were measured in no-load and load tests. The permanent magnet losses at no load were separated by measuring the friction losses without permanent magnets in the rotor and calculating the stator Joule losses by Cedrat's Flux2D/3D. At load also the stator copper losses are taken into account. Of course, there occurred also some inverter-caused time-harmonic-based losses in the measurements; however, these losses were not studied in detail in the thesis.

## **5.1 Future Work**

In the analytic calculation of Joule losses, a considerable uncertainty still remains, and hence, the calculation methods should be further developed. Optimization of the magnet width and the slot opening width to reduce cogging

in the proposed motor design should be carried out. The Joule losses in the magnets could maybe be further reduced by suitable means, for instance, by using semi-magnetic slot wedges. Moreover, the mechanical construction of the ironless rotor should be further developed to reach higher speeds and a more rigid rotor construction as a whole.

## REFERENCES

ABB, 2007. Product catalogue : *IEC Low Voltage Induction Motors 400 V 50 Hz*. [Online]. Available from <http://www.abb.com/> [Accessed 5 October 2009].

Amara, Y., Jiabin W. and Howe, D. 2005. "Analytical Prediction of Eddy-Current Loss in Modular Tubular Permanent-Magnet Machines." *IEEE Transactions on Energy Conversion*. Vol. 20, Issue 4, pp. 761–770.

Arrillaga, J. and Watson, N.R. 2003. *Power System Harmonics*. Chichester: John Wiley & Sons, Ltd.

Atallah, K., Howe, D., Mellor, P.H. and Stone, D.A. 2000. "Rotor Loss in Permanent Magnet Brushless AC Machines." *IEEE Transactions on Industry Applications*. Vol. 36, Issue 6, pp. 1612–1618.

Baracat, G., El-Meslouhi, T. and Dakyo, B. 2001. "Analysis of the Cogging Torque Behavior of a Two-Phase Axial-flux Permanent Magnet Synchronous Machine." *IEEE Transactions on Magnetics*. Vol. 37, Issue 4, pp. 2803–2805.

Bertotti, G., Boglietti, A., Chiampi, M., Chiarabaglio, D., Fiorillo F. and Lazzari, M. 1991. "An Improved estimation of Iron Losses in Electrical Machines." *IEEE Transactions on Magnetics*. Vol. 27, Issue 6, pp. 5007–5009.

Cedrat, 2009. Software solutions: Flux®. [Online]. Available from <http://www.cedrat.com/> [Accessed 2 April 2009].

Cistelecan, M.V. and Popescu, M. 2007. "Study of the Number of Slots/Pole Combinations for Low Speed Permanent Magnet Synchronous Generators." *In Proceedings Electric Machines & Drives Conference, IEMDC 2007*. Vol. 2, pp. 1616–1620.

Cogent, 2009. Product catalogue: *Non-oriented Fully Processed Electrical Steels*. [Online]. Available from <http://www.sura.se/> [Accessed 5 October 2009].

Cros, J., Viarouge, P. 2002. "Synthesis of High Performance PM Motors With Concentrated Windings." *IEEE Transactions on Energy Conversion*. Vol. 17, Issue 2, pp. 248–253.

Cros J., Viarouge, P., Carlson, R. and Dokonal, L.V. 2004. "Comparison of brushless DC motors with concentrated windings and segmented stator." *In Proceedings of the International Conference on Electrical Machines, ICEM 2004*. Krakow, Poland. CD.

- Deak, C., Binder, A. and Magyari, K. 2006. "Magnet Loss Analysis of Permanent Magnet Synchronous Motors with Concentrated Windings." In *Proceedings of the XVII International Conference on Electrical Machines, ICEM 2006*. Chania, Crete Island, Greece. CD.
- Deak, C., Petrovic, L., Binder, A., Mirzaei, M., Irimie, D. and Funieru, B. 2008. "Calculation of Eddy Current Losses in Permanent Magnets of Synchronous Machines." In *Proceedings of the International Symposium on Power Electronics, Electrical Drives, Automation and Motion, SPEEDAM 2008*. Ischia, Italy.
- Deng, F. 1999. "An Improved Iron Loss estimation for Permanent Magnet Brushless Machines." *IEEE Transactions on Energy Conversion*. Vol. 14, Issue 4, pp. 1391–1395.
- Dupas, F. and Espanet, C. 2009. "Analytical Solution of the Magnetic Field in Permanent-Magnet Motors Taking Into Account Slotting Effect: No-Load Vector Potential and Flux Density Calculation." *IEEE Transactions on Magnetics*. Vol. 45, Issue 5, pp. 2097–2109.
- Ede, J.D., Atallah K. and Jewell, G.W. 2007. "Effect of axial segmentation of permanent magnets on rotor loss in modular permanent-magnet brushless machines." *IEEE Transactions on Industry Applications*. Vol. 43, Issue 5, pp. 1207–1213.
- Ede J.D., Atallah, K., Jewell G.W., Wang J. and Howe, D. 2002. "Effect of Axial Segmentation of Permanent Magnets on Rotor Loss in Modular Permanent-Magnet Brushless Machines." In *Proceedings of the IEE International Conference on Power Electronics, Machines and Drives, PEMD 2002*. University of Bath, the UK, pp. 445–420.
- El-Refaie, A.M. and Jahns, T.M. 2006. "Scalability of surface PM Machines with concentrated windings designed to achieve wide speed ranges of constant power operation." *IEEE Transactions on Energy Conversion*. Vol. 21, Issue 2, pp. 362–369.
- El-Refaie, A.M. and Jahns, T.M. 2007. "Comparison of synchronous PM machine types for wide constant-power speed operation: converter performance." *IET Electric Power Applications*. Vol. 1, Issue 2, pp. 217–222.
- El-Rafaie, A.M. and Jahns, T.M. 2008. "Impact of Winding Layer Number and Magnet Type on Synchronous Surface PM Machines Designed for Wide Constant-Power Speed Range Operation." *IEEE Transactions on Energy Conversion*. Vol. 23, Issue 1, pp. 53–60.

- El-Refaie, A.M., Jahns, T.M., McCleer, P.J. and McKeever, J.W. 2006. "Experimental verification of optimal flux weakening in surface PM Machines using concentrated windings." *IEEE Transactions on Industry Applications*. Vol. 42, Issue 2, pp. 443–453.
- Gieras, F., Wang, R. and Kamper, M. 2008. *Axial Flux Permanent Magnet Machines*. Second edition. Dordrecht: Springer Science + Business Media B.V.
- Gieras, J.F., Wang, C. and Lai, J.C. 2006. *Noise of Polyphase Electric Motors*. Taylor & Francis Group, LLC.
- Gieras, F. and Wing, M. 1997. *Permanent Magnet Motor Technology – Design and Applications*. New York: Marcel Dekker, Inc.
- Hanselman, D. 2003. *Brushless Permanent Magnet Design*. Second edition. Cranston, Rhode Island: The Writers' collective.
- Heikkilä, Tanja. 2002. *Permanent magnet synchronous motor for industrial inverter applications - analysis and design*. D.Sc. (Tech) dissertation. Acta Universitatis Lappeenrantaensis 134. Lappeenranta, Finland.
- Heller, B. and Hamata, V. 1977. *Harmonic Field Effects in Induction Machines*. Amsterdam: Elsevier Scientific Publishing Company.
- Hendershot, J.R. Jr and Miller, T.J.E. 1994. *Design of Brushless Permanent-Magnet Motors*. Oxford: Magna physics publishing and Clarendon press.
- International Magnetics Association, 2000. MMPA standard No 0100-00. [Online]. Available from: <http://www.intl-magnetics.org/pdfs/0100-00.pdf> [Accessed 27 June 2009].
- Ishak, D., Zhu, Z.Q. and Howe, D. 2004. "Permanent Magnet Brushless Machines with Unequal Tooth Widths and Similar Slot and Pole Numbers." In *Proceedings of the Industry Applications Conference*. Vol. 2, pp. 1055–1061.
- Ishak, D., Zhu, Z.Q. and Howe D. 2005. "Eddy-current Loss in the Rotor Magnets of Permanent-Magnet Brushless Machines having a Fractional Number of Slots per Pole." *IEEE Transactions on Magnetics*. Vol. 41, Issue 9, pp. 2462–2469.
- Jokinen, T. 1973. *Utilization of Harmonics for Self-excitation of a Synchronous Generator by Placing an Auxiliary Winding in the Rotor*. D.Sc. (Tech) dissertation. Acta Polytechnica Scandinavica Electrical Engineering series, No. 32. Helsinki, Finland.



- Jussila, H., Salminen, P., Niemelä, M., Parviainen, A. and Pyrhönen, J. 2007. "Torque and Inductances of Concentrated Wound Permanent Magnet Machines." *International Review of Electrical Engineering (I.R.E.E.)*. Vol. 2, No. 5, September–October 2007, pp. 704–710.
- Kamper, M.J., Wang, R.-J. and Rossouw, F.G. 2007. "Analysis and Performance Evaluation of Axial Flux Air-Cored Stator Permanent Magnet Machine with Concentrated Coils." *In Proceedings Electric Machines & Drives Conference, IEMDC 2007*. Vol. 1, pp. 13–20.
- Kamper, M.J., Wang, R.-J. and Rossouw, F.G. 2008. "Analysis and Performance of Axial Flux Permanent-Magnet Machine With Air-Cored Nonoverlapping Concentrated Stator Windings." *IEEE Transactions on Industry Applications*. Vol. 44, Issue 5, pp. 1495–1504.
- Kinnunen, Janne. 2007. *Direct-On-Line Axial Flux Permanent Magnet Synchronous Generator Static and Dynamic Performance*. D.Sc. (Tech) dissertation. Acta Universitatis Lappeenrantaensis 284. Lappeenranta, Finland.
- Kume, M., Hayashi, M., Yamamoto, M., Kawamura, K. and Ihara, K. 2005. "Heat Resistant Plastic Magnets." *IEEE Transactions on Magnetics*. Vol. 41, Issue 10, pp. 3895–3897.
- Kurronen, P. 2003. *Torque vibration model of axial-flux surface-mounted permanent magnet synchronous machine*. D.Sc. (Tech) dissertation. Acta Universitatis Lappeenrantaensis 154. Lappeenranta, Finland.
- Libert, F. and Soulard, J. 2004. "Design Study of Different Direct-Driven Permanent-Magnet Motors for a Low Speed Application." *Proceedings of the Nordic Workshop on Power and Industrial Electronics, NORPIE 2004*. Trondheim, Norway. CD.
- Libert, F. and Soulard, J. 2004. "Investigation on Pole-Combinations for Permanent-Magnet Machines with Concentrated Windings." *In Proceedings of the International Conference on Electrical Machines, ICEM 2004*. Krakow, Poland. CD.
- Lindh, P., Jussila, H., Niemelä, M., Parviainen, A. and Pyrhönen, J. 2009. "Comparison of Concentrated Winding Permanent Magnet Motors with Embedded Magnets and Surface-Mounted Magnets." *IEEE Transactions on Magnetics*. Vol. 45, Issue 5, May 2009, pp. 2085–2089

Lindh, P., Pyrhönen, J., Parviainen, A., Jussila, H. and Niemelä, M. "Concentrated Wound PM Motors with Semiclosed Slots and with Open Slots." *IEEE Energy Conversion*. (Forthcoming).

Liu, Z.J., Li, J.T. 2007. "Analytical Solution of Air-Gap Field in Permanent-Magnet Motors Taking Into Account the Effect of Pole Transition Over Slots." *IEEE Transactions on Magnetics*. Vol. 43, Issue 10, pp. 3872–3883.

Magnussen, F. and Lendenmann, H. 2007. "Parasitic Effects in PM Machines With Concentrated Windings." *IEEE Transactions on Industry Applications*. Vol. 43, Issue 5, pp. 1223–1232.

Magnussen, F. and Sadarangani, C. 2003. "Winding Factors and Joule Losses of Permanent Magnet Machines with Concentrated Windings." In *Proceedings of the IEEE International Electric Machines and Drives Conference, IEMDC 2003*. Madison, Wisconsin, USA.

Magnussen, F., Svechkarenko, D., Thelin, P. and Sadarangani, C., 2004. "Analysis of a PM Machine with Concentrated Fractional Pitch Windings." In *Proceedings of the Nordic Workshop on Power and Industrial Electronics, NORPIE 2004*. Trondheim, Norway. CD.

Magnussen, F., Thelin, P. and Sadarangani, C., 2003. "Design of Compact Permanent Magnet Machines for a Novel HEV Propulsion System." In *Proceedings of Electric Vehicle Symposium, EVS-20*. Long Beach, USA. CD.

Markovic, M. and Perriard, Y. 2008. "A Simplified Determination of the Permanent Magnet (PM) Eddy Current Losses due to Slotting in a PM Rotating Motor." In *Proceedings of the IEEE International Conference on Electrical Machines and Systems, ICEMS 2008*. Wuhan, China.

Müller, G., Vogt, K. and Ponick, B. 2008. *Berechnung elektrischer Maschinen*, Sechste, völlig neu bearbeitete Auflage. Weinheim: VCH Verlag. (In German).

Nakano, M., Kometani, H., Kawamura, M. 2006. "A Study on Eddy-Current Losses in Rotors of Surface Permanent-Magnet Synchronous Machines." *IEEE Transactions on Industry Applications*. Vol. 42, Issue 2, pp. 429–435.

Neorem, 2009. Neorem Magnets. [Online]. Available from <http://www.neorem.fi> / [Accessed 27 June 2009].

Nerg, J., Niemelä, M., Pyrhönen, J. and Partanen, J. 2002. "FEM Calculation of Rotor Losses in a Medium Speed Direct Torque Controlled PM Synchronous Motor at Different Load Conditions." *IEEE Transactions on Magnetics*. vol. 38, Issue 5, pp. 3255–3257.

Parviainen, A. 2005. *Design of axial-flux permanent-magnet low-speed machines and performance comparison between radial and axial-flux machines*. D.Sc. (Tech) dissertation. Acta Universitatis Lappeenrantaensis 208. Lappeenranta, Finland.

Parviainen, A., Pyrhonen, J. and Kontkanen, P. 2005. "Axial Flux Permanent Magnet Generator with Concentrated Winding for Small Wind Power Applications." In *Proceedings Electric Machines & Drives Conference, IEMDC 2005*. Vol. 1, pp. 1187–1191.

Polinder, H. and Hoeijmakers, M.J. 1997. "Eddy-current losses in permanent magnets of a PM machine." In *Proceedings of the IEE International Conference on Electrical Machines and Drives, EMD97*. Cambridge, the UK, pp. 138–142.

Polinder, H. and Hoeijmakers, M.J. 1999. "Eddy-current losses in the segmented surface-mounted magnets of a PM machine." *IET Electric Power Applications*. Vol. 146, Issue 3, pp. 261–266.

Polinder, H. and Hoeijmakers, M.J. 2000. "Effect of a shielding cylinder on the rotor losses in a rectifier-loaded PM machine." In *Proceedings of the IEEE Conference on Industry Application*. Vol. 1, pp. 163–170.

Polinder, H., van der Pijl, F.F.A., de Vilder, G.-J. and Tavner, P.J. 2006. "Comparison of Direct-Drive and Geared Generator Concepts for Wind Turbines." *IEEE Transactions on Energy Conversion*. Vol. 21, Issue 3, pp. 725–733.

Pyrhönen, J. 1991. *The High Speed Induction Motor: calculating the effects of solid-rotor material on machine characteristics*. Dissertation. Acta Polytechnica Scandinavica, Electrical Engineering Series 68. Helsinki: The Finnish Academy of Technology. Available at <http://urn.fi/URN:ISBN:978-952-214-538-3>.

Pyrhönen, J., Jokinen, T. and Hrabovcová, V. 2008. *Design of Rotating Electrical Machines*. Chichester: John Wiley & Sons, Ltd.

- Reichert, K. 2004. "PM-Motors with concentrated, non overlapping Windings, Some Characteristics." In *Proceedings of the International Conference on Electrical Machines. ICEM 2004*. Krakow, Poland. CD.
- Richter, R. 1954. *Elektrische Maschinen, Band IV, Die Induktionsmaschinen*. Zweite Auflage. Basel and Stuttgart: Birkhäuser Verlag. (In German).
- Richter, R. 1963. *Elektrische Maschinen, Band II, Synchronmaschinen und Einankerumformer*. Dritte Auflage. Birkhäuser Verlag, Basel und Stuttgart, German. (In German).
- Richter, R. 1967. *Elektrische Maschinen, Band I, Allgemeine Berechnungselemente die Gleichstrommaschinen*. Dritte Auflage. Basel and Stuttgart: Birkhäuser Verlag. (In German).
- Rix, A.J., Kamper, M.J. and Wang, R-J. 2007. "Design and Performance Evaluation of Concentrated Coil Permanent Magnet Machines for In-Wheel Drives." In *Proceedings of the International Conference on Electric Machines & Drives, IEMDC 2007*. Vol. 1, pp. 770–775.
- Sahin, F., Tuckey, A.M. and Vandenput, A.J.A. 2001. "Design, development and testing of a high-speed axial-flux permanent-magnet machine." In *Proceedings of the IEEE Conference on Industry Applications*. Vol. 3, pp. 1640–1647.
- Salminen, P. 2004. *Fractional slot permanent magnet synchronous motor for low speed applications*. D.Sc. (Tech) dissertation. Acta Universitatis Lappeenrantaensis 198. Lappeenranta, Finland.
- Salminen, P., Jokinen, T. and Pyrhönen, J. 2005. "The Pull-Out Torque of Fractional-slot PM-Motors with Concentrated Winding." *IET Electric Power Applications*. Vol. 152, Issue 6, pp. 1440–1444.
- Salminen, P., Jussila H., Niemelä, M. and Pyrhönen, J. 2006. "Torque Ripple and Cogging Torque of Surface Mounted PM Machines with Concentrated Windings." In *Proceedings of the XVII International Conference on Electrical Machines, ICEM 2006*. Chania, Crete Island, Greece. CD.
- Salminen P., Pyrhönen J., Libert F. and Soulard J. 2005. "Torque Ripple of Permanent Magnet Machines with Concentrated Windings." In *Proceedings of the International Symposium on Electromagnetic Fields in Mechatronics, ISEF 2005*. Baiona, Spain.

- Slaets B., Van Roy P., Belmans R. 2000. "Determining the efficiency of induction machines, converters and softstarters." *Electromotion*. Vol. 7, Issue 2, pp. 73–80.
- Toda, H., Xia Z.P., Wang J., Atallah K. and Howe D. 2004. "Rotor eddy-current loss in permanent magnet brushless machines." *IEEE Transactions on Magnetics*. Vol. 40, Issue 4, pp. 2104–2106.
- Valtonen, M. 2007. *Performance Characteristics of an Axial-Flux Solid-Rotor-Core Induction Motor*. D.Sc. (Tech) dissertation. Acta Universitatis Lappeenrantaensis 285. Lappeenranta, Finland.
- Vizircanu, D., Brisset, S. and Brochet, P. 2006. "Design and Optimization of a 9-phase Axial-Flux PM Synchronous Generator with Concentrated Winding for Direct-Drive Wind Turbine." In *Proceedings of the Industry Applications Conference*. Vol. 4, pp. 1912–1918.
- Vogt, K. 1996. *Berechnung elektrischer Maschinen*. Weinheim: VCH Verlag.
- Wang, J., Xia, Z. P. and Howe, D. 2005. "Three-Phase Modular Permanent Magnet Brushless Machine for Torque Boosting on a Downsized ICE Vehicle." *IEEE Transactions on Vehicular Technology*. Vol. 54, Issue 3, pp. 809–816.
- Wrobel, R. and Mellor, P.H. 2005. "Design considerations of a direct drive brushless PM machine with concentrated windings." In *Proceedings Electric Machines & Drives Conference, IEMDC 2005*. Vol. 1, pp. 655–658.
- Zarko, D., Ban, D. and Lipo, T.A. 2006. "Analytical calculation of magnetic field distribution in the slotted air gap of a surface permanent-magnet motor using complex relative air-gap permeance." *IEEE Transactions on Magnetics*. Vol. 42, Issue 7, pp. 1828–1837.
- Zhu, Z.Q. and Howe, D. 1991. "Analytical prediction of the air-gap field distribution in permanent magnet motors accounting for the effect of slotting." In *Proceedings of the International Symposium on Electromagnetic Fields in Mechatronics, Electrical and Electronic Engineering, ISEF 1991*. Southampton, UK. pp. 181–184.
- Zhu, Z.Q. and Howe D. 1993. "Instantaneous Magnetic Field Distribution in Brushless Permanent Magnet dc Motors, Part 111: Effect of Stator Slotting." *IEEE Transactions on Magnetics*. Vol. 29, Issue 1, pp.143–151.

Zhu, Z.Q., Howe, D., Bolte, E. and Ackermann, B. 1993. "Instantaneous Magnetic Field Distribution in Brushless Permanent Magnet dc Motors, Part I: Open-circuit Field." *IEEE Transactions on Magnetics*. Vol. 29, Issue 1, pp. 124–135.

Zhu, Z.Q., Howe, D. and Chan, C.C. 2002. "Improved Analytical Model for Predicting the Magnetic Field Distribution in Brushless Permanent-Magnet Machines." *IEEE Transactions on Magnetics*. Vol. 38, Issue 1, pp. 229–238.

Zhu, Z.Q., Ng, K., Schofield, N. and Howe, D. 2004. "Improved analytical modelling of rotor eddy current loss in brushless machines equipped with surface-mounted permanent magnets." *IEE Electric Power Applications*. Vol. 151, Issue 6, pp. 641–650.

**ACTA UNIVERSITATIS LAPPEENRANTAENSIS**